Adaptive OFDM Cooperative Systems

by

Osama Mohammed Hussein Amin

A thesis
presented to the University of Waterloo
in fulfillment of the
thesis requirement for the degree of
Doctor of Philosophy
in
Electrical and Computer Engineering

Waterloo, Ontario, Canada, 2010

I hereby declare that I am the sole author of this thesis. This is a true copy of the thesis, including any required final revisions, as accepted by my examiners.

I understand that my thesis may be made electronically available to the public.

Abstract

Cooperative communication is a promising technique for wireless communication systems where wireless nodes cooperate together in transmitting their information. Such communication transmission technique, which realizes the multiple antenna arrays in a distributed manner over multiple wireless nodes, succeeds in extending the network coverage, increasing throughput, improving both link reliability and spectral efficiency.

Available channel state information at the transmitting nodes can be used to design adaptive transmission schemes for improving the overall system performance. Throughout our work, we adaptively change loaded power and/or bit to the Orthogonal Frequency Division Multiplexing (OFDM) symbol in order to minimize bit error rate or maximize the throughput.

In the first part of this dissertation, we consider single-relay OFDM system with amplify-and-forward relaying. We propose three algorithms to minimize the bit error rate under total power constraint and fixed transmission rate. These algorithms are optimal power loading, optimal bit loading and optimal bit and power loading. Through Monte Carlo simulations we study the proposed system performance and discuss the effect of relay location and channel estimation. This study shows that the proposed algorithms result in exploiting the multi-path diversity and achieving extra coding gain.

In the second part, we extend the problem to a multi-relay OFDM network but with decode-and-forward relaying. We propose an adaptive power loading algorithm to minimize the bit error rate under total power constraint based on two relay selection strategies. The proposed system leads to achieve both multi-path and cooperative spatial diversity using maximal-ratio combiner for the detection.

In the last part, we consider also multi-relay network but with amplify and forward relaying. We optimize the bit loading coefficients to maximize the throughput under target bit error rate constraint. The proposed algorithm is considered more practical since it takes into consideration the channel estimation quality. The considered adaptive system has less complexity compared with other adaptive systems through reducing the feedback amount. Furthermore, the full network channel state information is needed only at the destination.

Acknowledgements

I am thankful to Allah, the most merciful and most compassionate for blessing me with the strength to seek knowledge and complete this work.

I would like to express my deepest gratitude to my adviser, Professor Murat Uysal, who has provided me with a continuous support, assistance, and motivation. I am grateful for his insightful suggestions, valuable discussions and advices. It is my pleasure to thank my doctoral thesis committee members Dr. Eihab Abdel-Rahman, Dr. Patrick Mitran, Dr. Pin-Han Ho, and Dr. Teng Joon Lim for their valuable time and discussions. I thank also all professors who contributed in my educations and especially Dr. Mohamed Dabbagh whose office was open for me during my PhD study.

A special recognition for the Egyptian Ministry of Higher Education, Egyptian Cultural and Educational Bureau in Canada and Assiut University in Egypt for offering me this PhD scholarship.

I am very thankful to my research group, colleagues and friends for their valuable help, useful discussion and feedback during my PhD study especially, Hany Zeidan, Dr. Moataz El-Ayadi, Mohamed Feiteha, Dr. Salama Ikki, Suhail Al-Dharrab and Walid Abediseid. Special thank you to my big brother, Dr. Azmy Faisal, for supporting me and providing me with valuable advices.

Words cannot adequately express my heartiest thanks to my parents, my mother-in-law, my wife and other family members for their love, kindness, and prayers. Their support and encouragement was essential to achieve such accomplishments.

Last, but not least, I express my deep appreciation to numerous people who wished success to me or even smiled at me.

Dedication

To my parents, Marwa, Muhammad and ....

Table of Contents

List of Tables

List of Figures

List of Algorithms

List of Abbreviations

AF	Amplify-and-forward
APL	Adaptive power loading
AWGN	Additive white Gaussian noise
BER	Bit error rate
BICM	Bit interleaved coded modulation
CE	Channel estimation
CP	Cyclic prefix
CRC	Cyclic redundancy check
CSI	Channel state information
D-CE	Disintegrated channel estimation
DF	Decode-and-forward
EBPL	Equal bit and power loading
EPL	Equal power loading
FDM	Frequency division multiplexing
FIR	Finite impulse response
GBD	Generalized Benders decomposition
IBI	Interblock interference

IFFT	Inverse fast Fourier transform
IPS	Instantaneous power scaling
ISI	Intersymbol interference
KKT	Karush-Kuhn-Tucker
LMMSE	Linear minimum mean squared error
MIMO	Multiple-input multiple-output
ML	Maximum likelihood
M-PSK	M-ary phase shift keying
M-QAM	M-ary quadrature amplitude modulation
MRC	Maximal ratio combining
OBL	Optimal bit loading
OBPL	Optimal bit and power loading
OFDM	Orthogonal frequency division multiplexing
OPL	Optimal power loading
pdf	Probability density function
QPSK	Quadrature phase shift keying
RD	Receive diversity
RSM1	Relay selection method 1
RSM2	Relay selection method 2
SER	Symbol error rate performance
SIMO	Single input multiple output
SINR	Signal to interference plus noise ratio
SISO	Single input single output

SNR Signal-to-noise ratio

STD Simplified transmit diversity

TD Transmit diversity

TDM Time division multiplexing

Chapter 1

Literature Review

Wireless communication networks have grown widely and effectively since 1980 and become an important part of our day life. This growth developed from voice-dominated stage represented in analogue first generation and digital second generation mobile systems to data-dominated stage in the current third generation system. As reaching the end of this decade, we are currently on the border of dominating our mobile system by video traffic. This development is motivated by the diffusion of new mobile devices in the market such as iPhone, Android platforms, iPad and the continued growth of netbooks and laptops [1].

Next decade is expected to testify many exciting changes in the wireless communication networks, enabling wireless broadband internet services on a wide range of communication devices. These changes are part of the wireless network evolution to fourth-generation (4G) technologies and network. The evolution to 4G is expected to permit new services and usage models with higher efficiency network to be used in roaming and communicating the network anytime, anywhere and with any technology.

The 4G mobile communication systems are required to support wide applications which

requires higher and reliable data rate. Multicarrier system, such as applied in WiMAX (Worldwide Interoperability for Microwave Access), is one of the candidate 4G systems which targeted to provide transmission rate of 1Gb/s or more [1]. This challenging objective is achieved by utilizing wide bandwidth for parallel data transmission across multiple subcarriers. To meet such demand, wireless communication system designers need to optimize the network performance to meet some challenging parameters such as better link reliability, higher data rates, fewer dropped connections and longer battery life.

1.1 Cooperative Communication

Cooperative communication became the focus of enormous research attention during the current decade. The cooperative techniques are used to improve communication coverage, increase data rate and combat fading in wireless networks. Cooperative diversity exploits the broadcast nature of wireless transmission and creates a virtual (distributed) antenna array through cooperating nodes to extract spatial diversity. The source node and its nearby relaying nodes share their antennas and send the same message through independent fading paths. Cooperative transmission has succeeded in reaping many advantages of multiple-input multiple-output (MIMO) systems while overcoming some of its shortcomings as well. Particularly it provides a powerful alternative in various wireless applications where the deployment of multiple antennas might be problematic due to size and power limitations [2, 3].

Based on the relaying mode, cooperative transmission can be categorized into two main groups [4, 5]. In non-regenerative amplify-and-forward (AF) relaying, the relay receives an attenuated version of the transmitted signal and retransmits it after scaling the received

signal to meet the average transmit power constraint. In regenerative decode-and-forward (DF) relaying, the relay needs to detect the signal first and then re-encodes it (possibly using a different codebook) for transmission to the destination. DF relaying is favorable if the relay is equipped with an efficient and fast processor. AF mode is preferable in case of analogue systems and when the relay does not have sufficient processing ability.

Either AF or DF relaying can be combined with various cooperation protocols. In their pioneering work [5], Laneman et al. consider a multi-relay cooperation scenario where the source signal is transmitted to a destination terminal through a number of half-duplex terminals and demonstrate that the receiver achieves full spatial diversity. Their proposed user cooperation protocol is built upon a two-phase transmission scheme. In the first transmission phase (i.e., broadcasting phase), the source broadcasts to the destination and relay terminals. In the second transmission phase (i.e., relaying phase), the relays transmit processed version of their received signals to the destination using either orthogonal subchannels (repetition based cooperative diversity) or the same subchannel (space-time coded cooperative diversity).

In [6], Nabar et al. establish a unified framework for cooperation protocols in single-relay scenarios and consider so-called transmit diversity (TD) protocol, receive diversity (RD) protocol, and simplified transmit diversity (STD) protocol [1]. RD protocol is essentially the same as orthogonal cooperation protocol proposed in [5] and realizes a single input multiple output (SIMO) system in a distributed manner. Multi-hop transmission can be considered as a special case of the RD protocol where the destination node only switches on relaying phase. In TD protocol, the first transmission phase is the same as in RD protocol where the source terminal broadcasts to the relay and destination terminals.

[1]These protocols are referred as Protocol I, Protocol II, and Protocol III in [6]. Here, we use the protocol names as proposed in [7].

However, in the second transmission phase, unlike RD protocol, both the relay and source terminals communicate with the destination terminal. Since TD protocol can potentially convey different signals to the relay and destination terminals, this makes possible the deployment of various conventional space-time codes (originally proposed for co-located antennas) in a distributed scenario. STD protocol is similar to TD protocol except that the destination terminal does not receive from the source during the first transmission phase for reasons which are possibly imposed from the upper-layer networking protocols. For example, the destination terminal may be engaged in data transmission to another terminal during the first phase.

After the pioneering works in [4,5,8,9], a large number of publications have appeared in the area of cooperative communications investigating variety of topics such as information theoretic bounds, cooperation protocols, distributed space-time code design, distributed source coding, optimum power allocation, cross-layer design etc. among others. Detailed surveys of various issues in cooperative communication systems can be found in recent books [10, 11].

1.2 OFDM

There is an increasing demand on broadband wireless communication applications such as video and data streaming, i.e., real-time multimedia applications. A major design challenge in high-speed broadband communication is intersymbol interference (ISI) which is a result of the dispersive nature of underlying frequency-selective fading channels [12]. As a multi-carrier solution, orthogonal frequency division multiplexing (OFDM) converts the transmitted stream into substreams to be transmitted through different sub-channels

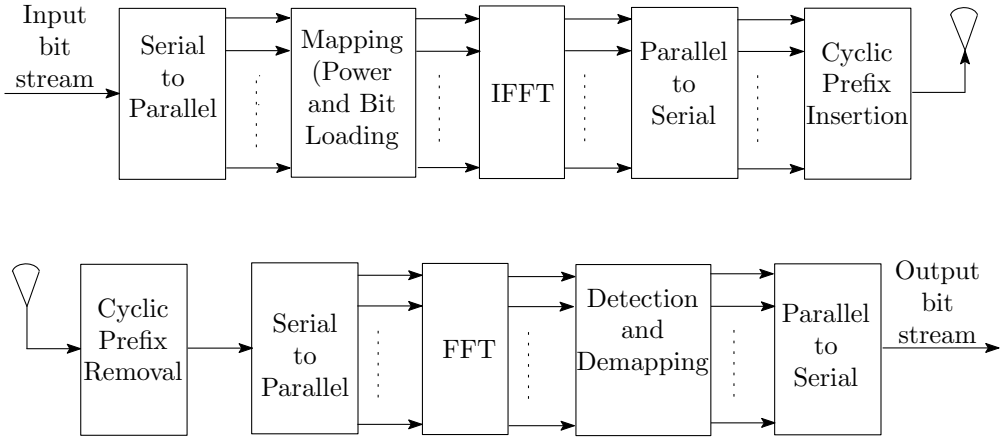

Figure 1.1: Block diagram of uncoded OFDM system.

exhibiting flat fading characteristics.

A generic uncoded SISO (single input single output) OFDM system, as illustrated in Figure 1.1, consists of symbol mapping system which maps the input binary data to the corresponding symbols for a given modulation scheme [13]. The serial symbol stream is then converted to N parallel substreams which are fed to N-IFFT (inverse fast Fourier transform). To prevent the interblock interference (IBI) between the successive blocks, cyclic prefix (CP) symbols are added to each data-symbols block. At the receiver, first the CP is removed, and then the received signals pass through serial-to-parallel converter which is fed to N-FFT (fast Fourier transform) system. After parallel-to-serial conversion, signals are detected by a maximum likelihood (ML) decoder.

Although uncoded OFDM is able to mitigate the degrading fading effects, it is not able to exploit the underlying rich multipath diversity of frequency-selective channels. Outer coding or precoding can be combined with OFDM to extract the multipath diversity. Bit interleaved coded modulation (BICM) OFDM system uses a convolutional coder at the transmitter and a Viterbi detector at the receiver to extract the multipath diversity [14,15].

The binary data stream is first encoded using a convolutional coder. In addition to that, a random bit-based interleaving is done at the transmitter to mitigate the deep fading in frequency domain.

Another effective way to exploit the multipath diversity is precoding method introduced in [16]. Precoded OFDM transmitter structure is similar to the uncoded system except after the IFFT system, a linear constellation precoder is added. The precoder matrix coefficients are designed to achieve maximum diversity and coding gain. Each output substream of the precoded system is a subset of the parallel input signals. Therefore, the detection process cannot be carried on separated received subchannels but it should be done jointly between dependent subchannels using Viterbi decoder.

1.3 Adaptive Transmission

Adaptive transmission aims to use any channel information available at the transmitter side to improve the overall system performance. In these closed loop systems, feedback channel is used to provide the transmitter with the channel state information (CSI) in order to adapt its power, rate or both together in order to attain a better system performance [17].

Since the 1990s, several researchers have studied adaptive transmission for point-to-point links. For example, [18–22] consider adaptive SISO systems while [23–28] focus on adaptive MISO and MIMO systems over frequency-flat fading channels. Adaptive transmission has been also studied in the context of multi-carrier communication. Although the subchannels in an OFDM system are considered to exhibit frequency-flat fading, the problem is essentially different from a single-carrier system. In a multicarrier adaptive system, rate and power optimization problems need to be solved for each of the subcarriers.

Adaptive transmission is considered for SISO OFDM systems in [29–34], for MISO OFDM systems in [35, 36] and for MIMO OFDM systems in [37–41].

Adaptive transmission has also been recently applied to cooperative networks which will be the focus of this thesis. We will provide an overview of the existing literature in the next sub-sections.

1.3.1 Adaptive Transmission for Frequency-Flat Fading Relay Channels

In [42], Ahmed et al. assume a single relay system with AF relaying over frequency-flat Rayleigh fading channels. They solve the power allocation problem aiming to minimize the outage probability for fixed rate transmission subject to power constraint. They further investigate the effect of limited feedback on the performance of their proposed scheme.

In [43], Ahmed and Aazhang propose rate and power control algorithms for DF relaying under power constraint assuming finite-rate feedback channels. A theoretical study for the achievable rates in adaptive DF and compress-and-forward relaying is further introduced in [19].

Considering multi-hop cooperative communication, Jingmei et al. solve the power allocation problem for a two-hop AF relaying scheme aiming to maximize the channel signal-to-noise ratio (SNR). In [44], Lau and Cui consider also the multi-hop cooperative system but for DF relaying mode. Their scheme aims to minimize the power consumption under a fixed bit error rate (BER) constraint. In [45], Ibrahim et al. consider a multi-relay scheme using RD cooperation protocol and DF relaying and investigate relay selection assuming DF mode based on the instantaneous CSI values.

Unlike the previous techniques that work under time division multiplexing (TDM) assumption, Adeane et al. propose a hybrid adaptive cooperative system which combines TDM and FDM (frequency division multiplexing) in [46]. They compute the optimal power allocation factors (i.e., the ratio between the users power to the power used to relay another users data) to minimize the BER.

1.3.2 Adaptive Transmission for Frequency-Selective Fading Relay Channels

In [47], Hammerstrom and Wittneben consider an uncoded two-hop OFDM system over frequency-selective channels and propose optimum power allocation schemes to maximize the instantaneous rate assuming AF relaying. They investigate this optimization problem for either fixed relay power or fixed source power and further study joint power allocation. In [48], they extend the same problem for a MIMO OFDM system.

Unlike [47, 48] which is built on multi-hopping, Ma et al. [49] consider RD protocol and solve the bit and power loading problem for AF and selection DF relaying. Their proposed algorithm assumes the availability of the CSI at all nodes and computes the bit and power loading coefficients at each subcarrier to minimize the power cost under a target throughput and symbol error rate performance (SER). In [50], Ying et al. employ power loading and subcarriers-pairing to maximize the instantaneous capacity under total power constraint for DF relaying. In [51], Yi et al. discuss rate maximization problem for DF relaying under individual power and SER constraints.

In [52], Can et al. consider TD, RD and STD cooperation protocols, adopt subchannel instantaneous SINR (signal to interference plus noise ratio) as a constraint, and aim to

maximize end-to-end throughput.

In [53], Gui and Cimini also consider RD protocol and present bit and power loading algorithms for OFDM DF cooperative systems with sub-carrier selection to minimize the total transmission power under a fixed rate assumption. In another work which builds on RD protocol [51, 54], Yi et al. propose a sub-optimal bit and power loading algorithm for OFDM cooperative system to maximize the throughput under individual power constraints and a target link error rate assuming AF and selective DF relaying. In [49], the same authors study bit and power loading algorithms to minimize the transmit power consumption for AF and selective DF modes at a target throughput. In [55], Hajiaghayi et al. address power loading for an OFDM AF system with RD protocol. They formulate two problems; one aims to maximize the system capacity and the other aims to minimize BER.

1.4 Constrained Optimization

In most cases, the design of adaptive transmission schemes can be formulated as constrained optimization problems. Optimization is the process of finding the best way to use available resources defined through optimization parameters, in order to improve certain performance metric through objective function, while at the same time not violating any of the conditions that are imposed by a constraint function [56–59].

Optimization parameters affect the value of both objective and constraint functions. They can be either continuous or discrete. An objective function has at least one global optimum which give the best improvement of the objective function, and may have multiple local optima. For continuous problems, minimization problem gives optimal solution when the objective and constraint function are convex functions.

Constraint functions can be equality or inequality or even both. Optimization problems are classified to different types according to the objective and constraint functions kinds. Linear optimization (or programming) problem deals with continuous variables in linear objective and constraint functions. While the non-linear optimization (or programming) problem which has either the objective function or constraint function is nonlinear or even both. Integer optimization (or programming) problem deals only with integer variables. In addition to these types, mixed types are considered such as mixed integer linear and mixed integer nonlinear optimization. In this dissertation, different optimization problems are considered such as nonlinear continuous optimization, nonlinear integer optimization and mixed integer non-linear optimization [56, 57].

In nonlinear optimization problem, the method of Lagrange multipliers provides a strategy for finding the maxima and minima of a function subject to one or multiple equality constraints. In this technique, the constrained problem is converted to unconstrained problems. Karush Kuhn Tucker conditions (also known as the Kuhn Tucker or KKT conditions) are a generalization of the Lagrange multiplier method where inequality constraint can be considered with equality constraint assuming more multipliers [56, 58].

As for nonlinear integer optimization, the dynamic programming has been widely used in dealing with such problems. The possibility to separate both the objective function / and constraint functions makes the dynamic programming method an ideal technique to solve this kind of problems. This method breaks the original problem into simpler sub problems, which try all possible values that can be assumed for the optimization parameter(s) [57,59].

Mixed-integer nonlinear programming problem includes both integer variables and continuous variables and can be solved by Generalized Benders Decomposition (GBD) approach. GBD generally relies on the successive solutions of closely related nonlinear pro-

gramming and mixed integer programming problems. The approaches described above only guarantee global optimality under (generalized) convexity. Deterministic algorithms for global optimization of non-convex problems require the solution of sub problems obtained via convex relaxations of the original problem [57–59].

1.5 Thesis Motivation and Contribution

Although adaptive cooperative transmission has attracted some attention lately, there exist many open problems to be pursued particularly over frequency-selective channels. Most of the current work considers power, instantaneous capacity, rate or throughput as the performance metrics. Another performance metric of practical concern is the error rate which has not been much investigated so far in the context of adaptive cooperative networks. This encourages us to study adaptive power and bit loading problems considering BER as the performance metric. Another research direction pursued to design the adaptive OFDM system for cooperative networks taking into account the quality of imperfect channel estimation. To the best of our knowledge, existing literature on adaptive transmission in OFDM-based cooperative systems does not consider the CSI estimation quality in the design.

In this dissertation, we consider in chapter 2 the problem of three nodes OFDM AF cooperative network and propose three algorithms to minimize BER for uncoded OFDM [60,61] These adaptive algorithms are based on power loading, bit loading and joint bit and power loading. Then we extend the problem in chapter 3 to multi-relay OFDM cooperative system and solve the problem of power loading for DF relaying. We assume relay selection scheme based on two strategies [62]. In chapter 4, we design adaptive bit loading system

for OFDM cooperative network considering the channel estimation quality [63, 64]. We aim to maximize the throughput for multi-relay with AF relaying mode.

Chapter 2

Bit and Power Loading for AF Cooperative Network

In this chapter, we investigate bit and power allocation strategies for a single-relay cooperative network over frequency-selective fading channels. We assume a single-relay OFDM system with AF relaying and RD protocol. Aiming to optimize the BER under total power constraint and for a given average data rate, we propose three adaptive algorithms. The first algorithm computes the optimal source and relay power loading coefficients under total power constraint and fixed subcarriers' rate. The second algorithm computes the optimal bit loading coefficients under fixed average transmission rate and equal power loading. The third algorithm computes the joint optimal power and bit loading coefficients under total power constraint and fixed average transmission rate. Through Monte-Carlo simulations, we demonstrate that our proposed schemes achieve full diversity and outperform conventional schemes with equal power loading as well as precoded systems. We further investigate the effect of practical considerations such as imperfect CSI and quantization on

the performance.

The rest of the chapter is organized as follows: The signal model for cooperative OFDM system under consideration is described in Section 2.1. Optimization problem to minimize BER is first formulated in Section 2.2 and then corresponding power and/or bit loading algorithms are presented. The simulated performance of proposed adaptive schemes is presented in Section 2.3. And finally Section 2.4 summarizes and concludes the chapter.

Notation: Bold upper-case letters denote matrices and bold lower-case letters denote vectors. $\mathbb{E}$ and $|.|$ denote respectively the expectation and the absolute value. $(.)^T$ and $(.)^H$ denotes transpose and conjugate transpose (i.e., Hermitian) operations, respectively. $Q(.)$ represents the Gaussian Q function. $\mathbf{Q}$ represents the $N \times N$ FFT matrix, i.e. $\mathbf{Q}(p,q) = (1/\sqrt{N}) \exp(-j2\pi(p-1)(q-1)/N)$, $p = 0, 1, ..., N-1$, $q = 0, 1, ..., N-1$.

2.1 Transmission Model

We consider a cooperative OFDM system with single relay. Source, relay, and destination nodes are equipped with single transmit/receive antennas and operate in half-duplex mode. The nodes are assumed to be located in a two-dimensional plane where d_{SD}, d_{SR} and d_{RD} denote the distances of source-to-destination (S→D), source-to-relay (S→R), and relay-to-destination (R→D) links, respectively (see Figure 2.1). In Figure 2.1, θ is the angle between lines representing S→R and R→D links.

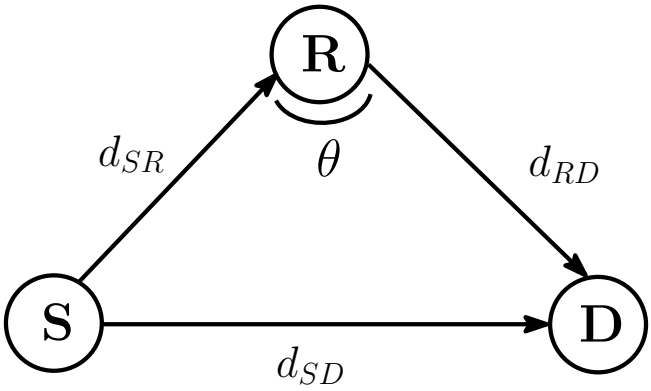

Figure 2.1: Cooperative system model.

To explicitly take into account the effect of relay location, we consider both long-term path loss and short-term frequency-selective Rayleigh fading. The path loss is proportional to d^{α} where d is the distance between nodes and α is the path loss exponent. By normalizing the path loss terms with respect to the direct S→D link, the so-called geometrical gains can be defined as $G_{SR} = (d_{SD}/d_{SR})^{\alpha}$ and $G_{RD} = (d_{SD}/d_{RD})^{\alpha}$ [7]. These are related through the cosines law by $G_{SR}^{2/\alpha} + G_{RD}^{2/\alpha} - 2G_{SR}^{1/\alpha}G_{RD}^{1/\alpha}\cos\theta = G_{SR}^{2/\alpha}G_{RD}^{2/\alpha}$. The frequency-selective fading channels are modeled as FIR (finite impulse response) filters with order of L_{SD}, L_{SR} and L_{RD}. They are represented by $\mathbf{h}_{SD} = [h_{SD}(0), \ldots, h_{SD}(L_{SD})]^T$, $\mathbf{h}_{SR} = [h_{SR}(0), \ldots, h_{SR}(L_{SR})]^T$ and $\mathbf{h}_{RD} = [h_{SR}(0), \ldots, h_{SR}(L_{SR})]^T$ for S→D, S→R, and R→D links, respectively. The entries of $\mathbf{h}_{SD}$, $\mathbf{h}_{SR}$, and $\mathbf{h}_{RD}$ are assumed to be zero mean, complex Gaussian distribution with their variance equal to $1/(L_{SD}+1)$, $1/(L_{SR}+1)$ and $1/(L_{RD}+1)$, respectively. The channels are assumed to remain constant over a block of OFDM symbols and change from one block to another independently.

Here, we assume RD cooperation protocol where the source and the relay nodes transmit in orthogonal transmission phases. In the first transmission phase, a bit-stream is fed into serial-to-parallel converter which maps them into modulation symbols chosen from

either M-PSK or M-QAM constellations. The k^{th} subcarrier symbol carries b_k bits based on the employed bit loading algorithm (which will be introduced later). Before passing through inverse FFT (IFFT), the power of each subcarrier symbol is adjusted based on the employed power loading algorithm (which will be introduced later). To prevent inter-block interference, a cyclic prefix (CP) is inserted between OFDM symbols with $L_{CP} \geq \max(L_{SR}, L_{RD}, L_{SD})$. Both relay and destination nodes receive the transmitted OFDM symbol. After removing CP and converting the OFDM symbol into parallel subcarrier symbols through FFT, the relay node scales the subcarriers power. Then it feeds the subcarrier symbols to IFFT and adds CP. In the second transmission phase, the relay node forwards the resulting signal to the destination while the source node remains silent. At the destination, both OFDM symbols received during the broadcasting and relaying phases are fed to maximum likelihood (ML) detector after removing CP and passing through FFT. Block diagrams of source, relay, and destination nodes are provided in Figures 2.2(a), 2.2(b) and and 2.2(c).

Let the subcarrier signal for the k^{th} carrier be denoted as $x(k)$, $k = 1, 2, ...N$ where N is the number of subcarriers. The received signals at the relay and the destination nodes during the broadcasting phase are given by

$$r_{D_1}(k) = \sqrt{E_{k,S}} \exp(j\phi_{k,S}) D_{SD}(k,k) x(k) + v_{D_1}(k) \tag{2.1}$$

$$r_R(k) = \sqrt{E_{k,S} G_{SR}} \exp(j\phi_{k,R}) D_{SR}(k,k) x(k) + v_R(k) \tag{2.2}$$

where $E_{k,S}$ and $\phi_{k,S}$ denote, respectively, the adjustable power and phase terms for k^{th} subcarrier. In the above $v_{D_1}(k)$, and $v_R(k)$ are the FFT of additive white Gaussian noise (AWGN) terms $n_{D_1}(k)$ and $n_R(k)$. $D_{SD}(k,k)$ and $D_{SR}(k,k)$ are the k^{th} diagonal el-

ements in the diagonal channel matrices $\mathbf{D}_{SD}$ and $\mathbf{D}_{SR}$. They are defined as $\mathbf{D}_{SD} = \text{diag}(\text{H}_{\text{SD}}(0),\ \text{H}_{\text{SD}}(1), \cdots \text{H}_{\text{SD}}(\text{N}-1))$ and $\mathbf{D}_{SR} = \text{diag}(\text{H}_{\text{SR}}(0),\ \text{H}_{\text{SR}}(1), \cdots \text{H}_{\text{SR}}(\text{N}-1))$ where $H_{SD}(k) = \sum_{l=1}^{N-1} h_{SD}(l) \exp(-j2\pi lk/N)$ and $H_{SR}(k) = \sum_{l=1}^{N-1} h_{SR}(l) \exp(-j2\pi lk/N)$. For the scaling at the relay node, we adopt a slightly modified version of so-called instantaneous power scaling (IPS) [65,66] which assumes perfect CSI. In IPS, scaling term is given by

$$\underset{v_R(k)}{\mathbb{E}} \left\{ \left| r_R(k) \right|^2 \right\} = E_{k,S} G_{SR} \left| D_{SR}(k,k) \right|^2 + N_0. \tag{2.3}$$

Here, instead we replace $E_{k,S}$ with the average value E. Such a modification does not significantly affect the overall performance, but simplifies the ensuing optimization problem. After scaling the received signal, the relay node amplifies the k^{th} subcarrier with power $E_{k,R}$ and adjusts the phase by adding $\phi_{k,R}$. Then it feeds the subcarriers to IFFT and adds CP before it forwards the resulting signal to destination node.

The destination node removes CP and converts the received OFDM symbol into subcarrier symbols. The k^{th} subcarrier signal is given by

$$r_{D_2}(k) = \frac{\sqrt{G_{SR} G_{RD} E_{k,S} E_{k,R}}}{\sqrt{E G_{SR} \left| D_{SR}(k,k) \right|^2 + N_0}} \exp\left(j(\phi_{k,S} + \phi_{k,R}) \right) D_{SR}(k,k)\, D_{RD}(k,k)\, x(k) + v'_{D_2}(k) \tag{2.4}$$

In (2.4), $v'_{D_2}(k)$ represents the effective noise term and is given by

$$v'_{D_2}(k) = \frac{\sqrt{G_{RD} E_{k,R}} D_{RD}(k,k) \exp(j\phi_{k,R})}{\sqrt{E G_{SR} \left| D_{SR}(k,k) \right|^2 + N_0}} v_R(k) + v_{D_2}(k) \tag{2.5}$$

where $v_{D_2}(k)$ is the FFT of AWGN term at the destination during the relaying phase. Effective noise is conditionally Gaussian with zero mean and variance of ϖ where $\varpi =$

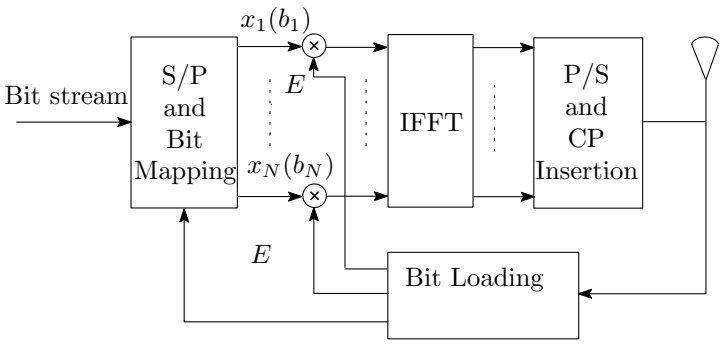

(a) Source

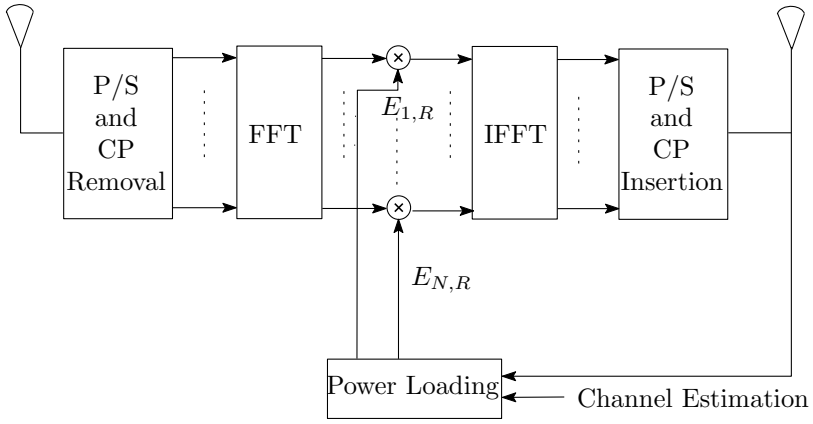

(b) Relay

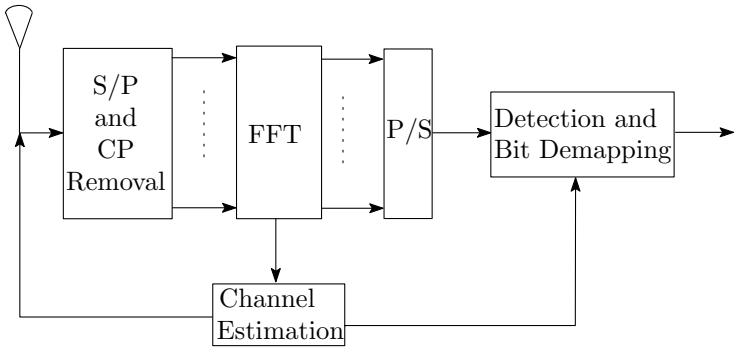

(c) Destination

Figure 2.2: Block diagrams of source, relay, and destination nodes.

$\sqrt{1+E_{k,R}G_{RD}|D_{RD}(k,k)|^2/\left(EG_{SR}|D_{SR}(k,k)|^2+N_0\right)}$. Normalizing (2.5) with ϖ, we have

$$\tilde{r}_{D_2}(k)=\frac{\sqrt{E_{k,S}E_{k,R}}D_{k,2}\exp\left(j\left(\phi_{k,S}+\phi_{k,R}\right)\right)}{\sqrt{E_{k,R}D_{k,R}+D_{k,0}}}x(k)+\tilde{v}_{D_2}(k) \tag{2.6}$$

where $\tilde{v}_{D_2}(k)$ is the output noise with variance N_0. In (2.6), $D_{k,R}$, $D_{k,0}$, $D_{k,1}$, and $D_{k,2}$ are defined as $D_{k,R}=G_{RD}\left|D_{RD}(k,k)\right|^2$, $D_{k,0}=EG_{SR}\left|D_{SR}(k,k)\right|^2+N_0$, $D_{k,1}=D_{SD}(k,k)$ and $D_{k,2}=\sqrt{G_{SR}G_{RD}}D_{SR}(k,k)\,D_{RD}(k,k)$. Based on the received signals given by (2.1) and (2.6) and assuming perfect CSI, the destination node performs ML detection using the metric

$$\hat{x}(k)=\arg\min_{x(k)}\left\{\left|r_{D_1}(k)-\sqrt{E_{k,S}}\exp\left(j\phi_{k,S}\right)D_{k,1}x(k)\right|^2\right.$$
$$\left.+\left|\tilde{r}_{D_2}(k)-\frac{\sqrt{E_{k,S}E_{k,R}}\exp\left(j\left(\phi_{k,S}+\phi_{k,R}\right)\right)D_{k,2}}{\sqrt{E_{k,R}D_{k,R}+D_{k,0}}}x(k)\right|^2\right\} \tag{2.7}$$

2.2 Adaptive Loading Algorithms for BER Optimization

In this section, we propose three adaptive bit and/or power loading algorithms to minimize the BER. Based on the availability of instantaneous CSI, approximate BER expressions for M-PSK and rectangular M-QAM are given by [67]

$$P\approx\sum_{k=1}^{N}c_kQ\left(\sqrt{a_k\varepsilon_k}\right) \tag{2.8}$$

where c_k, a_k and ε_k are defined as

$$\varepsilon_k = E_{k,S} \left| D_{k,1} \right|^2 + \frac{E_{k,S} E_{k,R} \left| D_{k,2} \right|^2}{(E_{k,R} D_{k,R} + D_{k,0})} \tag{2.9}$$

$$c_k = \begin{cases} \frac{(M_k - 1)}{\sum_{k=1}^{N} \log_2 M_k}, & \text{for M} - \text{PSK} \\ \frac{4}{\sum_{k=1}^{N} \log_2 M_k} \left(\frac{\sqrt{M_k} - 1}{\sqrt{M_k}} \right), & \text{for M} - \text{QAM} \end{cases} \tag{2.10}$$

$$a_k = \begin{cases} \frac{2}{N_0} \sin^2 \left(\frac{\pi}{M_k} \right), & \text{for M} - \text{PSK} \\ \frac{3}{N_0 (M_k - 1)}, & \text{for M} - \text{QAM} \end{cases} \tag{2.11}$$

where M_k is the constellation size for the k^{th} subcarrier.

2.2.1 Optimal Power Loading (OPL)

In this subsection, we aim to find OPL coefficients for source and relay subcarriers to minimize the BER under total power constraint and fixed subcarrier rate (i.e., fixed modulation scheme for all subcarriers). Total power constraint dictates $(1/N) \sum_{k=1}^{N} (E_{k,S} + E_{k,R}) = 2E$. On the other hand, under fixed subcarrier rate, we have $M_k = M$ which yields constant values $c_k = c$ and $a_k = a$ for all subcarriers. Let us define $\mathbf{E}_{k,S} = [\ E_{1,S} \quad E_{2,S} \quad \cdots \quad E_{N,S}\ ]^T$ and $\mathbf{E}_{k,R} = [\ E_{1,R} \quad E_{2,R} \quad \cdots \quad E_{N,R}\ ]^T$ as the vectors representing source and relay power

loading coefficients. Therefore, the optimization problem can be expressed as

$$\min_{\mathbf{E}_{k,S},\mathbf{E}_{k,R}} c\sum_{k=1}^{N} Q\left(\sqrt{a\varepsilon_k}\right) \tag{2.12}$$

subject to the constraint of

$$\frac{1}{N}\sum_{k=1}^{N}\left(E_{k,S}+E_{k,R}\right)=2E, \quad E_{k,S}>0, \quad E_{k,R}\geq 0 \quad b_k=B,\,\forall\, k \tag{2.13}$$

Since $Q\left(.\right)$ is convex, objective function in (2.12) is also convex as proved in the appendix. Therefore, its solution will provide global optimum results.

Factoring the constraint into the objective function, we formulate Lagrangian problem as

$$\Psi = c\sum_{k=1}^{N} Q\left(\sqrt{a\varepsilon_k}\right)+\lambda\left(\frac{1}{N}\sum_{k=1}^{N}\left(E_{k,S}+E_{k,R}\right)-2E\right)-\sum_{k=1}^{N}\mu_k E_{k,S}-\sum_{k=1}^{N}\eta_k E_{k,R} \tag{2.14}$$

where λ is the Lagrange multiplier. Eq. (2.13) can be rewritten as

$$\nabla_g \Psi = \mathbf{0} \tag{2.15}$$

where we define $\mathbf{g}$ as

$$\mathbf{g}=[E_{1,S},\cdots,E_{N,S},E_{1,R},\cdots,E_{N,R},\mu_1,\cdots\mu_N,\eta_1,\cdots\eta_N,\lambda,\phi_{1,S},\cdots,\phi_{N,S},\phi_{1,R},\cdots,\phi_{N,R}] \tag{2.16}$$

and ∇_g is the gradient operator with respect to elements of $\mathbf{g}$. Since Ψ is independent of $\phi_{k,S}$ and $\phi_{k,R}$, they will not affect the optimization. Therefore, we set $\phi_{k,S}=\phi_{k,R}=0$.

The KKT conditions for the optimization problem at hand can be then written as [58]

$$\frac{\partial \Psi}{\partial E_{k,S}} = -c\sqrt{\frac{a}{8\pi\varepsilon_k}}\exp\left(-\frac{a\varepsilon_k}{2}\right)\frac{\partial \varepsilon_k}{\partial E_{k,S}} + \frac{\lambda}{N} - \mu_k = 0 \tag{2.17}$$

$$\frac{\partial \Psi}{\partial E_{k,R}} = -c\sqrt{\frac{a}{8\pi\varepsilon_k}}\exp\left(-\frac{a\varepsilon_k}{2}\right)\frac{\partial \varepsilon_k}{\partial E_{k,R}} + \frac{\lambda}{N} - \eta_k = 0 \tag{2.18}$$

$$\frac{1}{N}\sum_{k=1}^{N}\left(E_{k,S} + E_{k,R}\right) - 2E = 0 \tag{2.19}$$

$$\mu_k E_{k,S} = 0 \tag{2.20}$$

$$\eta_k E_{k,R} = 0 \tag{2.21}$$

$$E_{k,R} \geq 0, \;\; E_{k,S} > 0 \tag{2.22}$$

$$\eta_k \geq 0, \;\; \mu_k \geq 0, \;\; \lambda \geq 0 \tag{2.23}$$

Optimum values of power loading coefficients $E_{k,S}$, $E_{k,R}$ can be then obtained by simultaneously solving (2.17)-(2.23). Eqs. (2.20) and (2.21) have the following four possible solutions:

$$\mu_k = 0, \;\; \eta_k = 0 \tag{2.24}$$

$$\mu_k = 0, \;\; E_{k,R} = 0 \tag{2.25}$$

$$\eta_k = 0, \;\; E_{k,S} = 0 \tag{2.26}$$

$$E_{k,S} = 0, \;\; E_{k,R} = 0 \tag{2.27}$$

The third and fourth solutions in (2.26) and (2.27) are not feasible and can be ignored under our assumption of fixed subcarrier rate. The second solution (2.25) means *no coop-*

eration for the k^{th} subcarrier and is adopted only for *unreliable* subcarriers (which will be elaborated later). On the other hand, solution (2.24) represents the cooperation case which is adopted for *reliable* subcarriers. Inserting $\mu_k = 0, \;\; \eta_k = 0$ in (2.17) and (2.18), we can readily find out $\partial\varepsilon_k/\partial E_{k,S} = \partial\varepsilon_k/\partial E_{k,R}$. Using this relation and after some mathematical mainpulations, we can express $E_{k,S}$ in terms of $E_{k,R}$ as

$$E_{k,S} = \frac{D_{k,R}}{D_{k,0}} \left(\frac{|D_{k,1}|^2 D_{k,R}}{|D_{k,2}|^2} + 1 \right) E_{k,R}^2 + \left(2D_{k,R} \frac{|D_{k,1}|^2}{|D_{k,2}|^2} + 1 \right) E_{k,R} + \frac{D_{k,0} |D_{k,1}|^2}{|D_{k,2}|^2} \quad (2.28)$$

then we can rewrite (2.14) in terms of $E_{k,R}$ as

$$\Psi = c \sum_{k=1}^{N} Q\left(\sqrt{a\varepsilon_k}\right) + \lambda \left(\frac{1}{N} \sum_{k=0}^{N} \left(\frac{D_{k,R}}{D_{k,0}} \gamma_k E_{k,R}^2 + 2\gamma_k E_{k,R} + \alpha_k \right) - 2E \right) \quad (2.29)$$

where ε_k is expressed in terms of $E_{k,R}$ as

$$\varepsilon_k = \frac{|D_{k,2}|^2}{D_{k,0}} \left(\gamma_k E_{k,R} + \alpha_k \right)^2 \quad (2.30)$$

Here, α_k and γ_k are defined as

$$\alpha_k = D_{k,0} |D_{k,1}|^2 / |D_{k,2}|^2 \quad (2.31)$$

$$\gamma_k = 1 + D_{k,R} |D_{k,1}|^2 / |D_{k,2}|^2 \quad (2.32)$$

Solving $\partial\Psi/\partial E_{k,R} = 0$ yields

$$f\left(E_{k,R}\right) = \exp\left(-a \frac{|D_{k,2}|^2}{2D_{k,0}} \left(\gamma_k E_{k,R} + \alpha_k \right)^2 \right) - \lambda \left(\frac{\sqrt{8\pi} \left(D_{k,R} E_{k,R} + D_{k,0} \right)}{cN \left| D_{k,2} \right| \sqrt{aD_{k,0}}} \right) = 0 \quad (2.33)$$

From (2.33), it can be found out that some relay subcarriers will have negative power values if the following condition given as

$$\exp\left(-a\frac{|D_{k,2}|^2}{2D_{k,0}}\alpha_k^2\right) < \lambda\left(\frac{\sqrt{8\pi D_{k,0}}}{cN\,|D_{k,2}|\,\sqrt{a}}\right) \tag{2.34}$$

is satisfied. These basically correspond to unreliable relay subchannels. Since negative power is physically meaningless, the power of such subcarriers should be forced to zero. This indicates that the optimum solution will yield the non-cooperative case for the unreliable subcarriers. Replacing $\mu_k = 0, \quad E_{k,R} = 0$ in (2.17) and (2.18) and imposing KKT conditions, we have

$$E_{k,S} = \frac{1}{a\,|D_{k,1}|^2}\mathrm{W}\left(\left(\frac{|D_{k,1}|^2\,caN}{2\sqrt{2\pi}\lambda}\right)^2\right) \tag{2.35}$$

where W in (2.35) is the Lambert function, i.e., the inverse function of $f(x) = x\exp(x)$ [68]. Based on the above derivation steps, we can summarize the proposed algorithm as in Algorithm 1.

As an example, we illustrate power distribution among subcarriers for given CSIs in Figure 2.3. The curves labelled by D_{SD}, D_{SR} and D_{RD} denote fading channel realizations. The curves labelled by E_S and E_R denote the power loading coefficients for source and relay assuming $N = 32$. It can be observed that OPL algorithm effectively equalizes bad sub-channels assigning more power onto them.

2.2.2 Optimal Bit Loading (OBL)

In this subsection, we aim to find OBL coefficients assuming equal power loading and fixed average transmission rate. Under these assumptions, we have $E_{k,S} = E_{k,R} = E \quad \forall k$ and

Algorithm 1 OPL Algorithm

1: Choose an initial interval for λ as $[\lambda_a, \lambda_b]$.

2: For each subcarrier, check if (2.33) is satisfied. If it is valid, set the subcarriers' power as

$$E_{k,R} = 0 \quad \text{and} \quad E_{k,S} = \frac{1}{a\left|D_{k,1}\right|^2} \mathrm{W}\left(\left(\frac{\left|D_{k,1}\right|^2 caN}{2\sqrt{2\pi\lambda}}\right)^2\right).$$

If (2.33) is not satisfied, compute $E_{k,R}$ and $E_{k,S}$ by solving the following equations, respectively,

$$\exp\left(-a\frac{\left|D_{k,2}\right|^2}{2D_{k,0}}\left(\gamma_k E_{k,R} + \alpha_k\right)^2\right) - \lambda\left(\frac{\sqrt{8\pi}}{cN\left|D_{k,2}\right|\sqrt{aD_{k,0}}}\right)\left(D_{k,R}E_{k,R} + D_{k,0}\right) = 0,$$

$$E_{k,S} = \frac{D_{k,R}}{D_{k,0}}\left(\frac{\left|D_{k,1}\right|^2 D_{k,R}}{\left|D_{k,2}\right|^2} + 1\right)E_{k,R}^2 + \left(2D_{k,R}\frac{\left|D_{k,1}\right|^2}{\left|D_{k,2}\right|^2} + 1\right)E_{k,R} + \frac{D_{k,0}\left|D_{k,1}\right|^2}{\left|D_{k,2}\right|^2}.$$

3: Compute the power constraint function given as

$$C_f\left(\mathbf{E}_S, \mathbf{E}_R\right) = \frac{1}{N}\sum_{k=1}^{N}\left(E_{k,S} + E_{k,R}\right) - 2E$$

4: Update the $[\lambda_a, \lambda_b]$ interval and repeat from step 1 until convergence, i.e., the C_f reaches zero.

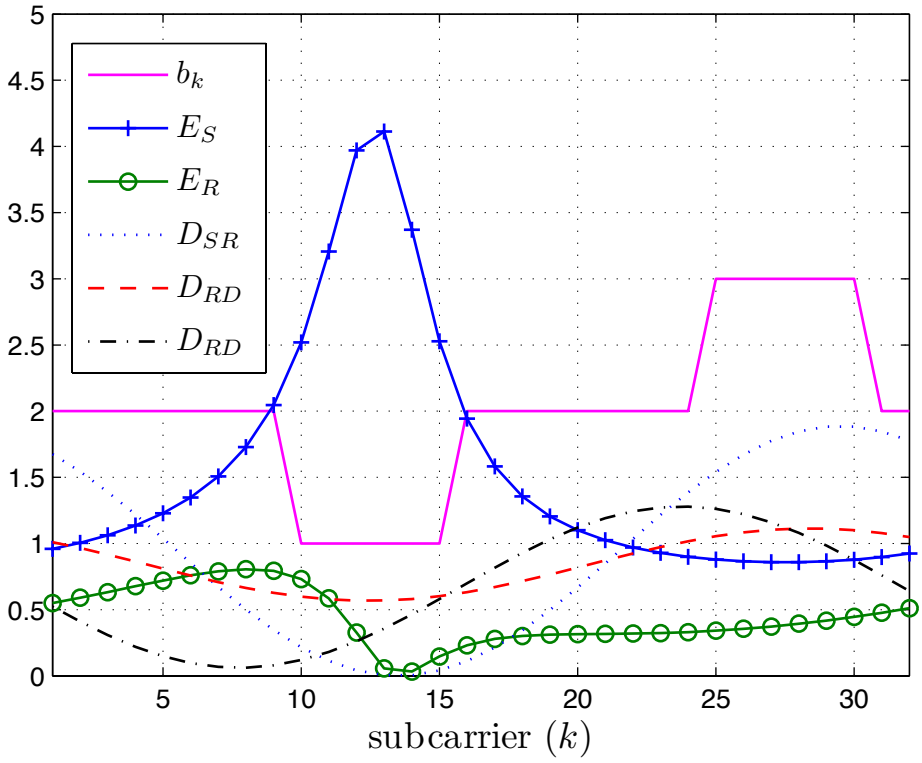

Figure 2.3: Power and loading coefficients for a given channel realization.

$\sum_{k=1}^{N} b_k = NB$ where $b_k = \log_2 M_k$ denotes the bit value assigned to the k^{th} subcarrier bit loading coefficient. Therefore, the optimization problem is given by

$$\min_{\mathbf{b}} \sum_{k=1}^{N} c_k Q\left(\sqrt{a_k \varepsilon_k}\right) \tag{2.36}$$

subject to the following constraints

$$\sum_{k=1}^{N} b_k = NB, \quad 0 \leq b_k \leq NB, \quad E_{k,S} = E_{k,R} = E \quad \forall k \tag{2.37}$$

The optimization problem of finding $\mathbf{b} = [b_1, b_2, ...b_N]$ is classified as an integer op-

timization problem of separable objective functions. The optimal solution can be found using the dynamic programming approach [59] where the objective function in (2.36) is simplified by dividing it into simpler sub-problems which are then solved recursively. In our case, we define the recursive functions associated with sub-problems as

$$f^{(k)}(p) = \min_{\mathbf{b}_j} \sum_{j=1}^{k} f_j(b_j) \tag{2.38}$$

subject to $\sum_{j=1}^{k} b_j = p$. Here, $f_j(b_j) = c_j Q\left(\sqrt{a_j \varepsilon_j}\right)$, b_j is a non-negative integer $j = 1, 2, \cdots, k$, $k = 1, 2, \cdots, N$ and $p = 0, 1, \cdots, NB$. Starting with the initial condition $f^{(1)}(p) = f_1(p), p = 0, 1, \cdots, NB$ we recursively need to compute $f^{(k)}(p)$ which are functions of c_p and a_p, c.f. (2.10) and (2.11). At $k = N$ and $p = NB$, we obtain $f^{(N)}(NB)$ which yields the OBL coefficients. The proposed algorithm can be summarized as in Algorithm 2. As an example, we illustrate bit loading values for given CSIs in Figure 2.3. As expected, OBL algorithm loads more bits to reliable channels.

Algorithm 2 OBL Algorithm

1: Initiate $k = 1$. Calculate $f^{(1)}(p)$ as $f^{(1)}(p) = f_1(p) = c_p Q\left(\sqrt{a_p \varepsilon_1}\right)$

2: Define $b_k(p) = p$

3: $k = k + 1$

4: For $p = 0, 1, \cdots, NB$ and $l = 0, 1, \cdots, p$, compute $f^{(k-1)}(p-l) + f_k(l)$. Let $l_{\min}$ denote the value of l which minimizes $f^{(k-1)}(p-l) + f_k(l)$. Set $f^{(k)}(p) = f^{(k-1)}(p - l_{\min}) + f_k(l_{\min})$ and $b_k(p) = l_{\min}$.

5: If $k < N - 1$ go to step 3, otherwise continue

6: For $k = N$ and $p = NB$, compute $f^{(N-1)}(NB - l) + f_N(l)$. Let $b_N(NB)$ denote the value of l which minimizes $f^{(N-1)}(NB - l) + f_N(l)$.

7: Compute OBL coefficients $\mathbf{b}$ as follows,
$\mathbf{b} = [b_{opt}(1), b_{opt}(2), ...b_{opt}(N)]$
$b_{opt}(N) = b_q(NB)$ where $q = N$ and

a. $q = q - 1$

b. $p_{opt} = N - \sum_{j=q-1}^{N} b_{opt}(j)$

c. $b_{opt}(q) = b_q(p_{opt})$

d. If $q > 1$ go to step 7.a otherwise stop.

2.2.3 Optimal Bit and Power Loading (OBPL)

In the previous two problems, we have fixed either subcarrier power or subcarrier rate and computed the optimal value for the other parameter. In this section, we present a joint OBPL scheme which simultaneously optimizes subcarrier rate and power to minimize BER. This problem can be expressed as

$$\min_{\mathbf{E}_S,\, \mathbf{E}_R,\, \mathbf{b}} \; \gamma\left(\mathbf{E}_S,\; \mathbf{E}_R,\; \mathbf{b}\right) = \sum_{k=1}^{N} c_k Q\left(\sqrt{a_k \varepsilon_k}\right) \tag{2.39}$$

subject to the following constraints

$$\begin{aligned} &\frac{1}{N}\sum_{k=1}^{N}\left(E_{k,S} + E_{k,R}\right) = 2E, \quad E_{k,S} > 0, \quad E_{k,R} \geq 0, \\ &\sum_{k=1}^{N} b_k = B, \quad 0 \leq b_k \leq NB \end{aligned} \tag{2.40}$$

The current problem is a mixed integer nonlinear convex optimization problem [57]. Here, we use GBD method [57] which converts the joint optimization problem into upper and lower bound optimization problems. The upper bound problem is a nonlinear optimization problem for the computation of the power loading coefficients. On the other hand, the lower bound problem is an integer optimization problem for the computation of the bit loading coefficients. The joint optimal solution can be obtained by iteratively solving the two problems each of which uses the others output until convergence. The proposed OPBL algorithm based on GBD method can be summarized as in Algorithm 3.

Algorithm 3 OBPL Algorithm

1: For $q = 1$ initiate $\mathbf{b} = \mathbf{b}^{(q)}$ and set $\alpha^0 = -\infty, LB^0 = -\infty$ and $UB^0 = \infty$.

2: For a given bit loading coefficients vector $\mathbf{b}^{(q)}$, find OPL coefficients $\mathbf{E}_S^{(q)}$, $\mathbf{E}_R^{(q)}$ and the Lagrange multiplier $\lambda^{(q)}$ by solving the upper bound optimization problem using the OPL algorithm (introduced in Section III-a).

3: Set $\mathrm{UB}^{(q)} = \min\left\{\mathrm{UB}^{(q-1)}, \gamma(\mathbf{E}_S^{(q)},\ \mathbf{E}_R^{(q)},\ \mathbf{b}^{(q)})\right\}$.

4: If $\mathrm{UB}^{(q)} = \gamma(\mathbf{E}_S^{(q)},\ \mathbf{E}_R^{(q)},\ \mathbf{b}^{(q)})$, set $(\mathbf{E}_{S,opt},\ \mathbf{E}_{R,opt}) = (\mathbf{E}_S^{(q)},\ \mathbf{E}_R^{(q)})$.

5: Define Lagrangian function $V(.)$ as

$$V(\mathbf{E}_S,\ \mathbf{E}_R,\ \mathbf{b}, \lambda) = \gamma(\mathbf{E}_S,\ \mathbf{E}_R,\ \mathbf{b}) + \lambda\left(\frac{1}{N}\sum_{k=1}^{N}(E_{k,S} + E_{k,R}) - 2E\right)$$

Using the OPL coefficients $(\mathbf{E}_{S,opt},\ \mathbf{E}_{R,opt})$ obtained in step 4, update the bit loading coefficients b through solving the lower bound integer optimization problem

$$\min_{\mathbf{b}^{(q+1)}} \quad V\left(\mathbf{E}_S^{(q)},\ \mathbf{E}_R^{(q)},\ \mathbf{b}^{(q)},\ \lambda^{(q)}\right) + \nabla_{\mathbf{M}}^T V\left(\mathbf{E}_S^{(q)},\ \mathbf{E}_R^{(q)},\ \mathbf{b}^{(q)},\ \lambda^{(q)}\right)\left(2^{\mathbf{b}} - 2^{\mathbf{b}^{(q)}}\right)$$

subject to $\sum_{k=1}^{N} b_k^{(q)} = NB$ and $\alpha^{(q)} \geq \alpha^{(q-1)}$, where

$$\alpha^{(q)} = V\left(\mathbf{E}_S^{(q)},\ \mathbf{E}_R^{(q)},\ \mathbf{b}^{(q)},\ \lambda^{(q)}\right) + \nabla_{\mathbf{M}}^T V\left(\mathbf{E}_S^{(q)},\ \mathbf{E}_R^{(q)},\ \mathbf{b}^{(q)},\ \lambda^{(q)}\right)\left(2^{\mathbf{b}^{(q+1)}} - 2^{\mathbf{b}^{(q)}}\right).$$

(see **Algorithm 4** for performing step (5))

6: Set $LB^{(q)} = \alpha^{(q)}$

7: If $LB^{(q)} \geq UB^{(q)}$, stop and the optimal solution will be given as $(\mathbf{E}_{S,opt},\ \mathbf{E}_{R,opt}, \mathbf{b}_{opt}) = \left(\mathbf{E}_S^{(q)},\ \mathbf{E}_R^{(q)}, \mathbf{b}^{(q)}\right)$. Otherwise, set $q = q + 1$ and go to step 2.

Algorithm 4 OBPL Sub-algorithm

Let $y_i(p) = \frac{\partial}{\partial M_i} V\left(E_{i,S}^{(q)},\ E_{i,R}^{(q)}, b_i^{(q)},\ \lambda^{(q)}\right)\left(2^p - 2^{b_i^{(q)}}\right)$

1: Initiate $k = 1$. For $p = 0, 1, \cdots, NB$, compute $y^{(1)}(p) = V\left(E_{1,S}^{(q)},\ E_{1,R}^{(q)}, b_1^{(q)},\ \lambda^{(q)}\right) + y_1(p)$.

2: Define $b_k(p) = p$

3: Set $k = k + 1$

4: For $p = 0, 1, \cdots, NB$ and $l = 0, 1, \cdots, p$, compute $y^{(k-1)}(p-l) + y_k(l)$. Let $l_{\min}$ denote the value of l which minimizes $y^{(k-1)}(p-l) + y_k(l)$. Set $b_k(p) = l_{\min}$ and $y^{(k)}(p) = y^{(k-1)}(p - l_{\min}) + y_k(l_{\min})$.

5: If $k < N - 1$ go to step 3, otherwise continue

6: For $k = N$ and $p = NB$, compute $y^{(N-1)}(NB - l) + y_N(l)$. Let $b_N(NB)$ denote the value of l which minimizes $y^{(N-1)}(NB - l) + y_N(l)$ subject to $\alpha^{(q)} \geq \alpha^{(q-1)}$.

7: Compute OBL coefficients $\mathbf{b}$ as follows,
$\mathbf{b} = [b_{opt}(1), b_{opt}(2), ...b_{opt}(N)]$,
$b_{opt}(N) = b_q(NB)$ where $q = N$ and

a. $q = q - 1$

b. $p_{opt} = N - \sum_{j=q-1}^{N} b_{opt}(j)$

c. $b_{opt}(q) = b_q(p_{opt})$

d. If $q > 1$ go to step 7.a otherwise stop.

2.3 Simulation Results

In this section, we investigate the BER performance of proposed OPL, OBL, and OBPL algorithms through Monte Carlo simulations. We assume $\alpha = 2$, $\theta = \pi$ and $N = 32$. The channel lengths for the three links are assumed to be equal to 2, i.e., $L_{SR} = L_{RD} = L_{SD} = L = 1$, SNR is defined to be E/N_0, where E is the average subcarrier power.

Example 1 (Performance of OBPL)

In this simulation example, we study the performance of the OBPL algorithm with perfect CSI assuming an average transmission rate of 2 and 4 bits/subcarrier, respectively, in Figures 2.4 and 2.5. We consider $G_{SR}/G_{RD} = 30$ dB, -30 dB, and 0 dB. These respectively correspond to cases where the relay is close to the source, close to the destination, and at the midpoint between the source and the destination. The performance of non-adaptive scheme with equal bit and power loading (EBPL) is included as a benchmark.

As observed in Figures 2.4 and 2.5, EBPL scheme achieves only a diversity of two. This diversity gain results from the spatial diversity for the single-relay scenario under consideration. Therefore, EBPL system is not able to extract the underlying multipath diversity. On the other hand, the proposed OBPL scheme is able to extract a diversity order of $2(L+1) = 4$ and significantly outperforms EBPL scheme. For example, in Figure 2.4, at BER=10^{-3}, OBPL outperforms EBPL by 3.5 dB assuming $G_{SR}/G_{RD} = 0$ dB. This climbs up to 5.8 dB for $G_{SR}/G_{RD} = -30$ dB. It is also interesting to note that each scheme attains its best performance at different locations. EBPL attains its best performance when the relay is at the midpoint (i.e.,$G_{SR}/G_{RD} = 0$ dB). On the other hand, the performance of OBPL gets better when the relay is placed close to the destination

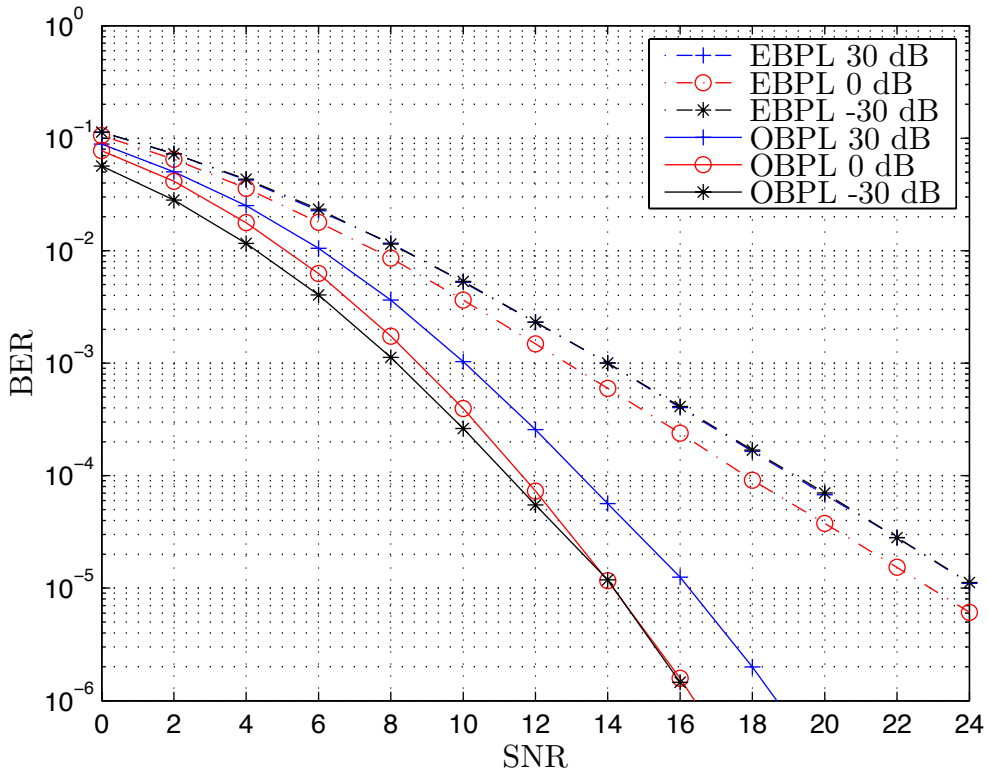

Figure 2.4: Performance comparison of EBPL and OBPL schemes for different relay locations with average transmission of 2bits/subcarrier.

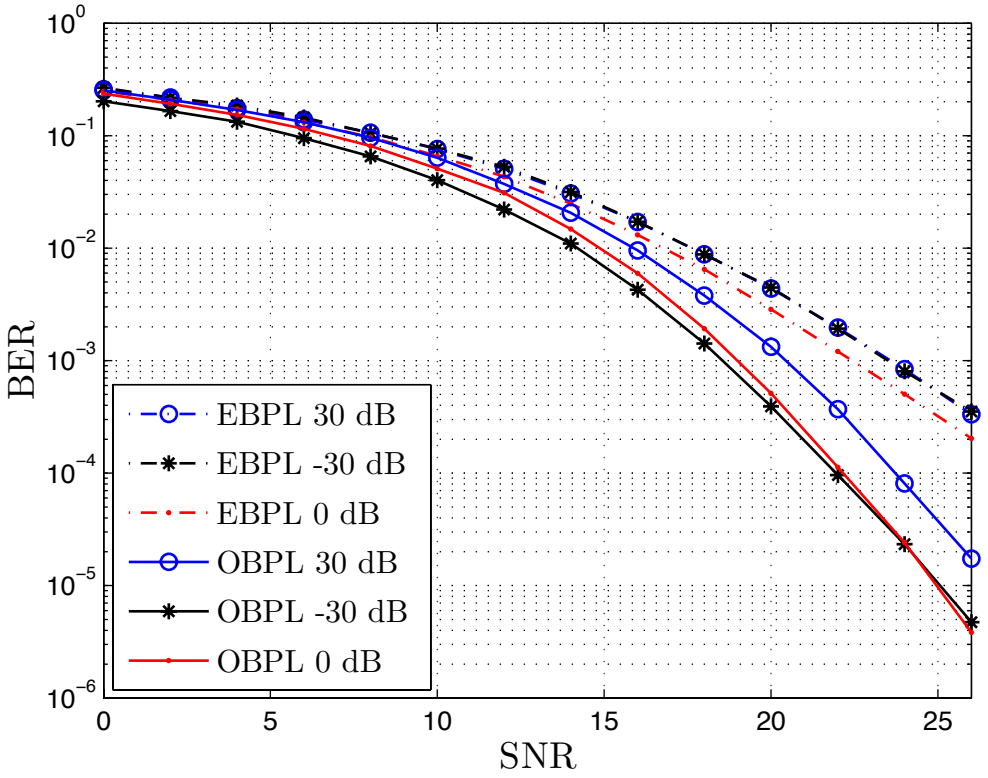

Figure 2.5: Performance comparison of EBPL and OBPL schemes for different relay locations with average transmission of 4bits/subcarrier.

(i.e.,$G_{SR}/G_{RD} = -30$ dB). Similar observations hold for Figure 2.5 where an average transmission rate of 4 bits/subcarrier is assumed, where at BER=10^{-3}, OBPL outperforms EBPL by 3 dB assuming $G_{SR}/G_{RD} = 0$ dB. Also the improvement reaches its maximum at $G_{SR}/G_{RD} = -30$ dB where 5 dB is achieved. From these results, we conclude that dealing with higher rates reduces performance improvement.

Example 2 (OBPL versus other schemes)

In this example, we first compare the performance of OBPL to OPL and OBL schemes. Through this comparison, we are particularly interested in finding out whether bit or power

loading is more rewarding in performance optimization. In our simulations, we assume perfect CSI, an average transmission rate of 2 bits/subcarrier and $G_{SR}/G_{RD} = -30$ dB. From Figure 2.6, we observe that, at BER=10^{-4}, performance gap between OBPL and OBL is 3.6 dB. On the other hand, performance gap between OBPL and OPL reduces to 1.1 dB. Therefore, it can be concluded that power loading is more dominant (important) in performance optimization.

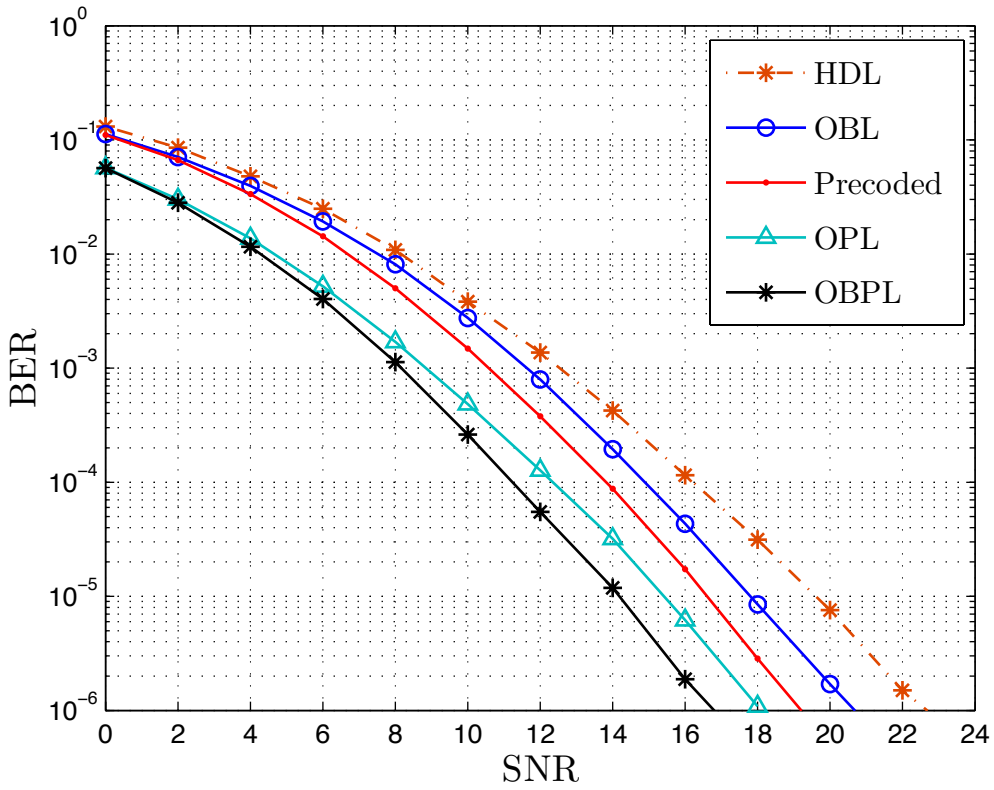

Figure 2.6: Performance comparison of OBPL, OPL, OBL algorithms and competing schemes.

For comparison with existing systems in the literature, we also include the performance of a precoded cooperative OFDM [16] in Figure 2.6 . It is observed that the proposed

schemes and the precoded system are both able to extract the full diversity and achieve the same diversity order. However, OBPL and OPL systems are able to outperform the precoded system by 2.6 dB and 1.5 dB, respectively, at BER=10^{-4}. On the other hand, OBL remains inferior to the precoded system by $\sim$1 dB. It should be further emphasized that, besides performance improvements, OBPL and OPL have advantage over the precoded systems in terms of receiver complexity. The receiver complexity of proposed algorithms is independent of the channel length while the detector complexity in precoded systems is exponentially proportional to the channel length [16].

Another comparison in Figure 2.6 is with the power loading scheme proposed in [55] by Hajiaghayi et.al. which also aims to optimize the BER performance (named as HDL scheme in our figure). Our results illustrate the superiority of proposed algorithms over HDL scheme. Specifically at BER=10^{-3} , we observe that OBL, OPL and OBPL outperform HDL by 0.8 dB, 3.2 dB and 4.3 dB respectively. It should be noted that HDL scheme is derived under the high SNR assumption and considers identical subcarrier power at source and relay nodes. Our schemes avoid such restricting assumptions and are therefore able to provide a better performance.

Example 3 (Effect of Relay Location)

In this example, we study the effect of relay location on the performance of EBPL, OBL, OPL, and OBPL schemes. Under the assumption of average transmission rate of 2 bits/subcarrier and a target fixed BER of 10^{-3}, we plot the required SNR versus the relay location. Figure 2.7 illustrates that the best location (i.e. requires the lowest SNR to achieve the BER= 10^{-3}) for OBPL and OPL is near to destination. For OBL and EBPL, mid-locations between source and destination become more favourable. For near-to-destination and near-to-source locations, they exhibit identical channel statistical properties [69] and

therefore yield symmetric performance around 0 dB location.

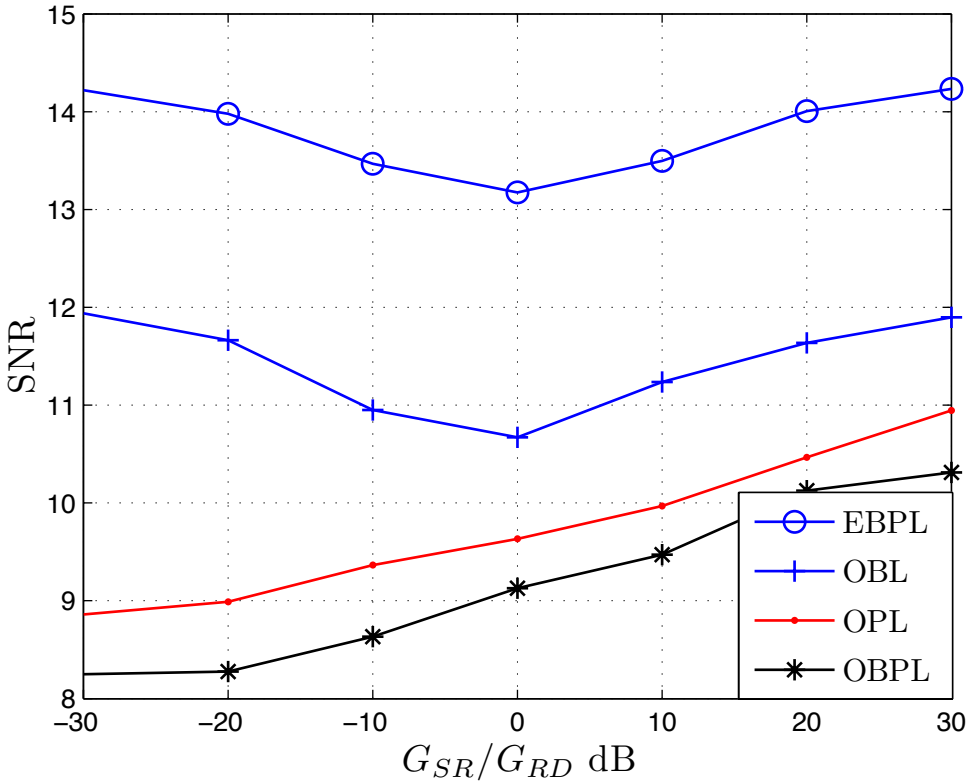

Figure 2.7: Effect of relay location on different adaptive algorithms.

Example 4 (Effect of Channel Estimation)

In this example, we study the effect of channel estimation on the proposed schemes. The adaptive algorithms assume that perfect CSI is available at source, relay and destination nodes. In practice, CSI information needs to be estimated. CSI for the direct link (i.e., S→D) and relaying link (i.e., S→R and R→D) is also used at the destination for detection process. For the estimation of relaying path, we adopt the so-called disintegrated channel estimation (D-CE) approach [69] in which S→R and R→D channels are estimated separately. In this approach, the relay node is equipped with a channel estimator and

feed-forwards the S→R channel estimate to the destination terminal as well as feedbacks it to the source [69]. Channel estimates for S→D and R→D links are obtained at the destination which sends them to the source and the relay via a feedback channel.

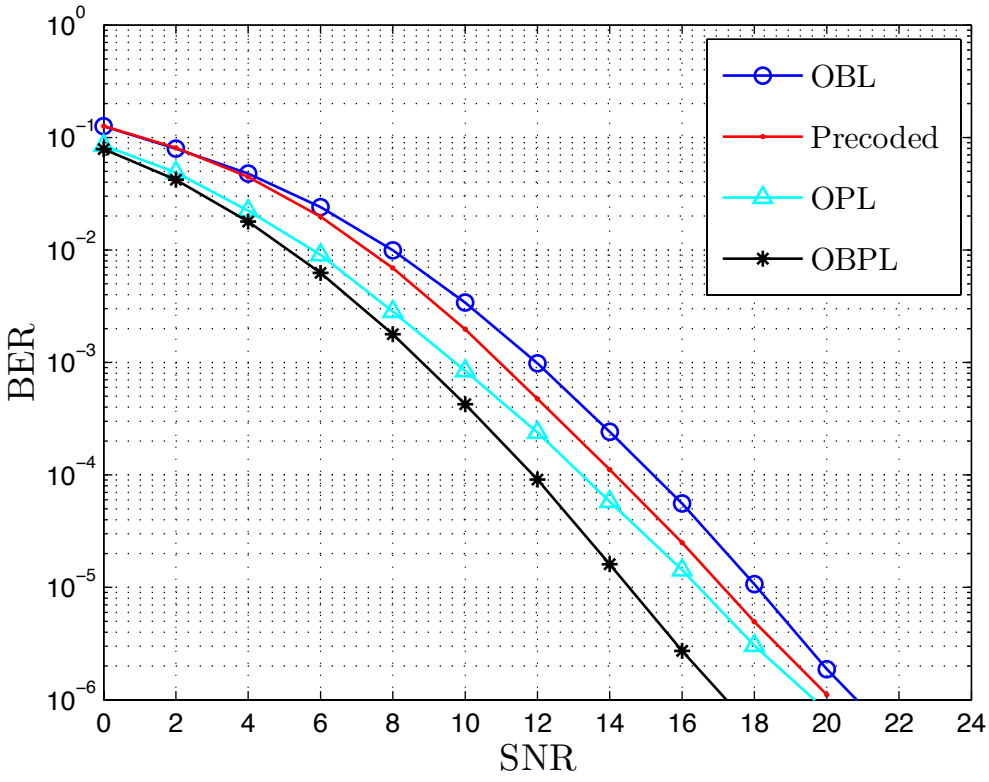

Figure 2.8: Performance of OBPL, OPL, OBL algorithms with imperfect channel estimation.

In Figure 2.8, we assume the employment of linear minimum mean squared error estimator (LMMSE) [70] and perfect feedback of the estimates. We consider the case where the relay is near to the destination, i.e., $G_{SR}/G_{RD} = -30$ dB and an average transmission rate of 2bits/subcarrier. Note that the precoded system which is used as a diversity benchmark does not need CSI at the transmitter side. Figure 2.8 illustrates that, at BER=10^{-4}, OBPL and OPL schemes with imperfect channel estimation at the transmitter side are

still able to outperform the precoded system by 2.3 dB and 0.9 dB.

In Figure 2.9, we study the effect of finite-rate feedback which is required to transfer the quantized CSIs in the practical implementation of our proposed schemes. Figure 2.9 shows that we need as small as 5 bits/subcarrier to achieve a similar performance to the ideal system with perfect feedback. When 6 bits/subcarrier is used, it gives an identical performance to that of perfect feedback. The corresponding performance curve is not included in the figure for the sake of presentation.

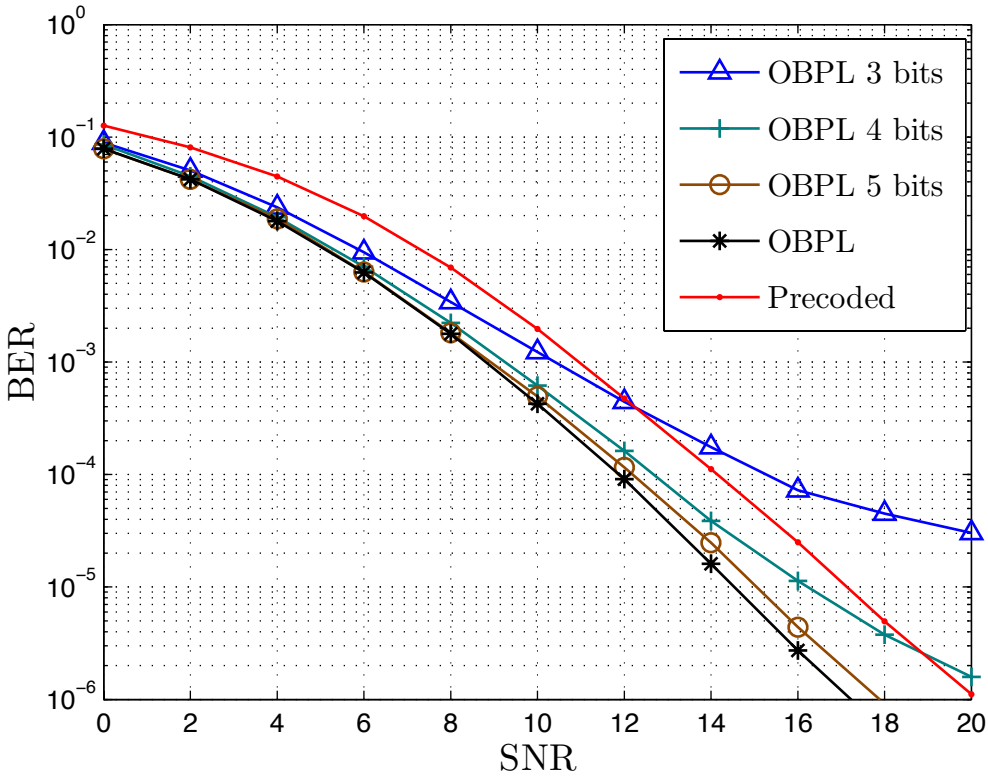

Figure 2.9: Effect of finite-rate feedback on the performance of OPBL algorithm.

2.4 Conclusion

In this chapter, we have investigated adaptive bit and/or power loading for a cooperative OFDM system with AF relaying. We have adopted BER as the objective function and formulated three optimization problems leading to different adaptive algorithms. The first algorithm, named as OPL, computes the optimal source and relay power loading coefficients under total power constraint and fixed subcarriers rate. The second algorithm, named as OBL, computes the optimal bit loading coefficients under fixed average transmission rate and equal power loading. The third one, named as OBPL, computes the joint optimal power and bit loading coefficients. Through Monte-Carlo simulations, we have demonstrated the superiority of our schemes over conventional non-adaptive cooperative OFDM systems. For example, assuming relay is located close to the destination, OBPL outperforms non-adaptive system (i.e., equal bit and power loading) by 5.8 dB at a target BER=10^{-3}. OBPL and OPL systems are also able to outperform the precoded cooperative OFDM systems while OBL turns out to be inferior. This also indicates that power loading is more dominant in the performance optimization where continuous optimization gives more degrees of freedom than the discrete optimization deployed in bit loading. We have further provided simulation results to quantify the effect of relay location, imperfect channel estimation and finite-rate quantized feedback on the BER performance of proposed schemes. Considering the result of power loading importance over bit loading for BER minimization, next chapter extends the problem for multi-relay network and focus only on the power loading problem for DF network.

Chapter 3

Power Loading for DF Cooperative Network

In this chapter, we propose an adaptive power loading algorithm for an OFDM-based multi-relay DF network with relay selection. The proposed scheme is based on selecting the "best" relays according to different strategies and distributing the power adaptively among the subcarriers of source and selected relay(s) as to minimize BER. Our Monte Carlo simulation results demonstrate supreme performance gains through power loading with respect to conventional equal power loading schemes. The effects of imperfect channel estimation and relay location on the BER performance are further discussed.

The rest of the chapter is organized as follows: In Section 3.1, the system model under consideration is described. In Section 3.2, first optimization problem to minimize BER is formulated, then corresponding power loading algorithm is presented. The simulated performance of proposed adaptive schemes and the effect of channel estimation on their performances are presented in Section 3.3. Finally, Section 3.4 concludes the chapter.

3.1 System Model

3.1.1 System Description and Relay Selection Methods

We consider a cooperative OFDM system with L relays. Source, relay, and destination nodes are equipped with single transmit/receive antennas and operate in half-duplex mode. The nodes are assumed to be located in a two-dimensional plane where d_{SD}, d_{SR_i} and d_{R_iD} denote the distances of source-to-destination (S $\rightarrow$ D), source-to-i^{th} relay (S $\rightarrow$ R$_i$) and i^{th} relay-to-destination (R$_i$ $\rightarrow$ D) links, respectively (see Figure 3.1). In Figure 3.1, θ_i is the angle between lines representing S $\rightarrow$ R$_i$ and i^{th} and R$_i$ $\rightarrow$ D links.

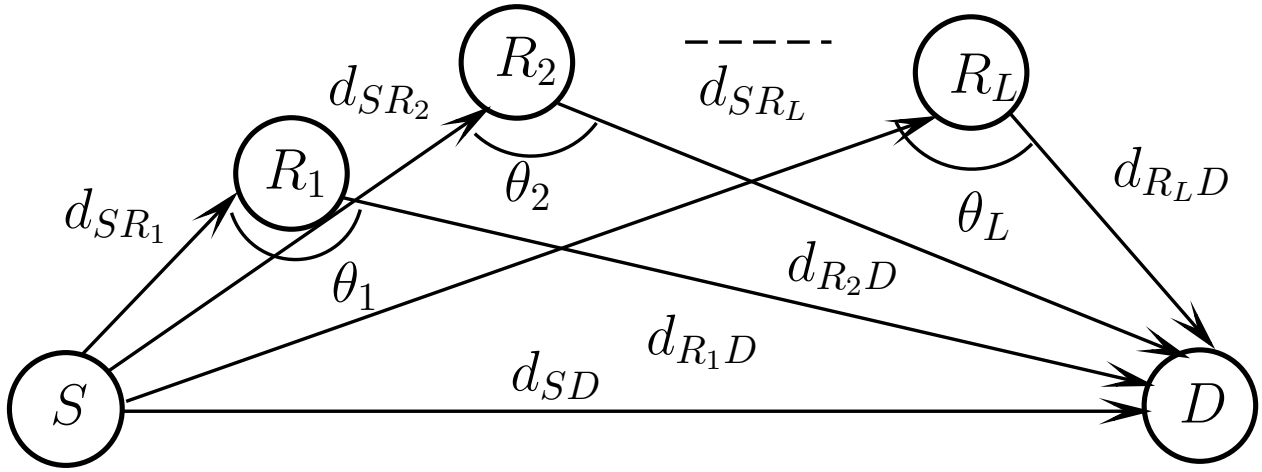

Figure 3.1: Multi-relay cooperative network.

To explicitly take into account the effect of relays location, we consider both long-term path loss and short-term frequency-selective Rayleigh fading. The path loss is inversely proportional to α where d is the distance between nodes and α is the path loss exponent. By normalizing the path loss terms with respect to the direct (S $\rightarrow$ D) link, the so-called geometrical gains [7] can be defined as $G_{SR_i} = (d_{SD}/d_{SR_i})^{\alpha}$ and $G_{R_iD} = (d_{SD}/d_{R_iD})^{\alpha}$, $i =$

$1, 2...L$. These are related through the cosines law by $G_{SR_i}^{2/\alpha} + G_{R_iD}^{2/\alpha} - 2G_{SR_i}^{1/\alpha} G_{R_iD}^{1/\alpha} \cos\theta_i = G_{SR_i}^{2/\alpha} G_{R_iD}^{2/\alpha}$. The frequency-selective quasi-static fading channels under consideration are modeled as FIR (finite impulse response) filters with orders L_{SD}, L_{SR_i} and L_{R_iD}. They are represented by $\mathbf{h}_{SD} = [h_{SD}(0), \ldots, h_{SD}(L_{SD})]^T$, $\mathbf{h}_{SR_i} = [h_{SR_i}(0), \ldots, h_{SR_i}(L_{SR_i})]^T$ and $\mathbf{h}_{R_iD} = [h_{R_iD}(0), \ldots, h_{R_iD}(L_{R_iD})]^T$ for S $\rightarrow$ D, S $\rightarrow$ R_i, and R_i $\rightarrow$ D links, respectively. The entries of $\mathbf{h}_{SD}$, $\mathbf{h}_{SR_i}$ and $\mathbf{h}_{R_iD}$ are assumed to be zero-mean complex Gaussian with their variances being equal to $1/(L_{SD}+1)$, $1/(L_{SR_i}+1)$ and $1/(L_{R_iD}+1)$, respectively. The frequency-domain expression for the k^{th} subcarrier is found through the Fourier transform and given by $H(k) = \sum_{l=1}^{N-1} h(l) \exp(-j2\pi lk/N)$ where the subscripts for underlying links are dropped for convenience.

Here, we assume RD cooperation protocol where the source and the relay nodes transmit in orthogonal transmission phases. In the first transmission phase (i.e., broadcasting), a bit stream is fed into serial-to-parallel converter which maps them onto modulation symbols chosen from either M-ary PSK or M-ary square QAM constellations. Each k subcarrier symbol modulates b bits where $M = 2^b$. Before passing through IFFT, the power of each subcarrier symbol is adjusted based on the employed power loading algorithm (which will be later introduced). To prevent inter-block-interference, a CP is inserted between OFDM symbol blocks with $L_{CP} \geq \max(L_{SR_i}, L_{R_iD}, L_{SD})$ as shown in Figure 3.2(a). All relays and the destination node receive the transmitted OFDM symbol. Then according to the deployed selection method, the "best" relay will be selected for all *or* each subcarrier(s). We consider two relay selection methods which are modified versions of [71]:

Relay Selection Method 1 (RSM1) - "Best" relay selection for each subcarrier - : In this selection method, the "best" relay (in the sense of SNR maximization) is

selected for each subcarrier. Therefore, selection criteria is given by

$$R_{sel}(k) = \arg\max_{R_i} \left\{ \min \left(\gamma_{SR_i}(k), \gamma_{R_iD}(k) \right) \right\}, \quad k = 1, 2, \cdots, N \tag{3.1}$$

where $\gamma_{SR_i}(k)$ and $\gamma_{R_iD}(k)$ are the instantaneous SNR of S $\rightarrow$ R$_i$ and R$_i$ $\rightarrow$ D links, respectively. Through this method although all relays L relays are busy, they can save some power by switching off unused subcarriers.

Relay Selection Method 2 (RSM2) -"Average best" relay selection- : In this alternative selection method, only a single relay is selected based on the maximization of the sum of subchannels SNR. Each subchannel SNR is chosen to be the minimum SNR between S $\rightarrow$ R$_i$ and R$_i$ $\rightarrow$ D links.

$$R_{sel} = \arg\max_{R_i} \left\{ \sum_{k=1}^{N} \left(\min \left(\gamma_{SR_i}(k), \gamma_{R_iD}(k) \right) \right) \right\} \tag{3.2}$$

In this method, one relay will participate in the relaying phase while others will be switched off. These relays will be therefore available to engage in any possible communication during this phase. Detection is performed at selected relay subcarriers after removing CP and converting the OFDM symbol into parallel subcarrier symbols through FFT. Regenerated subcarrier symbols are fed to IFFT and CP is added as depicted in Figure 3.2(b). In the relaying phase, the relay(s) forward the resulting signal to the destination while the source node remains silent. At the destination, both OFDM symbols received during the broadcasting and relaying phases are fed to ML detector after removing CP and passing through FFT as illustrated in Figure 3.2(c).

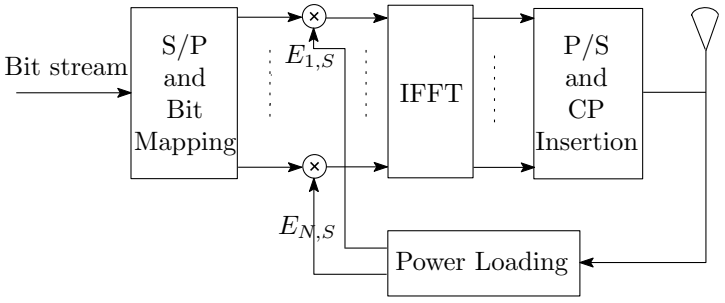

(a) Source

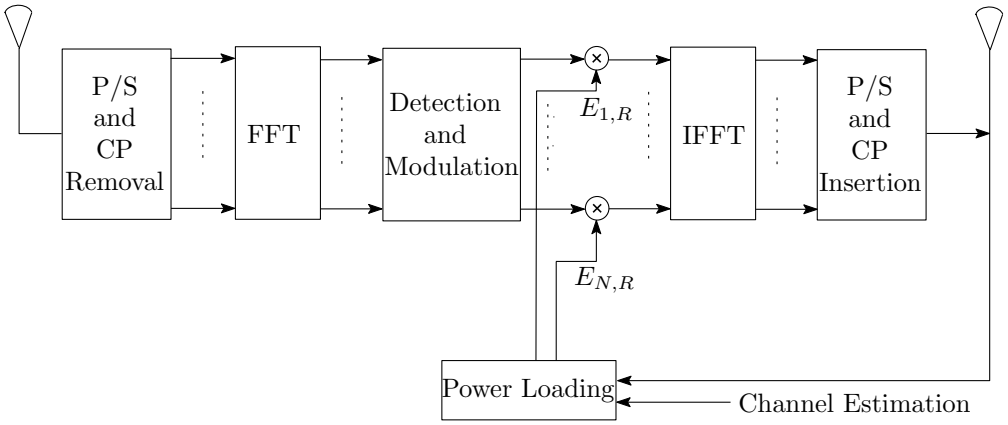

(b) Relay

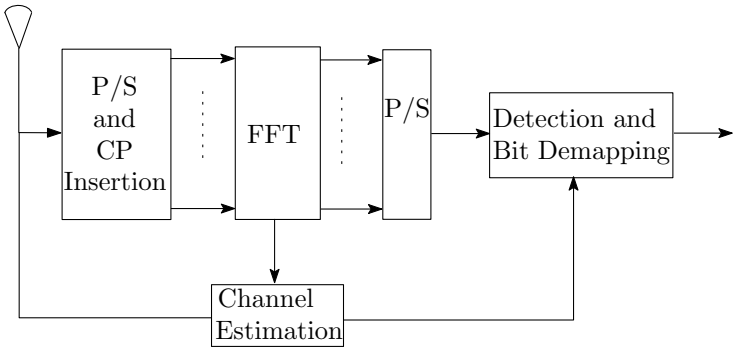

(c) Destination

Figure 3.2: Block diagrams of source, relay, and destination nodes.

3.1.2 System Equations

In the broadcasting phase, the received signal on the k^{th} subcarrier at the destination node (after FFT and CP removal) is given by

$$r_{D_1}(k) = \sqrt{E_{k,S}} D_{SD}(k,k)\, x(k) + v_{D_1}(k), \quad k = 1, 2, ...N \tag{3.3}$$

where $E_{k,S}$ is the source nodes k^{th} subcarrier power and $v_{D_1}(k)$ is the additive AWGN noise with variance N_0. Here, $D_{SD}(k,k)$ denotes the k^{th} diagonal element in the diagonal channel matrix $\mathbf{D}_{SD}$ which is defined as $\mathbf{D}_{SD} = diag(H_{SD}(0),\ H_{SD}(1), \cdots H_{SD}(N-1))$. After FFT and CP removal, the k^{th} subcarrier of i^{th} relay node is given by

$$r_{R_i}(k) = \sqrt{E_{k,S}}\sqrt{G_{SR_i}} D_{SR_i}(k,k)\, x(k) + v_{R_i}(k) \tag{3.4}$$

where $v_{R_i}(k)$ is the additive AWGN noise with variance N_0 and $D_{SR_i}(k,k)$ is the diagonal element of matrix $\mathbf{D}_{SR_i}$ defined as $\mathbf{D}_{SR_i} = diag(H_{SR_i}(0),\ H_{SR_i}(1), \cdots H_{SR_i}(N-1))$. For the employed DF relaying method, the signal to be transmitted is decided through the ML decision metric

$$\hat{x}_{R_i}(k) = \min_{x} \left| r_{R_i}(k) - \sqrt{E_{k,S}}\sqrt{G_{SR_i}} D_{SR_i}(k,k)\, x(k) \right|^2. \tag{3.5}$$

Here, the i^{th} relay will not transmit the signal if the subchannel is unreliable for transmission which can be determined through the proposed adaptive algorithm.

In the relaying phase, the received k^{th} subcarrier signal at the destination (after FFT

and CP removal) is given by

$$r_{D_2}(k) = \sqrt{E_{k,R_i}}\sqrt{G_{R_iD}}D_{R_iD}(k,k)\,\hat{x}_{R_i}(k) + v_{D_2}(k), \quad k = 1, 2, ...N \tag{3.6}$$

where $v_{D_2}(k)$ is additive AWGN noise with variance N_0 and $D_{R_iD}(k,k)$ is the diagonal element of matrix $\mathbf{D}_{R_iD}$ defined as $\mathbf{D}_{R_iD} = diag(H_{R_iD}(0),\ H_{R_iD}(1), \cdots H_{R_iD}(N-1))$. Based on (3.3) and (3.5), ML detection is performed at the destination

$$\begin{aligned}\hat{x}(k) = \arg\min_{x} \Bigg\{ &\left| r_{D_1}(k) - \sqrt{E_{k,S}}D_{SD}(k,k)\,x(k) \right|^2 \\ &+ \left| r_{D_2}(k) - \sqrt{E_{k,R_i}}\sqrt{G_{R_iD}}D_{R_iD}(k,k)\,x(k) \right|^2 \Bigg\}\end{aligned} \tag{3.7}$$

3.2 Power Loading Scheme

In this section, we propose a power loading scheme for a multi-relay OFDM network. The power loading coefficients are computed to minimize the BER for the received subcarriers signals under the assumption of the ability of relays in perfectly detecting errors, i.e., genie relays. This simplifies the ensuing BER analysis and provides a lower bound on the performance of the actual system. In practice, the relay can decide that an incorrect decision has been made through cyclic redundancy check (CRC) deployment [4]. The probability of error for the k^{th} subcarrier assuming that it belongs to ith relay which is allowed for transmission, $i \in \{1, 2, ..., L\}$, can be expressed as [1]

$$P_{e_i}(k) = (1 - P_{e,SR_i}(k))\,P_{e,COOP_i}(k) + P_{e,SR_i}(k)P_{e,SD}(k) \tag{3.8}$$

[1] i changes per subcarrier for RSM1 while it is fixed for all subcarriers in RSM2,

where $P_{e_i}(k)$ is the end-to-end error probability, $P_{e,SR_i}(k)$ is the error probability of S $\rightarrow$ R$_i$ link for the kth subcarrier, $P_{e,SD}(k)$ is the error probability of S $\rightarrow$ D link for the k^{th} subcarrier and $P_{e,COOP_i}(k)$ is the error probability in the cooperative links (i.e., S $\rightarrow$ D and R$_i$ $\rightarrow$ S, when the k^{th} subcarrier participates in transmission). The first term at the right hand side of (3.8) is the error probability when the k^{th} subcarrier in the i^{th} relay detects the signal correctly, but the signal resulting from the cooperative links S $\rightarrow$ D and R$_i$ $\rightarrow$ S is detected wrong. The second term represents the case when the k^{th} subcarrier of the relay cannot participate in transmission because of incorrect decision. In this case, the error probability results only from the direct link S $\rightarrow$ D. The error probability in (3.8) can be upper bounded as in [49]

$$P_{e_i}(k) \leq P_{e,COOP_i}(k) + P_{e,SR_i}(k)P_{e,SD}(k) \tag{3.9}$$

Therefore, under the assumption of perfect channel knowledge at the transmitters [2] , the average BER of N-subcarrier OFDM symbol can be approximated as

$$\begin{aligned} P_{e_i} \leq & \sum_{k=1}^{N} cQ\left(\sqrt{a\left(\left|\mathbf{D}_{SD}(k,k)\right|^2 E_{k,S} + \left|\mathbf{D}_{R_iD}(k,k)\right|^2 G_{R_iD}E_{k,R_i}\right)}\right) \\ & + \sum_{k=1}^{N} \alpha Q\left(\sqrt{a\left|\mathbf{D}_{SD}(k,k)\right|^2 E_{k,S}}\right) Q\left(\sqrt{a\left|\mathbf{D}_{SR_i}(k,k)\right|^2 G_{SR_i}E_{k,S}}\right) \end{aligned} \tag{3.10}$$

where a, c, and α are given by

$$a = \begin{cases} \frac{2}{N_0}\sin^2\left(\frac{\pi}{M}\right) & \text{M} - \text{PSK} \\ \frac{3}{N_0(M-1)} & \text{M} - \text{QAM} \end{cases}, \tag{3.11}$$

[2]For a given value of the fading coefficient, we are practically dealing with a deterministic multiplicative channel (i.e., determined by a fixed coefficient) in the presence of AWGN [67].

$$c = \begin{cases} \frac{(M-1)}{N \log_2 M}, & \text{forM} - \text{PSK} \\ \frac{4}{N \log_2 M} \left(\frac{\sqrt{M}-1}{\sqrt{M}} \right), & \text{forM} - \text{QAM} \end{cases}, \tag{3.12}$$

and

$$\alpha = \begin{cases} \frac{(M-1)^2}{N(\log_2 M)}, & \text{forM} - \text{PSK} \\ \frac{16}{N(\log_2 M)} \left(\frac{\sqrt{M}-1}{\sqrt{M}} \right)^2, & \text{forM} - \text{QAM} \end{cases}. \tag{3.13}$$

We aim to the minimize BER in (3.10) under total power constraint and fixed subcarriers transmission rate. The optimization problem can be formulated as

$$\begin{aligned} &\min_{E_{k,S},\ E_{k,R}} P_e \\ &\text{s.t.} \, (1/N) \textstyle\sum_{k=1}^{N} (E_{k,S} + E_{k,R_i}) = 2E, \quad E_{k,R_i} \geq 0, \quad E_{k,S} > 0 \end{aligned} \tag{3.14}$$

As shown in Appendix B, P_e is a convex function. Therefore (3.14) would yield an optimal global minimum [56] . The Lagrangian problem can be formulated using Lagrange multipliers, λ, μ_k, η_k as,

$$\Psi = P_e + \lambda \left(\frac{1}{N} \sum_{k=1}^{N} (E_{k,S} + E_{k,R}) - 2E \right) - \sum_{k=1}^{N} \mu_k E_{k,S} - \sum_{k=1}^{N} \eta_k E_{k,R} \tag{3.15}$$

The KKT conditions for the optimization problem are [56]

$$\partial \Psi / \partial E_{k,S} = 0 \tag{3.16}$$

$$\partial \Psi / \partial E_{k,R_i} = 0 \tag{3.17}$$

$$\frac{1}{N} \sum_{k=1}^{N} (E_{k,S} + E_{k,R_i}) - 2E = 0 \tag{3.18}$$

$$\mu_k E_{k,S} = 0 \tag{3.19}$$

$$\eta_k E_{k,R_i} = 0 \tag{3.20}$$

$$E_{k,R_i} \geq 0;\ E_{k,S} > 0 \tag{3.21}$$

$$\eta_k \geq 0;\ \ \mu_k \geq 0;\ \ \lambda \geq 0 \tag{3.22}$$

Differentiating Ψ with respect to $E_{k,S}$ yields (3.16) as

$$\begin{aligned} &\tfrac{\alpha\sqrt{G_{SR_i}}\left|\mathbf{D}_{SR_i}(k,k)\right|}{\sqrt{E_{k,S}}} Q\left(\sqrt{a\left|\mathbf{D}_{SD}(k,k)\right|^2 E_{k,S}}\right)\exp\left(-\tfrac{a}{2}\left|\mathbf{D}_{SR_i}(k,k)\right|^2 G_{SR_i}E_{k,S}\right) \\ &+\tfrac{\alpha|\mathbf{D}_{SD}(k,k)|}{\sqrt{E_{k,S}}}\exp\left(-\tfrac{a}{2}\left|\mathbf{D}_{SD}(k,k)\right|^2 E_{k,S}\right) Q\left(\sqrt{a\left|\mathbf{D}_{SR_i}(k,k)\right|^2 G_{SR_i}E_{k,S}}\right) \\ &+\tfrac{c|\mathbf{D}_{SD}(k,k)|^2}{\sqrt{\beta_{k,i}}}\exp\left(-\tfrac{a}{2}\beta_{k,i}\right) - \sqrt{\tfrac{8\pi}{a}}\tfrac{\lambda}{N} + \sqrt{\tfrac{8\pi}{a}}\mu_k = 0 \end{aligned} \tag{3.23}$$

where $\beta_{k,i} = \left|\mathbf{D}_{SD}(k,k)\right|^2 E_{k,S} + \left|\mathbf{D}_{R_iD}(k,k)\right|^2 G_{R_iD}E_{k,R_i}$ Differentiating Ψ with respect to $E_{k,R}$ yields (17) as

$$\frac{c\left|\mathbf{D}_{R_iD}(k,k)\right|^2 G_{R_iD}}{\sqrt{\beta_{k,i}}}\exp\left(-\frac{a}{2}\beta_{k,i}\right) - \sqrt{\frac{8\pi}{a}}\frac{\lambda}{N} + \sqrt{\frac{8\pi}{a}}\eta_k = 0 \tag{3.24}$$

Eqs. (3.19) and (3.20) have four possible solutions given by

$$\mu_k = 0,\ \ \eta_k = 0 \tag{3.25}$$

$$\mu_k = 0,\ \ E_{k,R_i} = 0 \tag{3.26}$$

$$\eta_k = 0,\ \ E_{k,S} = 0 \tag{3.27}$$

$$E_{k,S} = 0,\ \ E_{k,R_i} = 0 \tag{3.28}$$

The fourth solution in (3.28) is not feasible and is ignored under our assumption of fixed subcarriers rate. The third solution in (3.27) is also ignored because it is physically meaningless, i.e., relay cannot transmit without the presence of a source signal to be forwarded. Solution given by (3.26) assumes no cooperation for the k^{th} subcarrier and can be ignored as well. This leaves us with the solution given by (3.25) which is the general cooperation scenario. Therefore, by replacing (3.25) in (3.23) and (3.24), we can obtain

$$\begin{aligned}&\left(1-\frac{|\mathbf{D}_{SD}(k,k)|^2}{\left|\mathbf{D}_{R_iD}(k,k)\right|^2 G_{R_iD}}\right)\frac{\lambda}{\alpha N}\sqrt{\tfrac{8\pi}{a}}\sqrt{E_{k,S}}=\\&\left|\mathbf{D}_{SR_i}(k,k)\right|\sqrt{G_{SR_i}}Q\left(\sqrt{a\left|\mathbf{D}_{SD}(k,k)\right|^2 E_{k,S}}\right)\exp\left(-\tfrac{a}{2}\left|\mathbf{D}_{SR_i}(k,k)\right|^2 G_{SR_i}E_{k,S}\right)\\&+\left|\mathbf{D}_{SD}(k,k)\right|\exp\left(-\tfrac{a}{2}\left|\mathbf{D}_{SD}(k,k)\right|^2 E_{k,S}\right)Q\left(\sqrt{a\left|\mathbf{D}_{SR_i}(k,k)\right|^2 G_{SR_i}E_{k,S}}\right)\end{aligned}\tag{3.29}$$

For a given λ, channel fading coefficients and specific modulation scheme, there is only one solution for (3.29) since its root is the intersection of increasing convex function in left hand side of (3.29) and decreasing convex function in right hand side of (3.29). Thus, the solution for the k^{th} source subcarriers power will be feasible (i.e. positive) if and only if

$$\left|\mathbf{D}_{R_iD}(k,k)\right|^2 G_{R_iD} > \left|\mathbf{D}_{SD}(k,k)\right|^2 \tag{3.30}$$

If (3.30) is satisfied, E_{k,R_i} can be found from (3.24) and (3.25) to be

$$E_{k,R_i}=\frac{1}{a\left|\mathbf{D}_{R_iD}(k,k)\right|^2 G_{R_iD}}\left(\mathrm{W}\left\{\left(\left|\mathbf{D}_{R_iD}(k,k)\right|^2 G_{RD}\frac{caN}{2\sqrt{2\pi}\lambda}\right)^2\right\}-a\left|\mathbf{D}_{SD}(k,k)\right|^2 E_{k,S}\right) \tag{3.31}$$

where $\mathrm{W}\{.\}$ is the Lambert function [68]. E_{k,R_i} has a feasible solution if and only if

$$\mathrm{W}\left\{\left(\left|\mathbf{D}_{R_iD}(k,k)\right|^2 G_{R_iD}\frac{caN}{2\sqrt{2\pi}\lambda}\right)^2\right\}\geq a\left|\mathbf{D}_{SD}(k,k)\right|^2 E_{k,S} \tag{3.32}$$

If (3.30) is not satisfied, $E_{k,S}$ will yield negative values. This means that assuming (3.25) as a solution for (3.23) and (3.24) is not acceptable and we have to switch to the solution of (3.26) . This can be physically interpreted that the cooperation is not worth for this subcarrier and we need to work with direct transmission. Then by substituting (3.26) in (3.23) , we obtain,

$$\begin{aligned}
&\tfrac{\lambda}{N}\sqrt{\tfrac{8\pi}{a}}\sqrt{E_{k,S}} = c\left|\mathbf{D}_{SD}(k,k)\right|\exp\left(-\tfrac{a}{2}\left|\mathbf{D}_{SD}(k,k)\right|^2 E_{k,S}\right)\\
&+\alpha\left|\mathbf{D}_{SR_i}(k,k)\right|\sqrt{G_{SR_i}}Q\left(\sqrt{a\left|\mathbf{D}_{SD}(k,k)\right|^2 E_{k,S}}\right)\exp\left(-\tfrac{a}{2}\left|\mathbf{D}_{SR_i}(k,k)\right|^2 G_{SR_i}E_{k,S}\right)\\
&+\alpha\left|\mathbf{D}_{SD}(k,k)\right|\exp\left(-\tfrac{a}{2}\left|\mathbf{D}_{SD}(k,k)\right|^2 E_{k,S}\right)Q\left(\sqrt{a\left|\mathbf{D}_{SR_i}(k,k)\right|^2 G_{SR_i}E_{k,S}}\right)
\end{aligned} \tag{3.33}$$

Eq. (3.33) has a positive unique solution of $E_{k,S}$ because the solution is the intersection of increasing convex function in left hand side of (3.33) and decreasing convex function in its right hand side. Based on the derived steps above, the flowchart of proposed power loading algorithm is provided in Figure 3.3. Starting from initial interval to λ, i.e. $[\lambda_a,\ \lambda_b]$, the corresponding constraint functions $F_a,\ F_b$ are computed from

$$F = (1/N)\sum\nolimits_{k=1}^{N}\left(E_{k,S} + E_{k,R_i}\right) - 2E \tag{3.34}$$

Then by using any bracketing minimization method, as the bisection method, and by defining a desired tolerance ε, a solution of λ can be found and thus $E_{k,S},\ E_{k,R_i}$ values are computed.

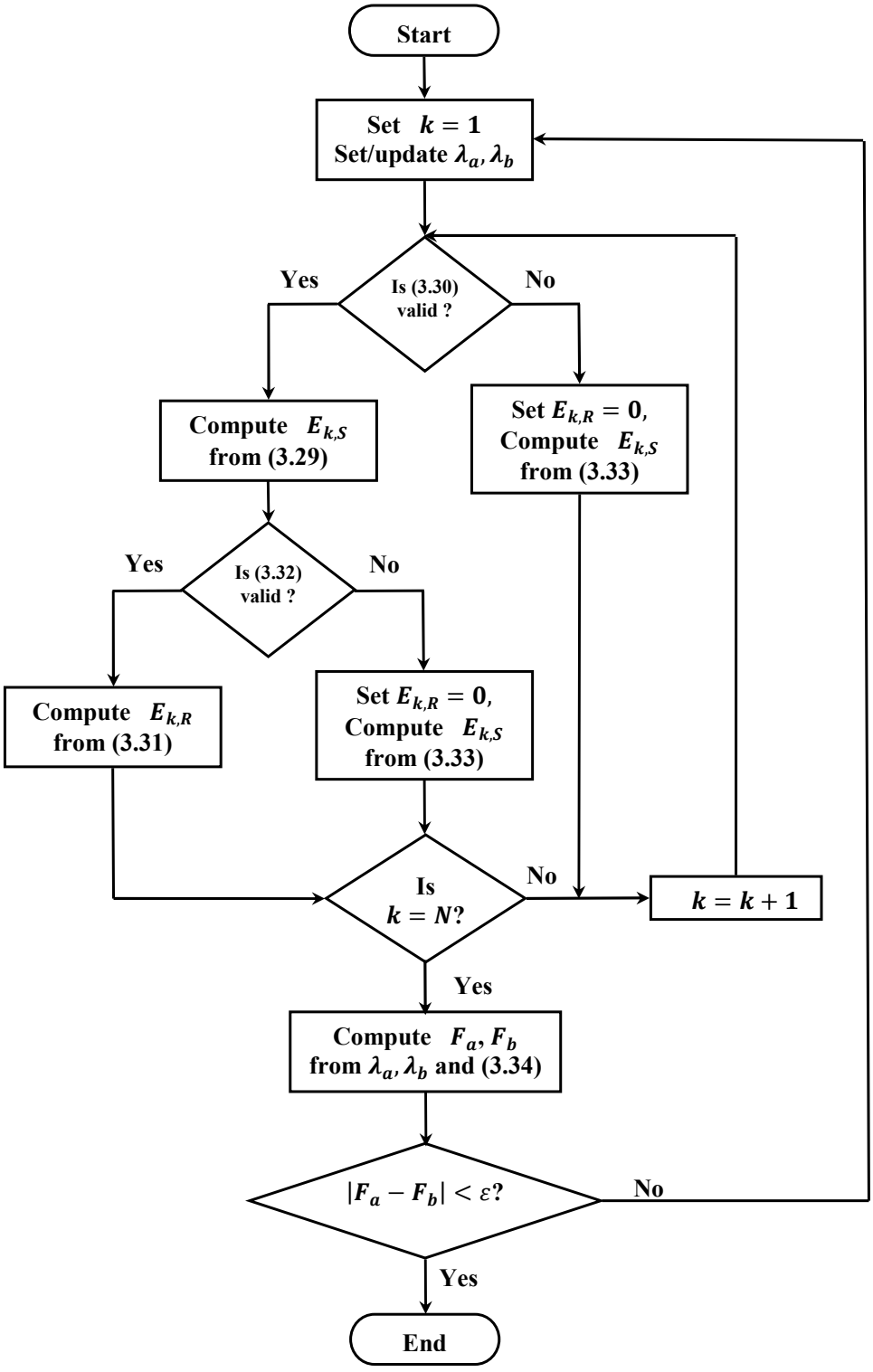

Figure 3.3: The flowchart of the proposed adaptive algorithm.

3.3 Simulation Results and Discussion

In this section, we investigate the performance of the proposed system through Monte Carlo simulations. We assume quadrature phase shift keying (QPSK) modulation, $N = 32$, $\alpha = 2$, $\theta = \pi$ and $L_{SD} = L_{SR_i} = L_{R_iD} = 1$.

Example 1 (Single-relay case): We first consider the proposed adaptive power loading scheme in a single-relay scenario which will be used as a benchmark in the later examples. We assume three representative relay locations: G_{SR}/G_{RD}=30 dB, -30 dB and 0 dB which respectively indicate locations near to source, near to destination and midway. Figure 3.4 illustrates that equal power loading (EPL) scheme can extract the spatial diversity only for relay location near the source and fails to do it so in the other relay locations because of error propagation resulting from incorrect decisions at the relay.

On the other hand, the proposed scheme (denoted by APL) is able to extract the full diversity in all cases and significantly outperforms EPL. Specifically, at BER=10^{-3}, APL outperforms EPL by 11.5 dB, 11 dB and 4 dB for $G_{SR}/G_{RD}= -30$ dB, 0 dB and 30 dB respectively. The APL scheme succeeds to extract both spatial diversity and multipath diversity and yields a diversity order of 4. It can be also observed that, for EPL scheme, best performance is attained near to the source while, for the APL scheme, best performance is obtained at the midway.

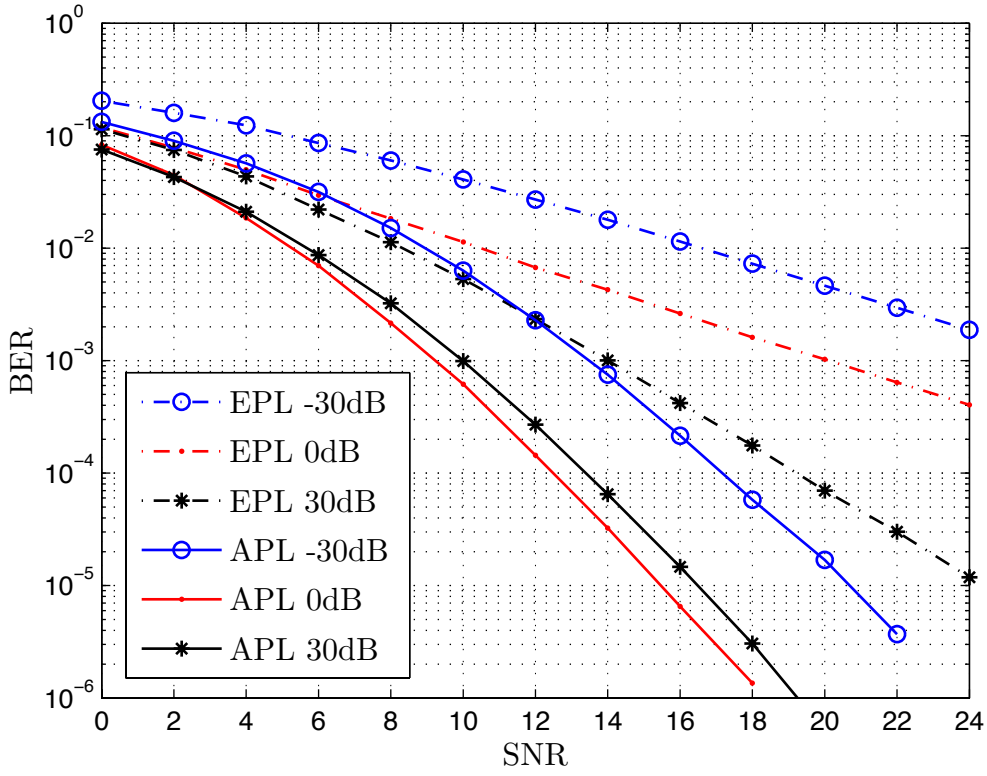

Figure 3.4: Performance comparison of EPL and APL in a single-relay scenario.

Example 2 (Multi-relay case): In this example, we first compare the performance of EPL and APL for a two-relay system with geometrical gains given by G_{SR}/G_{RD}=30 dB and −30 dB. We consider both relay selection methods earlier described. In Figure 3.5, we observe that APL-RSM1 scheme outperforms EPA-RSM1 scheme by 5.2 dB at a target BER of 10^{-3}. Deployment of RSM2 further increases the performance improvement and APL-RSM2 scheme outperforms EPA-RSM2 by 10.7 dB. RSM1 achieves better performance than RSM2 because the selection is made based on per subcarriers SNR not on average relays SNR. Further performance improvements are possible as the number of relays increases (See Figure 3.6). In this figure, only APL is considered. For RSM1,

two-relay deployment brings a performance improvement of 4.8 dB over single-relay case while improvement in three-relay deployment climbs up to 7.2 dB at a target BER of 10^{-3}. For RSM2, performance gains of 3.4 dB and 5.2 dB are observed, respectively, for two and three relays.

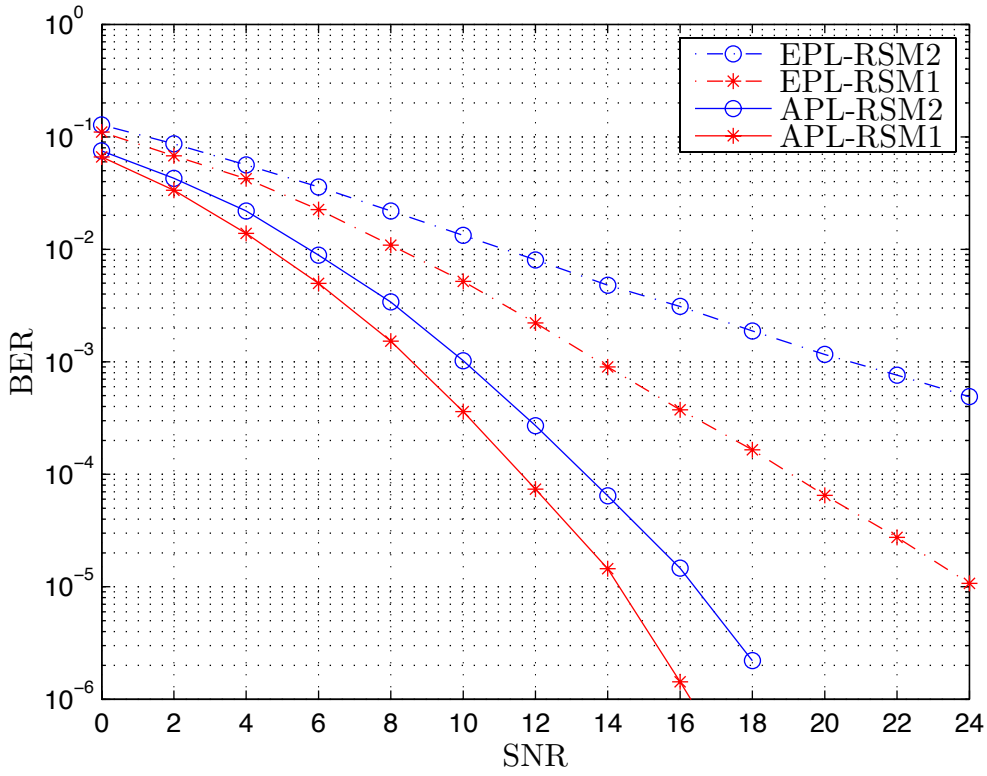

Figure 3.5: Performance comparison of EPL and APL in a two-relay scenario with different relay selection methods.

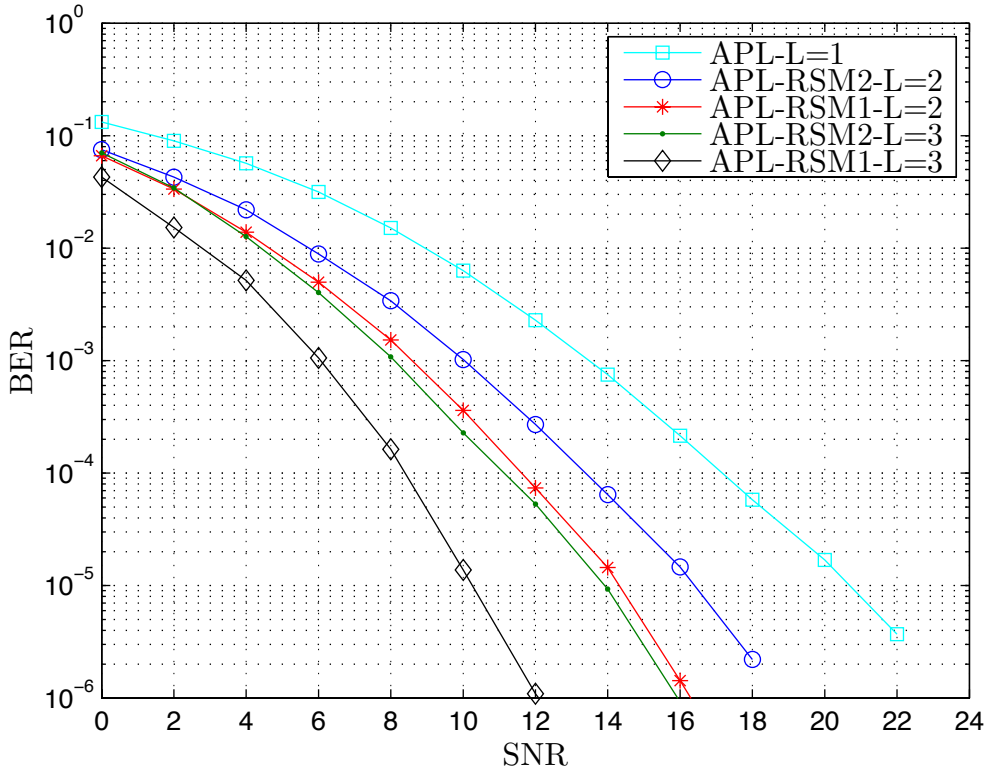

Figure 3.6: Performance of APL for various number of relays.

Example 3 (Effect of relay location): In this example, we investigate the effect of relay location on the error rate performance in a two-relay scenario. We plot the received SNR of direct link required to achieve BER=10^{-3} for different relays locations considering APL-RSM1 and APL-RSM2 versus the locations of two relays. Figure 3.7 shows that APL-RSM1 outperforms APL-RSM2 for all relay locations; specifically the maximum performance gap is around 2 dB when both relays are near-to-destination. On the other hand, the minimum difference is 1 dB which occurs when both relays are near-to-source. Both methods achieve their best performance when both relays are located in the middle location.

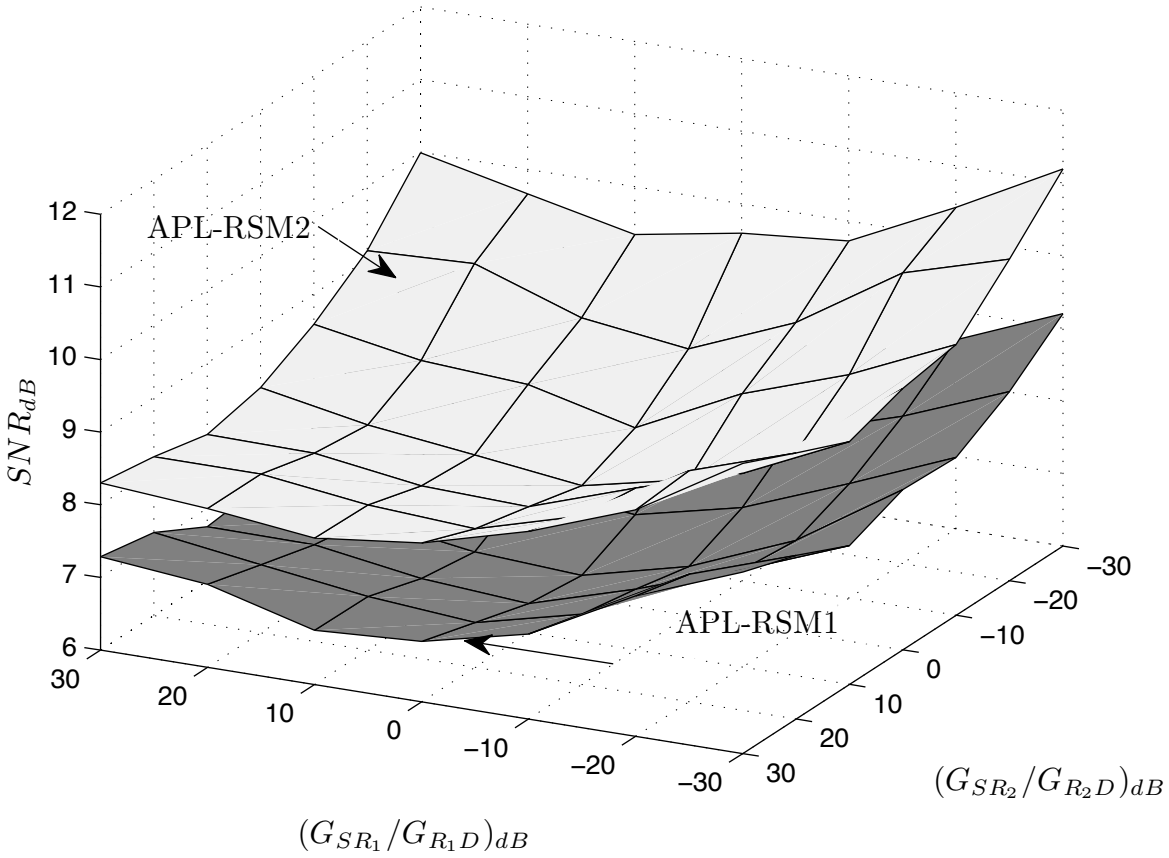

Figure 3.7: Performance of APL for various number of relays.

Example 4 (Effect of channel estimation): Adaptive algorithms depend on the availability of fading channel coefficients which are estimated and fed back to the transmitters. In this example, we study the effect of channel estimation on the BER performance. We assume the D-CE estimation method [69] and deploy LMMSE estimator at the relay and the destination nodes. One pilot symbol is employed through each subcarrier with equal power . We further assume two relay scenario with locations G_{SR}/G_{RD}=30 dB and −30 dB. Figure 3.8 illustrates that, at BER=10^{-3}, a small performance degradation of 0.5

dB and 0.8 dB is with respect to perfect CSI is observed for APL-RSM1 and APL-RSM2, respectively.

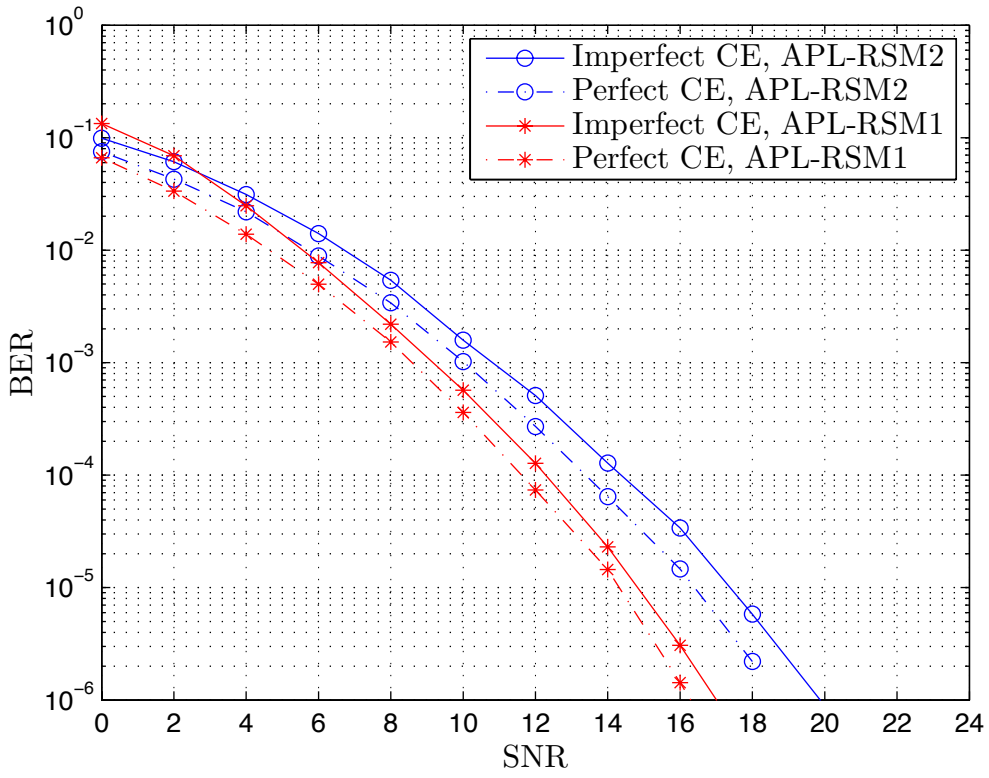

Figure 3.8: Effect of imperfect channel estimation on the BER performance.

3.4 Conclusion

In this chapter, we have proposed an adaptive power loading algorithm for a multi-relay OFDM system with detect-and-forward relaying and relay selection. In the adaptive algorithm design, we have chosen the minimization of BER as the objective function and performed power loading under total power constraint. As for relay selection methods, we have employed so-called RSM 1 and 2 which respectively depends on the best relay selection for each subcarrier and the average best relay selection for all subcarriers. Through Monte Carlo simulations, we have demonstrated that the proposed adaptive algorithm encoupled with these relay selection methods is able to achieve full diversity and presents significant performance gains over conventional equal power loading schemes. For example, in a two-relay scenario, performance gains up to 10.7 dB are observed depending on the relay location and relay selection method. We have further presented simulation results to demonstrate the effects of imperfect channel estimation and relay location on the performance. And rather than studying the effect of imperfect channel estimation on adaptive systems, we will consider the quality of channel estimation in designing the adaptive OFDM cooperative system in next chapter.

Chapter 4

Bit Loading for AF Cooperative Network with Imperfect Channel Estimation

In this chapter, we introduce an adaptive bit loading scheme for an AF OFDM cooperative system with relay selection. The proposed bit loading scheme maximizes the throughput for a targeted error rate taking into account the quality of imperfect channel estimation. It relies on estimated CSI at the destination node and partial CSI (which involves the number of loaded bits) at the source node. We provide extensive Monte-Carlo simulation results to present the throughput and the no-transmission probability performance of proposed scheme and discuss the effect of various system and channel parameters on the performance.

The rest of the chapter is organized as follows: In Section 4.1, we describe the system model under consideration. In Section 4.2, we first derive an expression for SNR at the destination and its probability density function (pdf), then use this pdf to obtain an

expression for the throughput. In Section 4.3, we formulate an optimization problem as to maximize the throughput and present its solution which yields our bit loading algorithm. In Section 4.4, we provide Monte Carlo simulation results to demonstrate the performance gains through adaptive bit loading and effects of various system and channel parameters on the performance. Finally, we conclude in Section 4.5.

Notation: $\otimes$ is the Kronecker product. $\mathbf{1}_N$ denotes vector of ones with length of N.

4.1 System Model

We consider an OFDM multi-relay wireless network with relay selection. The system model is the same as the multi-relay model in chapter 3 and depicted in Figure 3.1. In this work, we assume also RD cooperation protocol where the source and the relay nodes transmit in orthogonal transmission phases. In the first transmission phase (i.e., broadcasting), a bit stream is fed into serial-to-parallel converter which maps them onto modulation symbols chosen from either M-ary PSK or M-ary square QAM constellations. Assume that a constellation with size of M_n has been chosen based on the employed bit loading scheme which will be elaborated later. The n^{th} subcarrier symbol modulates $b_n = \log_2 M_n$ bits. Before passing through IFFT, the power of subcarriers' symbols is amplified with E after IPS. To prevent inter-block-interference, a CP is inserted between OFDM symbol blocks with $L_{CP} \geq \max(L_{SR_i}, L_{R_iD}, L_{SD})$ as shown in Figure 4.1(a). All relay nodes and the destination node receive the transmitted OFDM symbol.

Let the subcarrier signal for the n^{th} carrier be denoted as $x(n)$, $n = 1, 2, ...N$ where N is the number of subcarriers. The received signals at the relay and the destination nodes

during the broadcasting phase are given by

$$r_{D_1}(n) = \sqrt{E} D_{SD}(n,n)\, x(n) + v_{D_1}(n), \tag{4.1}$$

$$r_{R_i}(n) = \sqrt{G_{SR_i} E} D_{SR_i}(n,n)\, x(n) + v_{R_i}(n) \tag{4.2}$$

where $D_{SD}(n,n)$ and $D_{SR_i}(n,n)$ are the n^{th} diagonal elements in channel matrices defined as $\mathbf{D}_{SD} = diag(H_{SD}(0),\ H_{SD}(1), \cdots H_{SD}(N-1))$ and
$\mathbf{D}_{SR_i} = diag\left(H_{SR_i}(0),\ H_{SR_i}(1), \cdots H_{SR_i}(N-1)\right)$.

For each subcarrier, only a single relay is allowed to participate in the relaying phase. "Best" relay is chosen based on [72]

$$R_{sel}(n) = \arg\max_{R_i} \left\{\gamma_{SR_iD}(n)\right\}, \quad n = 1, 2, \cdots, N \tag{4.3}$$

where $\gamma_{SR_iD}(n)$ is the equivalent instantaneous *effective* SNR of S $\rightarrow$ R$_i$ $\rightarrow$ D link (i.e., taking into account the channel estimation errors. Through this selection method, relays can save some power by switching off unused subcarriers. After scaling the received signal [65], the selected relay node amplifies the selected n^{th} subcarrier with power E. Then it feeds the subcarriers to IFFT and adds CP before it forwards the resulting symbol to destination node. At the destination node, CP is removed and the received OFDM symbol is converted into subcarrier signals as shown in Figure 4.1(c). The n^{th} subcarrier signal is given by

$$r_{D_2}(n) = \frac{E\sqrt{G_{SR_i} G_{R_iD}} D_{SR_i}(n,n)\, D_{R_iD}(n,n)}{\sqrt{E G_{SR_i} \left|D_{SR_i}(n,n)\right|^2 + N_0}} x(n) + v'_{D_2}(n) \tag{4.4}$$

where $v'_{D_2}(n) = \left(\sqrt{E G_{R_iD}} D_{R_iD}(n,n) \Big/ \sqrt{E G_{SR_i} \left|D_{SR_i}(n,n)\right|^2 + N_0}\right) v_{R_i}(n) + v_{D_2}(n)$.

In (4.1), (4.2) and (4.4). $v_{D_1}(n)$, $v_R(n)$ and $v_{D_2}(n)$ are the FFT of AWGN terms with zero mean and variance equal to N_0.

The destination is assumed to have access only to imperfect channel estimates which will be used at the MRC. Let the channel estimates of the S $\rightarrow$ R$_i$ and S $\rightarrow$ D link be $\hat{D}_{SR_i}(n,n)$ and $\hat{D}_{SD}(n,n)$, respectively. We assume that $D_{SR_i}(n,n)$ and $\hat{D}_{SR_i}(n,n)$ are jointly ergodic and stationary Gaussian processes. We can therefore write $D_{SR_i}(n,n) = \hat{D}_{SR_l}(n,n) + e_{SR_i}(n)$ where $e_{SR_i}(n)$ denotes the channel estimation error which is modeled as complex Gaussian with zero mean and variance $\sigma^2_{e_{SR_i}}(n)$. Assuming the deployment of LMMSE estimator [70], the autocorrelation function of estimation error vector $\mathbf{e}_{SR_i} = diag\left(\mathbf{D}_{SR_i} - \hat{\mathbf{D}}_{SR_l}\right)$ is given by

$$\mathbf{R}_{SR_i} = \mathbb{E}\left[\mathbf{e}_{SR_i}\mathbf{e}^H_{SR_i}\right] = \mathbf{R}_{h_{SR_i}} - \mathbf{R}_{h_{SR_i}}\mathbf{X}^H_{SR_i}\mathbf{X}_{SR_i}\mathbf{R}_{h_{SR_i}}\left(\mathbf{X}^H_{SR_i}\mathbf{X}_{SR_i}\mathbf{R}_{h_{SR_i}} + N_0\mathbf{I}_N\right)^{-1} \quad (4.5)$$

where $\mathbf{X}_{SR_i} = \mathbf{1}_{N_p} \otimes \sqrt{G_{SR_i}E}\mathbf{I}_N$, N_p is the number of pilots, $\mathbf{R}_{h_{SR_i}} = \mathbf{Q}_{t,SR_i}\mathbf{Q}^H_{t,SR_i}/(L_{SR_i}+1)$ and $\mathbf{Q}_{t,SR_i}$ is the first $(L_{SR_i}+1)$ columns of the $\mathbf{Q}$ matrix. Therefore, we have $\sigma^2_{e_{SR_i}}(n) = \mathbf{R}_{SR_i}(n,n)$. Similarly, we have $\sigma^2_{e_{SD}}(n) = \mathbf{R}_{SD}(n,n)$ and $\sigma^2_{e_{R_iD}}(n) = \mathbf{R}_{R_iD}(n,n)$ where $\mathbf{R}_{SD}$ and $\mathbf{R}_{R_iD}$ are the corresponding autocorrelation functions. The received signals are fed to the MRC. Output signal at the n^{th} subcarrier signal is given by [73]

$$\lambda_n = W_{SD}(n)\, r_{SD}(n) + W_i(n)\, r_{R_iD}(n) \quad (4.6)$$

where the combiner coefficients are given by

$$W_{SD}(n) = \frac{\sqrt{E}}{N_0}\hat{D}^*_{SD}(n,n) \quad (4.7)$$

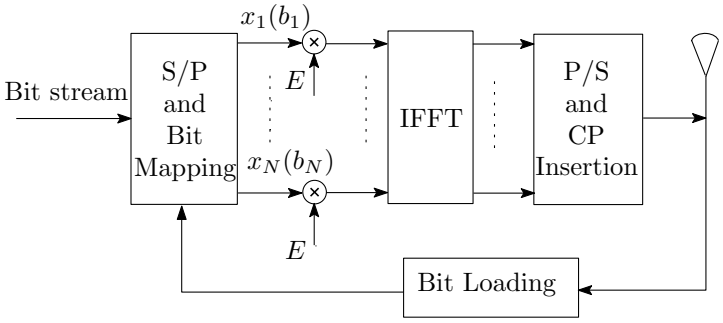

(a) Source

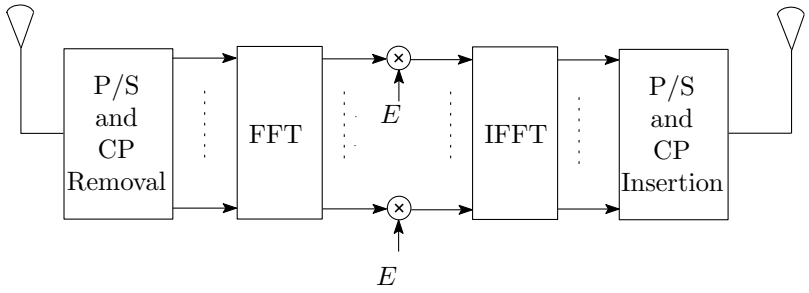

(b) Relay

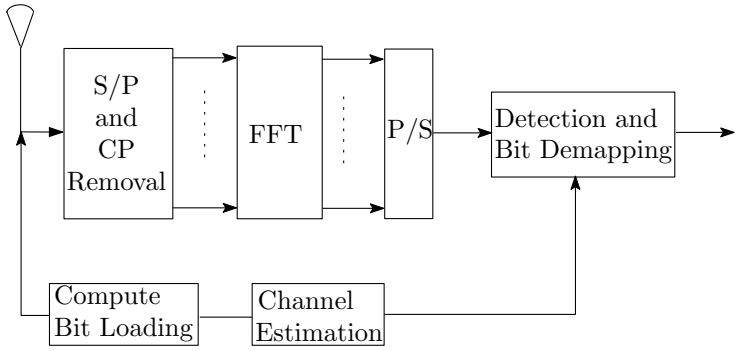

(c) Destination

Figure 4.1: Block diagrams of source, relay, and destination nodes for AF bit loading system.

$$W_i(n) = \frac{\sqrt{G_{R_iD}E}}{|\hat{D}^*_{SR_i}(n,n)|N_{tot}} \hat{D}^*_{SR_i}(n,n)\,\hat{D}^*_{R_iD}(n,n) \tag{4.8}$$

with

$$N_{tot} = N_0 + \frac{EG_{R_iD}}{EG_{SR_i}|\hat{D}_{SR_i}(n,n)|^2 + N_0}|\hat{D}_{R_iD}(n,n)|^2 N_0 \tag{4.9}$$

4.2 Instantaneous Effective SNR

In this section, we derive the *effective* SNR (i.e., incorporating the effects of channel estimation) at the destination and its corresponding pdf. Such a statistical characterization is essential for the derivation of performance measures under consideration.

From (4.6), it can be noticed that the combiners output consists of two terms coming either from the direct or indirect links. Specifically, $\lambda_{SD}(n) \stackrel{def}{=} W_{SD}(n) r_{SD}(n)$ is the term contributed by the S $\rightarrow$ D link and can be expanded as

$$\lambda_{SD}(n) = \underbrace{\frac{E|\hat{D}_{SD}(n,n)|^2}{N_0}x}_{\text{signal}} + \underbrace{\frac{\sqrt{E}\hat{D}^*_{SD}(n,n)}{N_0}\left(\sqrt{E}e_{SD}(n)x + v_{SD}(n)\right)}_{\text{effective noise}} \tag{4.10}$$

The instantaneous effective SNR of this term for the n^{th} subcarrier can be written as

$$\gamma_{SD}(n) = \frac{\hat{\gamma}_{S,D}(n)}{E\sigma^2_{e_{SD}}/N_0 + 1} \tag{4.11}$$

where $\hat{\gamma}_{SD}(n) = E|\hat{D}_{SD}(n,n)|^2/N_0$ is the estimated instantaneous SNR of S $\rightarrow$ D link. The average effective SNR can be further written as

$$\bar{\gamma}_{SD}(n) = \mathbb{E}\left(\gamma_{SD}(n)\right) = \frac{E\left(\Omega_{SD}(n) - \sigma^2_{e_{SD}}(n)\right)}{\left(E\sigma^2_{e_{SD}}(n) + N_0\right)} \tag{4.12}$$

where $\Omega_{SD}(n) = \mathbb{E}\left(|D_{SD}\left(n,n\right)|^2\right)$

Similarly, it can be noticed from (4.6) that $\lambda_{SR_iD}(n) \overset{def}{=} W_i(n) r_{R_iD}(n)$ is the term contributed by the indirect link via i^{th} relay node. It can be expanded as

$$\lambda_{SR_iD}\left(n\right) = \underbrace{\frac{\sqrt{G_{R_iD}}\hat{D}^*_{SR_i}\left(n,n\right)\hat{D}^*_{R_iD}\left(n,n\right)}{|\hat{D}_{SR_i}\left(n,n\right)|N_{tot}}\sqrt{\frac{G_{SR_i}}{G_i\left(n\right)}}\hat{D}_{SR_i}\left(n,n\right)\hat{D}_{R_iD}\left(n,n\right)Ex}_{\text{signal}}$$

$$+\underbrace{\sqrt{\frac{G_{R_iD}E}{G_i\left(n\right)}}\frac{\hat{D}^*_{SR_i}\left(n,n\right)\hat{D}^*_{R_iD}\left(n,n\right)}{|\hat{D}_{SR_i}\left(n,n\right)|N_{tot}}\left\{\sqrt{G_{SR_i}E}\hat{D}_{SR_i}\left(n,n\right)e_{g_i}x + \sqrt{G_{SR_i}E}\hat{D}_{R_iD}\left(n,n\right)e_{h_i}x\right.}_{\text{effective noise}}$$

$$\underbrace{\left.+\left(\hat{D}_{R_iD}\left(n,n\right)+e_{g_i}\right)v_{S,R_i} + \sqrt{G_i\left(n\right)}v_{R_iD}\right\}}_{\text{effective noise}} \tag{4.13}$$

where $G_i\left(n\right) = EG_{SR_i}|D_{R_iD}\left(n,n\right)|^2 + N_0$. This lets us write the corresponding instantaneous effective SNR as

$$\gamma_{SR_iD}(n) = \frac{\hat{\gamma}_{SR_i}(n)\hat{\gamma}_{R_iD}(n)}{\hat{\gamma}_{SR_i}(n)\left(\frac{G_{R_iD}E\sigma^2_{e_{R_iD}}(n)}{N_0}+1\right)+\hat{\gamma}_{R_iD}(n)\left(\frac{G_{SR_i}E\sigma^2_{e_{SR_i}}(n)}{N_0}+1\right)+\frac{G_{SR_i}G_{R_iD}E^2\sigma^2_{e_{SR_i}}(n)\sigma^2_{e_{R_iD}}(n)}{N_0^2}+\frac{G_{R_iD}E\sigma^2_{e_{R_iD}}(n)}{N_0}+1} \tag{4.14}$$

where $\hat{\gamma}_{SR_i}(n) = G_{SR_i}E|\hat{D}_{SR_i}\left(n,n\right)|^2/N_0$ and $\hat{\gamma}_{R_i,D}(n) = G_{R_iD}E|\hat{D}_{R_iD}\left(n,n\right)|^2/N_0$ are the estimated instantaneous SNR of the S $\rightarrow$ R$_i$ and R$_i$ $\rightarrow$ D links. Their average values are given by

$$\bar{\gamma}_{SR_i}(n) = \mathbb{E}\left(\hat{\gamma}_{SR_i}\left(n\right)\right) = \frac{G_{SR_i}E\left(\Omega_{SR_i}(n) - \sigma^2_{e_{SR_i}}(n)\right)}{\left(G_{SR_i}E\sigma^2_{e_{SR_i}}(n) + N_0\right)} \tag{4.15}$$

$$\bar{\gamma}_{R_iD}(n) = \mathbb{E}\left(\hat{\gamma}_{R_iD}\left(n\right)\right) = \frac{EG_{R_iD}\left(\Omega_{R_iD}(n) - \sigma^2_{e_{R_iD}}(n)\right)}{\left(EG_{R_iD}\sigma^2_{e_{R_iD}}(n) + N_0\right)} \tag{4.16}$$

where $\Omega_{SR_i}(n) = \mathbb{E}\left(|D_{SR_i}(n,n)|^2\right)$ and $\Omega_{R_iD}(n) = \mathbb{E}\left(|D_{R_iD}(n,n)|^2\right)$. Eq. (4.14) can be further simplified as

$$\gamma_{SR_iD}(n) = \frac{\gamma_{SR_i}(n)\gamma_{R_iD}(n)}{\gamma_{SR_i}(n) + \gamma_{R_iD}(n) + \varrho(n)} \tag{4.17}$$

where the instantaneous effective SNRs of $\mathrm{S} \to \mathrm{R}_i$ and $\mathrm{R}_i \to \mathrm{D}$ links defined as

$$\gamma_{SR_i}(n) = \hat{\gamma}_{SR_i}(n) \Big/ \left(G_{SR_i} E \sigma^2_{e_{SR_i}}(n)/N_0 + 1\right)$$

and

$$\gamma_{R_iD}(n) = \hat{\gamma}_{R_iD}(n) \Big/ \left(G_{R_iD} E_i \sigma^2_{e_{g_i}}(n)/N_0 + 1\right)$$

with $\varrho(n)$ given by

$$\varrho(n) = \frac{G_{SR_i} G_{R_iD} E^2 \sigma^2_{e_{SR_i}}(n)\sigma^2_{e_{R_iD}}(n) + G_{R_iD} E \sigma^2_{e_{R_iD}}(n) N_0 + N_0^2}{\left(G_{SR_i} E \sigma^2_{e_{SR_i}}(n) + N_0\right)\left(G_{R_iD} E \sigma^2_{e_{R_iD}}(n) + N_0\right)} \tag{4.18}$$

Finally, using (4.11) and (4.17), the effective total output SNR can be obtained as

$$\gamma_{tot}(n) = \gamma_{SD}(n) + \max_{i \in L} \gamma_{SR_iD}(n) \tag{4.19}$$

which can be bounded as [72] by

$$\gamma_{ub}(n) = \gamma_{SD}(n) + \max_{i \in L} \min\left(\gamma_{SR_i}(n), \gamma_{R_iD}(n)\right) \tag{4.20}$$

The pdf of the upper bound on the effective total SNR of the n^{th} subcarrier can be

expressed as [74]

$$f_{\gamma_{ub}}(\gamma) = \sum_{i=1}^{L}(-1)^{i+1}\sum_{K_1=1}^{L-i+1}\sum_{K_2=K_1+1}^{L-i+2}\cdots\sum_{K_i=K_{i-1}+1}^{L}\left(\frac{1}{1/\xi-\bar{\gamma}_{SD}}\exp\left(-\gamma\xi\right)\right.$$
$$\left.-\frac{1}{1/\xi-\bar{\gamma}_{SD}}\exp\left(-\frac{\gamma}{\bar{\gamma}_{SD}}\right)\right) \tag{4.21}$$

where $\xi_i = \sum_{j=1}^{i}(1/\bar{\gamma}_{R_{K_j}})$ and $\bar{\gamma}_i = \bar{\gamma}_{SR_i}\bar{\gamma}_{R_iD}/(\bar{\gamma}_{SR_i}+\bar{\gamma}_{R_iD})$. Considering independent identical distribution (i.i.d) channels, i.e. $\bar{\gamma}_{SD} = \bar{\gamma}_{SR_i} = \bar{\gamma}_{R_iD} = \bar{\gamma}$, (4.21) reduces as in [74] to

$$f_{\gamma_{up}^{iid}}(\gamma) = \sum_{q=1}^{M}\binom{M}{q}\frac{(-1)^{q-1}}{\bar{\gamma}\left(1-1/\left(2q\right)\right)}\left[\exp\left(-\frac{\gamma}{\bar{\gamma}}\right)-\exp\left(-\frac{2q\gamma}{\bar{\gamma}}\right)\right] \tag{4.22}$$

4.3 Adaptive Bit Loading

We aim to maximize the throughput of multi-relay network by adaptively changing the number of loaded bits per subcarrier under a target BER constraint. Assume that there are K different signal constellations (M-ary QAM or M-ary PSK) to choose from. Each modulation scheme $M_n(k)$ is used for a certain SNR region defined by $(\gamma_k,\ \gamma_{k+1})$, $k = 1, 2...K$ at the n^{th} subcarrier. Let $R_l(n)$ and $P_l(n)$, respectively, denote the throughput and the average BER through the n^{th} subcarrier assuming the deployment of the l^{th} relay. The optimization problem can be defined as

$$\max_{b_n\in B} R_l(n) \tag{4.23}$$

subject to the BER constraint given by

$$P_l(n) \leq P_{th} \quad \forall\, l \in \{1, 2, \cdots, L\}, \quad n \in \{1, 2, \cdots, N\} \tag{4.24}$$

where B is the set of allowable number of bits for the signal constellations under consideration and P_{th} is a desired threshold BER value. $R_l(n)$ in (4.23) can be expressed as

$$R_l(n) = \frac{1}{2} \sum_{k=1}^{K} b_n(k) \int_{\gamma_k}^{\gamma_{k+1}} f(\lambda)\, d\lambda \tag{4.25}$$

where $b_n(k)$ is the number of loaded bits for the n^{th} subcarrier and $f(\lambda)$ is the pdf of effective SNR when transmitting through the n^{th} subcarrier. Using the upper bound for pdf given by (4.21), (4.25) can be expressed as

$$\begin{aligned} R_l(n) = {} & \tfrac{1}{2} \sum_{k=1}^{K} b_n(k) \sum_{i=1}^{L} (-1)^{i+1} \sum_{K_1=1}^{L-i+1} \sum_{K_2=K_1+1}^{L-i+2} \cdots \sum_{K_i=K_{i-1}+1}^{L} \frac{1}{1/\xi - \bar{\gamma}_{SD}} \\ & \times \left[(\bar{\gamma}_{SD}) \exp\left(-\tfrac{\lambda}{\bar{\gamma}_{SD}} \right) - \tfrac{1}{\xi} \exp(-\lambda \xi) \right] \Big|_{\gamma_k}^{\gamma_{k+1}} \end{aligned} \tag{4.26}$$

In the case of i.i.d. channels, (4.25) reduces to

$$R_{l,iid}(n) = \frac{1}{2} \sum_{k=1}^{K} b_n(k) \sum_{q=1}^{M} \binom{M}{q} \frac{(-1)^{q-1}}{\bar{\gamma}\,(1 - 1/(2q))} \left[\frac{\bar{\gamma}}{2q} \exp\left(-\frac{2q\lambda}{\bar{\gamma}} \right) - \bar{\gamma} \exp\left(-\frac{\lambda}{\bar{\gamma}} \right) \right]_{\gamma_k}^{\gamma_{k+1}} \tag{4.27}$$

On the other hand, the average BER for the multicarrier system under consideration can be expressed as [75]

$$P_l(n) = \frac{1}{R_l(n)} \sum_{k=1}^{K} b_k P(k) \tag{4.28}$$

where $P(k)$ is the average BER for modulation scheme $M_n(k)$ and defined as

$$P(k) = \int_{\gamma_k}^{\gamma_{k+1}} \sum_i \alpha_i Q\left(\sqrt{\beta_i \gamma}\right) f(\gamma)\, d\gamma \tag{4.29}$$

Replacing the upper bound given by (4.21) in (4.29), we have

$$\begin{aligned} P(k) = \sum_{i=1}^{L} (-1)^{i+1} \sum_{K_1=1}^{L-i+1} \sum_{K_2=K_1+1}^{L-i+2} \cdots \sum_{K_i=K_{i-1}+1}^{L} \frac{1}{1/\xi_i - \bar{\gamma}_{SD}} \sum_j \frac{\alpha_j}{2} \Bigg\{ \bar{\gamma}_{SD} \sqrt{\frac{(\beta_j/2)\bar{\gamma}_{SD}}{(\beta_j/2)\bar{\gamma}_{SD}+1}} \\ \times \operatorname{erf}\left(\sqrt{\frac{(\beta_j/2)\bar{\gamma}_{SD}+1}{\bar{\gamma}_{SD}}}\gamma\right) + \left[\bar{\gamma}_{SD} \exp\left(-\frac{\gamma}{\bar{\gamma}_{SD}}\right) - \frac{1}{\zeta_i} \exp\left(-\zeta_i \gamma\right)\right] \operatorname{erfc}\left(\sqrt{(\beta_j/2)\,\gamma}\right) \\ - \frac{1}{\zeta_i} \sqrt{\frac{\beta_j/2}{\beta_j/2+\zeta_i}} \operatorname{erf}\left(\sqrt{(\beta_j/2+\zeta_i)\,\gamma}\right) \Bigg\}_{\gamma_k}^{\gamma_{k+1}} \end{aligned} \tag{4.30}$$

For i.i.d. scenario, (4.29) reduces to

$$\begin{aligned} P_{iid}(k) = \sum_{q=1}^{M} \binom{M}{k} \frac{(-1)^{q-1}}{\bar{\gamma}(1-1/(2q))} \sum_j \frac{\alpha_j}{2} \Bigg\{ \frac{\bar{\gamma}}{2q} \sqrt{\frac{(\beta_j/2)\bar{\gamma}/(2q)}{(\beta_j/2)\bar{\gamma}/(2q)+1}} \operatorname{erf}\left(\sqrt{\frac{(\beta_j/2)\bar{\gamma}/(2q)+1}{\bar{\gamma}/(2q)}}\gamma\right) \\ - \bar{\gamma} \sqrt{\frac{(\beta_j/2)\bar{\gamma}}{(\beta_j/2)\bar{\gamma}+1}} \operatorname{erf}\left(\sqrt{\frac{(\beta_j/2)\bar{\gamma}+1}{\bar{\gamma}}}\gamma\right) + \bar{\gamma}\left(\frac{1}{2q} \exp\left(-\frac{2q\gamma}{\bar{\gamma}}\right) - \exp\left(-\frac{\gamma}{\bar{\gamma}}\right)\right) \operatorname{erfc}\left(\sqrt{(\beta_j/2)\,\gamma}\right) \Bigg\}_{\gamma_k}^{\gamma_{k+1}} \end{aligned} \tag{4.31}$$

From (4.26), we observe that the optimization problem can be reformulated in terms of SNR threshold values γ_k instead of b_n in the original formulation. This reformulation enables us to solve the problem off-line and determine the bit loading coefficients once rather than using an iterative loading algorithm for each channel realization [49, 51, 53, 54, 59]. The Lagrangian optimization problem can be now given as

$$\Psi = R_l(n) + \mu \left(\sum_{k=1}^{K} b_k P(k) - R_l(n) P_{th} \right) \tag{4.32}$$

Deriving $\partial\Psi/\partial\gamma_k = 0$ and $\partial\Psi/\partial\mu = 0$, the SNR threshold values γ_k can be expressed in terms of γ_1 as in [76] to be

$$y_k(\gamma_k) = p_2(\gamma_1), \qquad k = 2, 3, \cdots, K-1 \tag{4.33}$$

$$y_k(\gamma_k) = \frac{1}{b_k - b_{k-1}} \left(b_k p_{m_k}(\gamma_k) - b_{k-1} p_{m_{k-1}}(\gamma_k) \right) \tag{4.34}$$

Replacing (4.33) and (4.34) in (4.28), we end up with a one dimensional problem in terms of γ_1 instead of the original $K-1$ dimensional problem. γ_1 can be then solved numerically and consequently the other SNR thresholds can be calculated from (4.33) and (4.34). The flowchart of proposed bit loading algorithm is provided in Figure 4.2.

In practice, the destination terminal needs to compute the SNR thresholds. Then, for each channel realization, the number of loaded bits per subcarrier is determined simply by determining the SNR region which instantaneous SNR value falls in. The number of loaded bits is sent to the source through a feedback signal. This feedback signal is an OFDM symbol with each carrier carrying the relevant number of bits. In contrast with [49, 51, 53, 54] which require the availability of full CSI at all communication nodes, our scheme relies on CSI only at the destination terminal and partial CSI (i.e., number of bits) at the source.

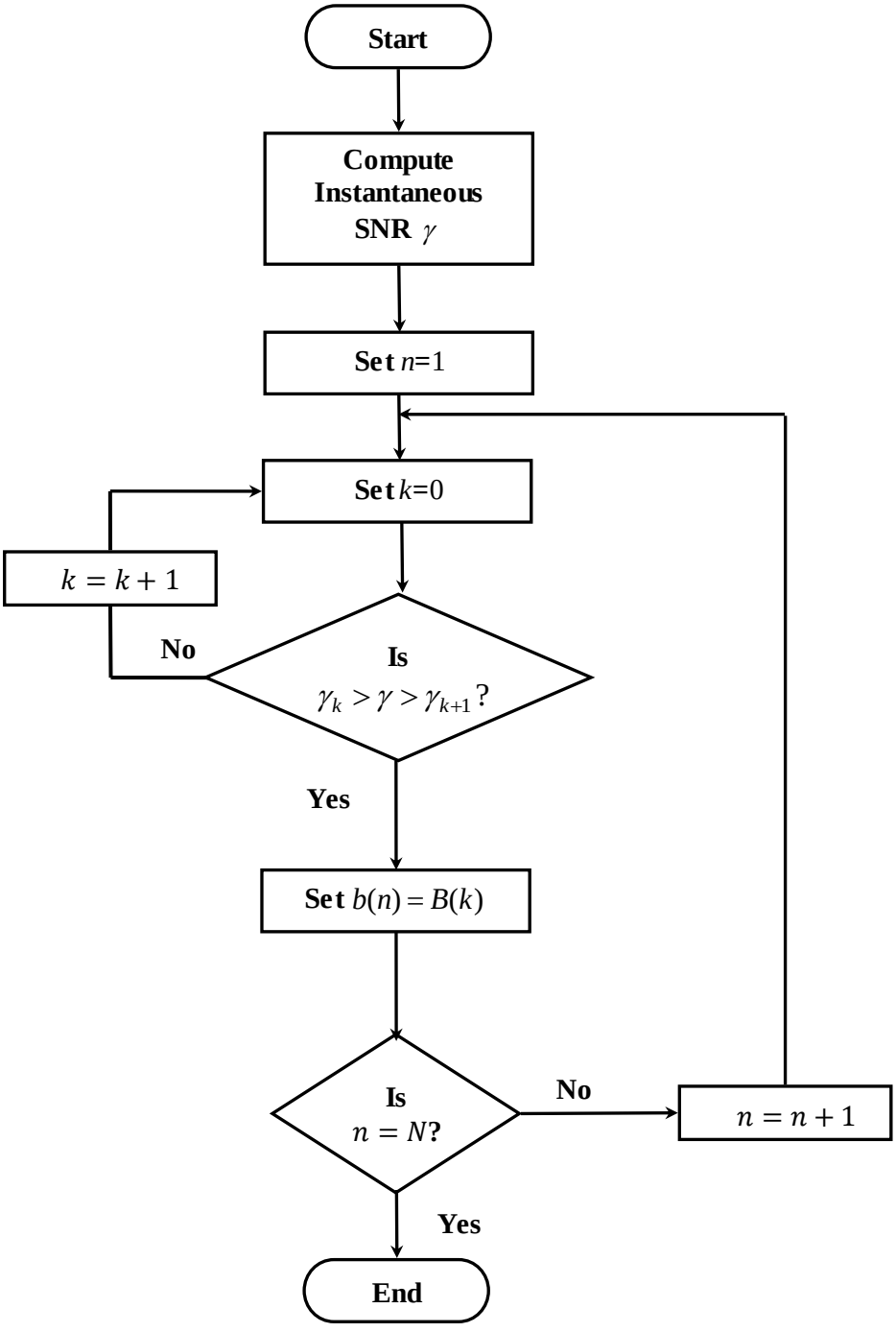

Figure 4.2: Flowchart of the adaptive bit loading scheme.

4.4 Simulation Results

In this section, we investigate the throughput performance of the proposed bit loading scheme through Monte Carlo simulations. We assume $\alpha = 2$ and $N = 32$. Unless otherwise mentioned, the number of relays is $L = 3$, the channel lengths of underlying links are assumed to be equal to each other as $L_{SR} = L_{RD} = L_{SD} = 1$ and the sub-channels are estimated using one pilot per subcarrier. M-ary QAM modulation schemes are deployed with $K = 5$, $M_n = \{0, 2, 4, 16, 64\}$, $B = \{0, 1, 2, 4, 6\}$ and parameters $\{\alpha_i, \beta_i\}$ can be found in [76]. The SNR thresholds (γ_k) are computed from (4.33) and (4.34) and the threshold BER is set as $P_{th} = 10^{-3}$. In the figures, SNR is defined as E/N_0.

Example 1 (Performance of Multi-Relay Systems with Bit Loading)

In this example, we demonstrate the performance of proposed system with bit loading for different number of relays. We consider three relay-assisted scenarios for $L = 1$, 2 and 3 with related parameters described in Table 4.1. From Figure 4.3, we observe that the SNR required to achieve a desired throughput decreases as the number of relays increases. Specifically, the SNR required to achieve a throughput of three bit/s/Hz/subcarrier is 26 dB, 24 dB and 22.5 dB for $L = 1$, 2 and 3 respectively. As for the probability of no-transmission (i.e., when $0 <$ SNR $< \gamma_1$) [76] illustrated in Figure 4.4, we observe that increasing the number of relays effectively decreases this probability especially at medium and high SNR. Therefore, although all three schemes achieve the same throughput at high SNR ($>$ 26 dB), deploying more relays has the advantage of decreasing the probability of no-transmission.

Table 4.1: Simulation scenarios.

	$L = 1$	$L = 2$	$L = 1$
G_{SR_i}/G_{R_iD} [dB]	-30	-30, 0	-30, 0, 30
θ_i	π	$\pi,\ \pi/3$	$\pi,\ \pi/3,\ \pi/6$

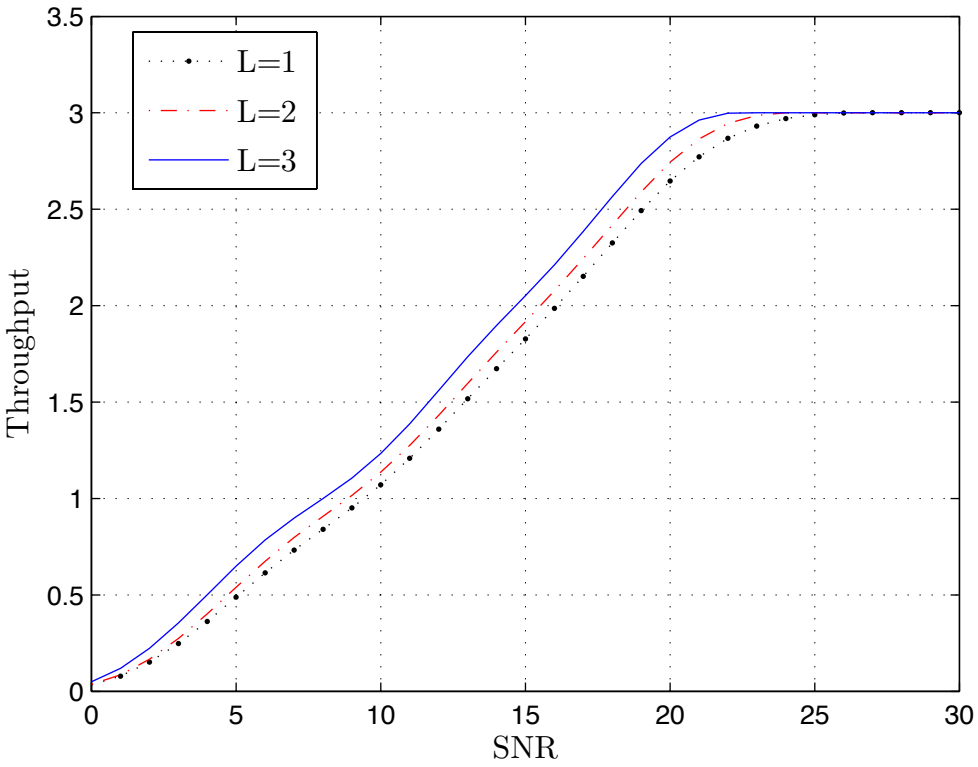

Figure 4.3: Throughput for different number of relays.

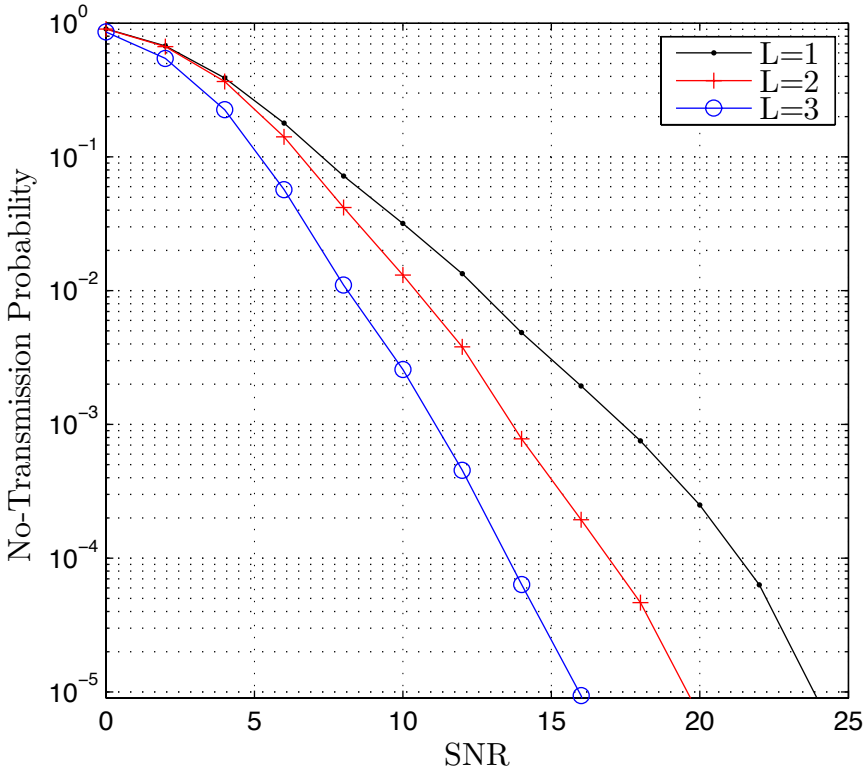

Figure 4.4: No-transmission probability for different number of relays.

Example 2 (Number of Pilot Symbols) In this example, we investigate the effect of number of pilot symbols on the performance. We assume the three-relay scenario described in Table 4.1. In Figure 4.5, we assume $L_{SR} = L_{RD} = L_{SD} = L_{ch} = 1$ with $N_p = 1$. It is observed that even single pilot is sufficient to provide a performance close to the perfect CSI case. In Figure 4.6, we consider $L_{SR} = L_{RD} = L_{SD} = 10$ and employ $N_p = 1$, 3 and 5 pilot symbols. For $N_p = 1$, we observe 1.3 dB between perfect and estimated performance. This reduces to 0.5 dB for $N_p = 3$. Further increase in pilot symbol number does not provide a significant performance gain.

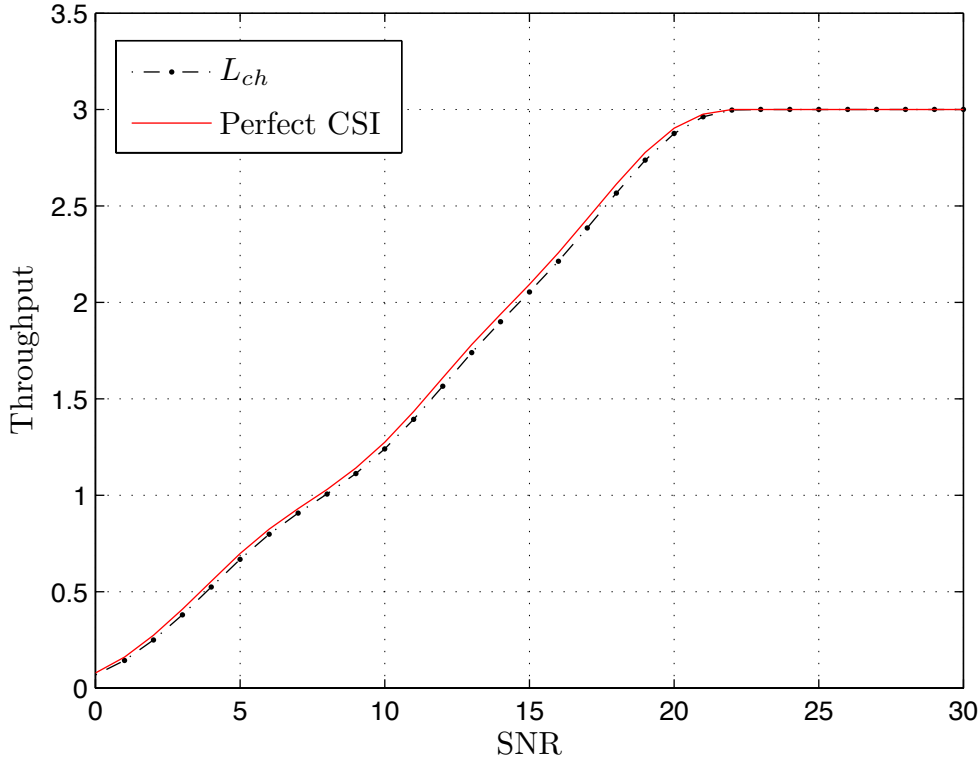

Figure 4.5: Throughput for perfect and imperfect channel estimation assuming $L_{SR} = L_{RD} = L_{SD} = L_{ch} = 1$ and $N_p = 1$.

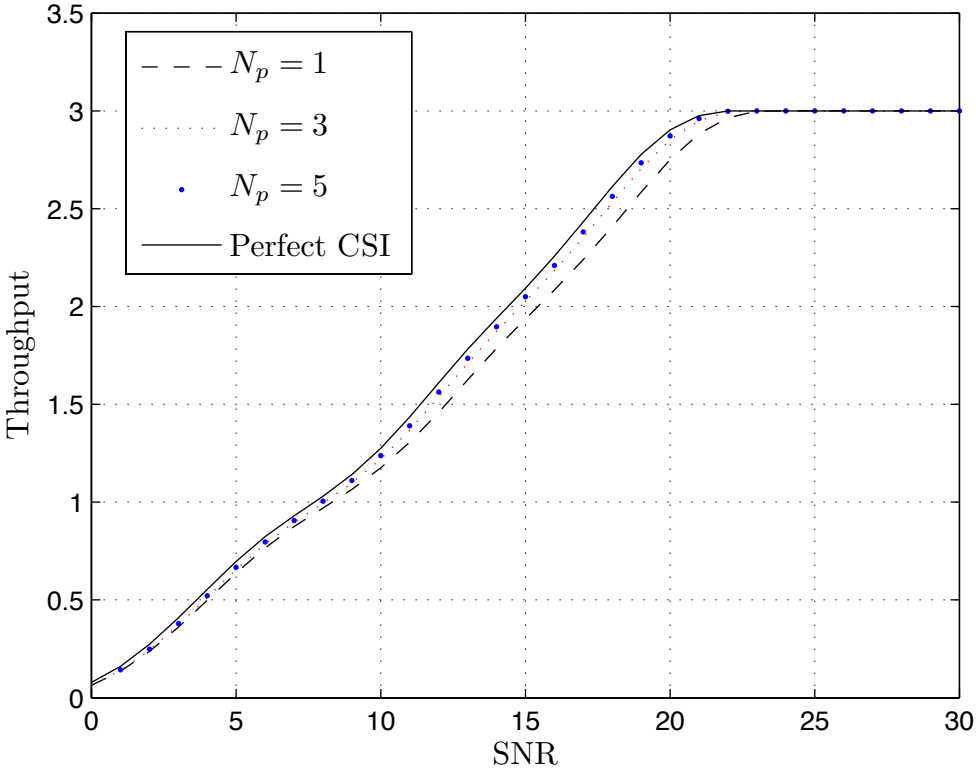

Figure 4.6: Effect of the number of pilots on the throughput.

Example 3 (Effect of Relay Location) To study the effect of relay location on the throughput, we assume single-relay scenario and consider various values of G_{SR}/G_{RD} and θ. In Figure 4.7, we illustrate the SNR required to achieve a throughput of 3 bits/Hz/subcarrier with respect to these two parameters. It is observed from Figure 4.7 that the best relay location is obtained for the combination of $G_{SR}/G_{RD} = 0$ dB and $\theta = \pi$ (i.e., relay is located at midway of the direct line between the source and the destination). At this location, SNR of $\sim$ 25 dB is required to achieve a throughput of 3 bits/s/Hz/subcarrier. As the angle θ become smaller, performance becomes worse and middle relay location becomes unfavorable in comparison to other locations.

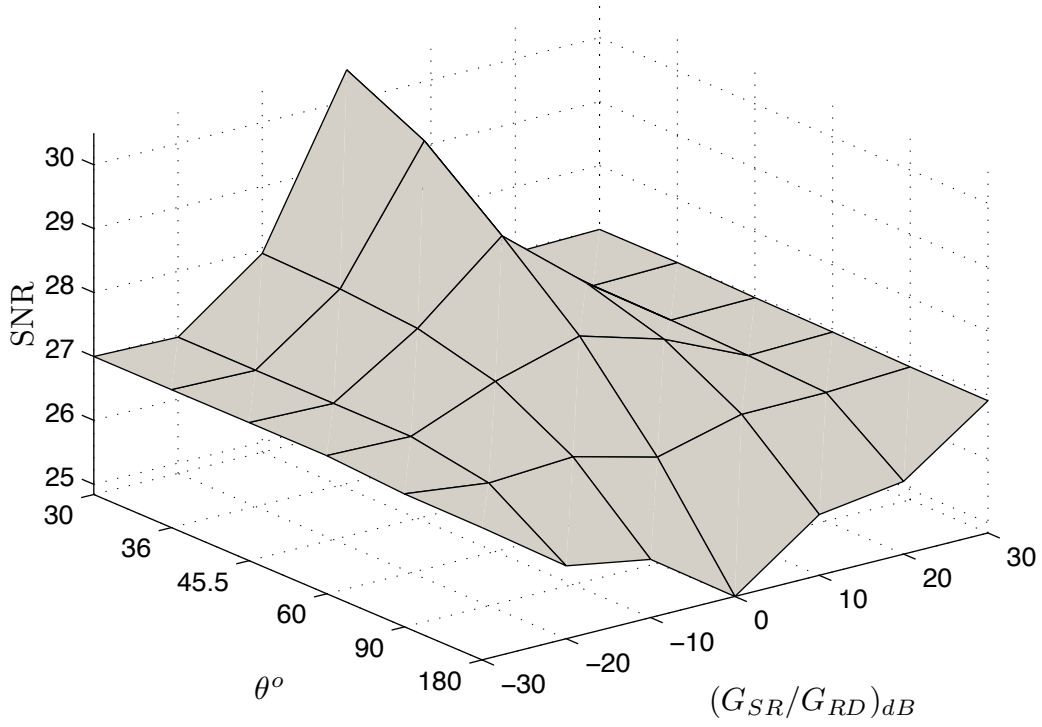

Figure 4.7: SNR required to achieve 3 bits/s/Hz/subcarrier versus relay location parameters.

Example 4 (Effect of Channel Length) In this example, we study the effect of channel lengths on the performance. We consider relay scenarios described in Table 4.1 and assume that channel lengths of underlying links are equal to each other, i.e., $L_{SR} = L_{RD} = L_{SD} = L_{ch}$. In our simulations, we consider $L_{ch} = 1, 5, 10$. Figure 4.8 shows that the throughput performance degradation increases with increasing channel order. Specifically, when the channel order increases from 1 to 5, a degradation of 0.5 dB is observed (to maintain a throughput of 3 bits/Hz/subcarrier). When the channel order increases from 1 to 10, the degradation becomes approximately 1.25 dB. Degradation with increasing channel order mainly originates from the degradation in channel estimation.

Figure 4.9 illustrates no-transmission probability with respect to channel order. A similar behavior is also observed in the no-transmission probability. The same performance is achieved for all channel lengths at low SNR values and differences appear at higher SNR values. Better performance is achieved as L_{ch} decreases.

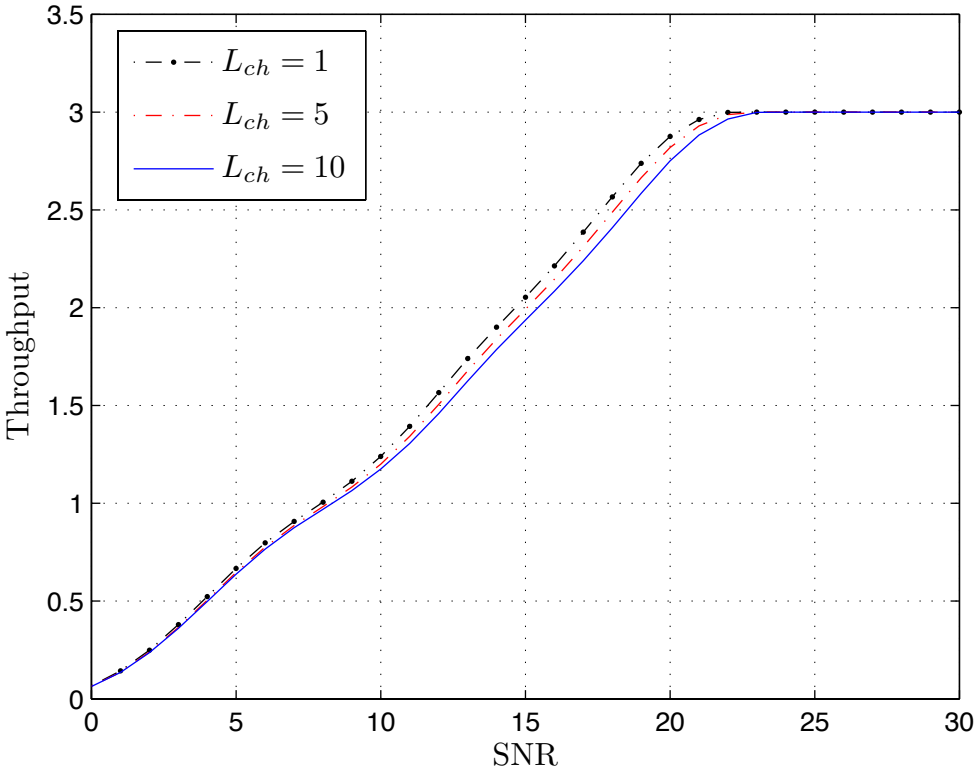

Figure 4.8: Throughput for different channel lengths.

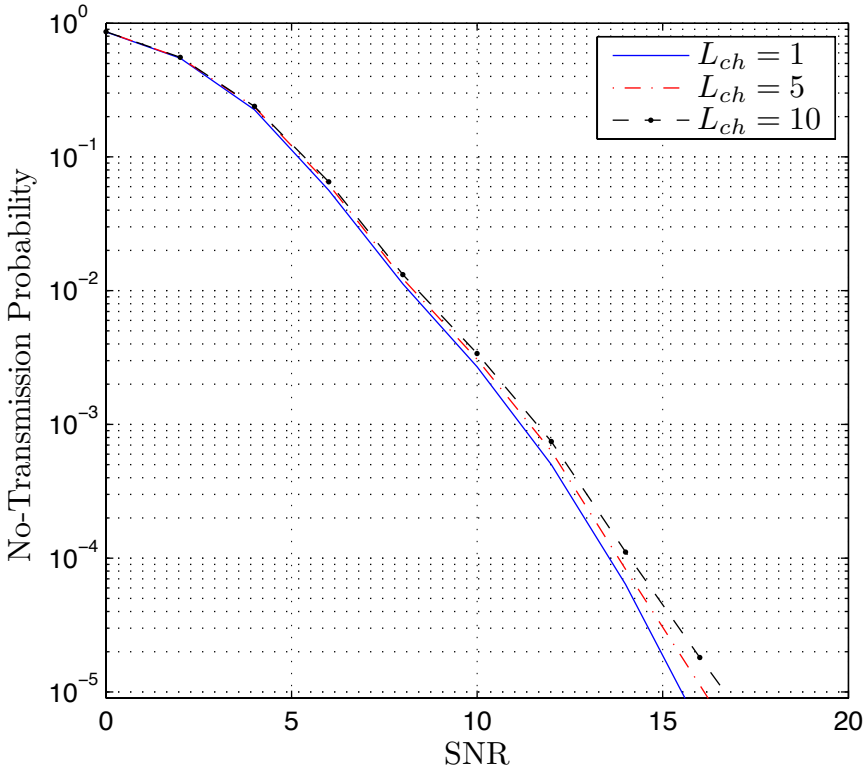

Figure 4.9: No-transmission probability for different channels lengths.

Example 5 (Target Error Rate) So far, we have assumed $P_{th} = 10^{-3}$ as the threshold BER. In this example, we study the effect of threshold error probability on the performance. We assume the three-relay scenario with $P_{th} = 10^{-2},\ 10^{-3}$ and 10^{-4}. As expected, Figure 4.10 shows that the SNR required to achieve a throughput of 3 bits/Hz/subcarrier increases as the target BER decreases. Specifically the SNR required to achieve error probabilities $10^{-2},\ 10^{-3}$ and 10^{-4} are 18, 22.5 and 25.5 dB, respectively. A similar effect occurs on the no-transmission probability as shown in Figure 4.11. Specifically, the system with target BER of 10^{-4} needs 2.2 dB more than the system with BER target of 10^{-3} to have an outage transmission of 10^{-3}.

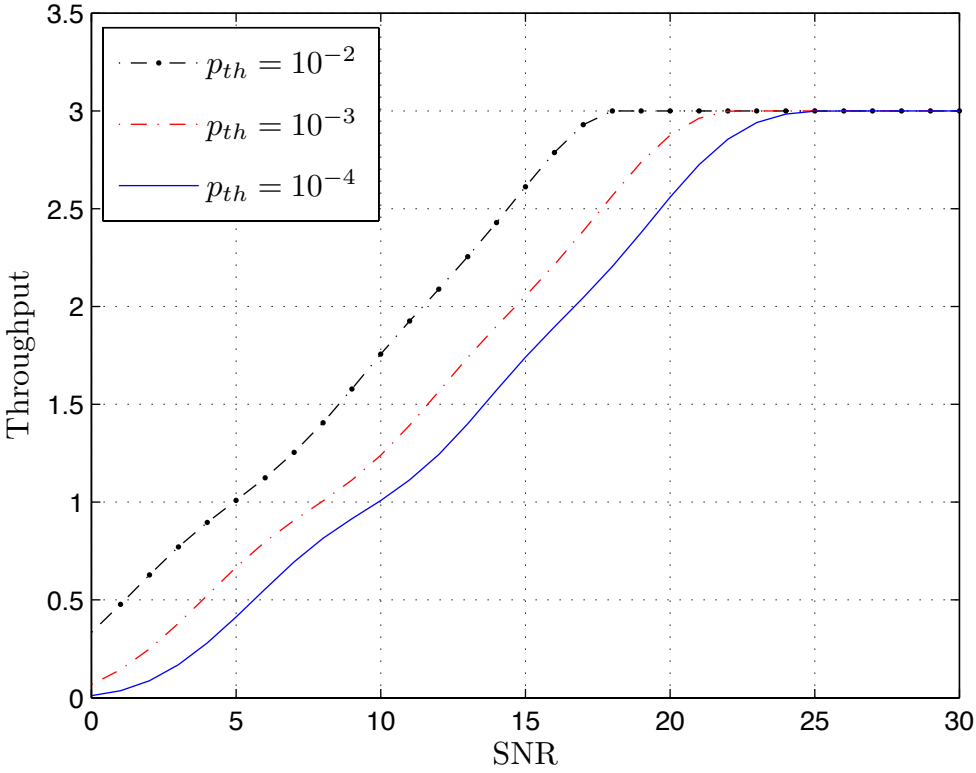

Figure 4.10: Effect of error probability threshold on the throughput.

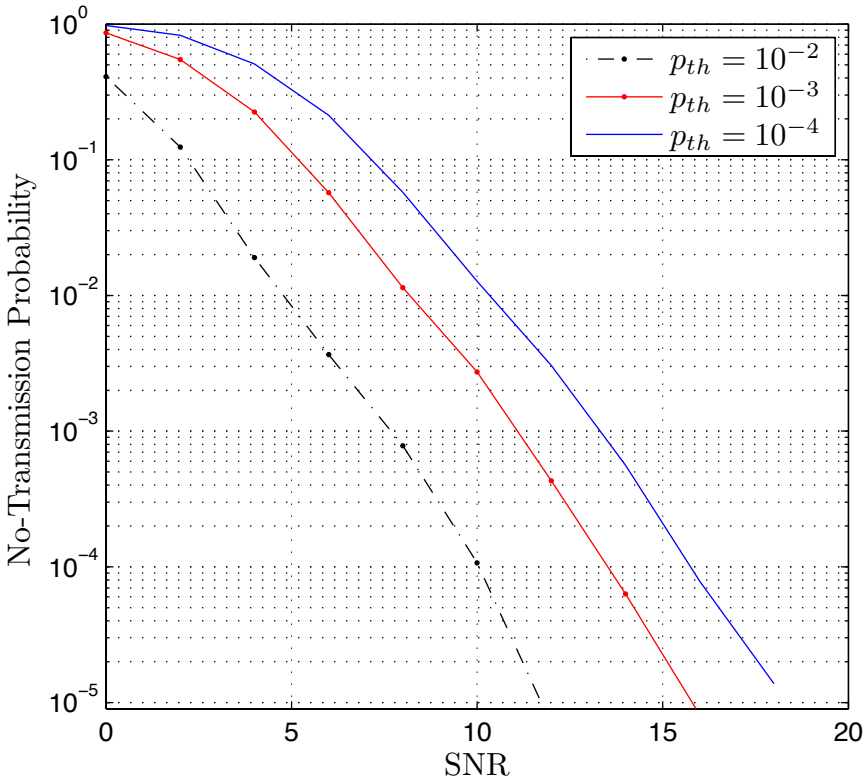

Figure 4.11: Effect of error probability threshold on the no-transmission probability.

4.5 Conclusion

In this chapter, we have introduced an adaptive bit loading scheme to maximize the throughput for a multi-relay AF OFDM network with relay selection. Taking into consideration the imperfect channel estimation, we have derived closed-form expressions for the received SNR and its pdf and used them to obtain the throughput. Optimization problem has been formulated in terms of SNR threshold values and its solution yields the bit loading scheme which relies only on the number of bits per carrier rather than the full CSI. We have presented extensive Monte-Carlo simulation results to demonstrate the performance of proposed scheme and the effect of various system and channel parameters on the performance. The proposed scheme has two advantages, considering the channel estimation quality in designing the adaptive system. The second advantage that full CSI is needed only at the destination not at transmission nodes as adaptive schemes introduced previously. In addition to that, the feedback signal is with finite rate which reduces the system reliability.

Chapter 5

Conclusions and Future Work

In this final chapter, we summarize the contributions presented in this dissertation and discuss several potential extensions to our work.

5.1 Research Contribution

Unlike the open loop OFDM cooperative communication, adaptive OFDM cooperative network allows variable bit and/or power loading for different transmission nodes according to the instantaneous CSI of the cooperative channel links. Available CSI at the transmitting nodes can be used to design adaptive transmission schemes for performance improvement. Our adaptive schemes spanned from the single relay to multi-relay OFDM cooperative network.

In the first research part, we considered three node cooperative network and we adopted BER as our desired performance metric. We proposed three adaptive algorithms to develop optimal bit and/or power loading to minimize BER under certain network power

and rate budget. We studied also the effect of relay location and channel estimation on our algorithms. Simulation results showed that in mid SNR region, best location for power loading and joint bit and power loading is for the near to destination location. On the other hand, bit loading best location is in the middle distance between the source and destination. Simulation results demonstrated that adaptive algorithms are able to extract full diversity when compared with collocated antenna systems besides collecting some coding gain depending on relay location. Also, we found that the power is more dominant than bit loading. It can be observed also that OPL algorithm effectively equalizes bad sub-channels by assigning more power onto them while OBL algorithm loads more bits to reliable channels.

In the second research part, we extended the single relay model to multi-relay assuming DF cooperative OFDM network. We employed two relay selection strategies depending on the best relay selection for each subcarrier and the average best relay selection for all subcarriers. We proposed the adaptive power loading algorithm based on the instantaneous CSI to minimize the BER under total power constraint and fixed subcarriers rate. Through Monte-Carlo simulations, we have demonstrated that the proposed adaptive algorithm coupled with the presented relay selection methods is able to achieve full diversity and presents significant performance gains over conventional equal power loading schemes. Also, we studied the effect of channel estimation and relays location. Specifically for 2 relays scenario, best location is when both relays are in the middle distance between source and destination for both selection methods.

In the third research part, we considered also multi-relay OFDM cooperative network working with AF relaying and using best relay per subcarrier selection method. We introduced adaptive bit loading algorithm to maximize the throughput under a target bit error

rate. Our proposed system has two main advantages; it takes into consideration the channel estimation quality parameters and reduces system complexity. Optimization problem has been formulated in terms of SNR threshold values and its solution yields the bit loading scheme which relies only on the number of bits per carrier rather than the full CSI. Full CSI is required only at the destination node and SNR thresholds are to be computed one time per the used cooperative network. We presented simulation results to demonstrate and validate the performance of the proposed scheme and the effect of various systems and channel parameters on the performance such as relay location, number of relays, channel length and number of pilots.

5.2 Future Work

For future research, the spectral efficiency of the assumed systems can be improved if the cooperation schemes work in two-way relaying rather than the one-way relaying mode. Two-way relaying mode has attracted much research attention recently [77–84]. In the two-way relaying, two terminals exchange their data with the help of one or multiple relays. The relay receives a mixture data from both terminals in the first transmission phase. In the second transmission phase, the relay forwards this data to both terminals. Then, each terminal can detect its counterpart data with the help of the knowledge of its previous transmitted data. Besides the same addressed problem in the thesis, other problems can be considered for the two-way relaying mode since the literature work still incomplete in this point [78, 79, 81–84]. For example the following problems can be considered, power and/or bit loading to minimize total power consumption under target bit error rate, maximize throughout under power constraint and maximize throughput under bit error rate

constraint.

Another possible research extension is to quantize the power loading coefficients, used for power loading purposes in chapter 2 and chapter 3, to optimized limited levels. To quantize the power coefficients, we need to define maximum power limit and number of levels and follow similar approach considered in chapter 4. Although this solution will not be optimum, the system complexity and feedback amount will be reduced.

Single-carrier frequency domain equalization (SC-FDE) provides a powerful alternative to multicarrier systems [85, 86]. In the last few years, there has been a renewed interest in SC-FDE. Although increasing research efforts target several topics in SC-FDE, there is only sparse work on adaptive SC-FDE, see for example, the bit-loading algorithm proposed in [87]. To the best of our knowledge, there has been no prior research on adaptive cooperative SC-FDE systems, which will be one of the possible future research topics.

Appendices

Appendix A

Convexity Proof of AF Problem

In this appendix, we provide the convexity proofs for OPL, OBL and OPBL optimization problems under consideration.

A.1 OPL

For this problem, the general objective function given by (2.8) reduces to

$$P \approx c \sum_{k=1}^{N} Q\left(\sqrt{a\varepsilon_k}\right). \tag{A.1}$$

Let $f_1 = Q\left(\sqrt{a\varepsilon_k}\right)$. First we need to prove the convexity of f_1 with respect to ε_k. Performing the second derivative of f_1 with respect to ε_k, we obtain

$$\frac{d^2 f_1}{d\varepsilon_k^2} = \left(\frac{a\sqrt{a}}{4\sqrt{2\pi\varepsilon_k}} + \frac{\sqrt{a}}{4\varepsilon_k\sqrt{2\pi\varepsilon_k}}\right) \exp\left(-\frac{a\varepsilon_k}{2}\right). \tag{A.2}$$

Since a and ε_k are positive quantities, (A.2) is always positive which proves that f_1 is a convex function. Second, we need to prove that ε_k is concave in $E_{k,S}$ and $E_{k,R}$. This will prove the convexity of f_1 with respect to $E_{k,S}$ and $E_{k,R}$ [56]. Rewriting ε_k given by (2.9) as

$$\varepsilon_k = g_1\left(E_{k,S}, E_{k,R}\right) + g_2\left(E_{k,S}, E_{k,R}\right) \tag{A.3}$$

where

$$g_1\left(E_{k,S}, E_{k,R}\right) = E_{k,S}\left|D_{k,1}\right|^2 \tag{A.4}$$

$$g_2\left(E_{k,S}, E_{k,R}\right) = \begin{cases} \frac{E_{k,S}E_{k,R}\left|D_{k,2}\right|^2}{\left(E_{k,R}D_{k,R}+D_{k,0}\right)} \text{original} \\ \frac{E_{k,S}E_{k,R}\left|D_{k,2}\right|^2}{\left(E_{k,R}D_{k,R}+E_{k,S}G_{SR}|D_{SR}(k,k)|^2+N_0\right)} \quad \text{modified} \end{cases} \tag{A.5}$$

In (A.5), we consider two cases. As earlier discussed, the original IPS scaling term is given by (2.3). The modified version involves replacing $E_{k,S}$ with the average value E in (2.3). **Modified IPS:** For the modified version, $g_2\left(E_{k,S}, E_{k,R}\right)$ can be expressed as,

$$g_2\left(E_{k,S}, E_{k,R}\right) = \frac{\left(\frac{\left|D_{k,2}\right|^2}{D_{k,R}D_{k,0}}\right)}{\left(\frac{1}{E_{k,R}E_{k,S}D_{k,R}} + \frac{1}{D_{k,0}E_{k,S}}\right)} \tag{A.6}$$

Since $D_{k,2}$, $D_{k,0}$, $D_{k,R}$ and $E_{k,S}$ are positive quantities, $g_2\left(E_{k,S}, E_{k,R}\right)$ is concave if and only if $1/(E_{k,R}E_{k,S}D_{k,R})$ and $1/(D_{k,0}E_{k,S})$ are convex functions. The term $1/(E_{k,R}E_{k,S}D_{k,R})$ is convex because

$$\frac{\partial^2}{\partial E_{k,S}^2}\left(\frac{1}{D_{k,0}E_{k,S}}\right) = \frac{2}{D_{k,0}E_{k,S}^2} > 0 \tag{A.7}$$

The Hessian matrix $\mathbf{H}_1$ of $1/(E_{k,R}E_{k,S}D_{k,R})$ is expressed as

$$\mathbf{H}_1 = \frac{1}{D_{k,R}E_{k,S}E_{k,R}} \begin{bmatrix} \frac{2}{E_{k,R}^2} & \frac{1}{E_{k,S}E_{k,R}} \\ \frac{1}{E_{k,S}E_{k,R}} & \frac{2}{E_{k,S}^2} \end{bmatrix} \tag{A.8}$$

If $\mathbf{x} = [\ x_1 \quad x_2\ ]^T$, where $x_1,\ x_2 \in \Re$ and not zero, then $\mathbf{x}^T\mathbf{H}_1\mathbf{x}$ is expressed as:

$$\mathbf{x}^T\mathbf{H}_1\mathbf{x} = \frac{2}{D_{k,R}E_{k,S}E_{k,R}} \left(\left(\frac{1}{\sqrt{2}E_{k,R}}x_1 + \frac{1}{\sqrt{2}E_{k,S}}x_2 \right)^2 + \frac{1}{2E_{k,R}^2}x_1^2 + \frac{1}{2E_{k,S}^2}x_2^2 \right) \tag{A.9}$$

Since $D_{k,R}$ is positive, therefore (A.9) is positive and $\mathbf{H}_1$ is positive define matrix which proves the convexity of $[1/(E_{k,R}E_{k,S}D_{k,R})]$ term. Thus $g_2\left(E_{k,S}, E_{k,R}\right)$ is a concave function.

Original IPS: For the original case, (A.5) can be expressed as,

$$g_2\left(E_{k,S}, E_{k,R}\right) = \frac{\left(\frac{4\left|D_{k,2}\right|^2}{N_0^2 D_{k,R}G_{SR}\left|D_{SR}(k,k)\right|^2} \right)}{\left(\frac{1}{E_{k,R}D_{k,R}+N_0/2} + \frac{1}{E_{k,S}G_{SR}\left|D_{SR}(k,k)\right|^2+N_0/2} \right)} \tag{A.10}$$

The Hessian matrix $\mathbf{H}_2$ of the term in denominator is given by

$$\mathbf{H}_2 = \begin{bmatrix} \frac{2G_{SR}\left|D_{SR}(k,k)\right|^2}{\left(E_{k,S}G_{SR}\left|D_{SR}(k,k)\right|^2+N_0/2\right)^3} & 0 \\ 0 & \frac{2D_{k,R}}{\left(E_{k,R}D_{k,R}+N_0/2\right)^3} \end{bmatrix} \tag{A.11}$$

It can be then shown that

$$\mathbf{x}^T\mathbf{H}_2\mathbf{x} = \frac{2G_{SR}\left|D_{SR}\left(k,k\right)\right|^2}{\left(E_{k,S}G_{SR}\left|D_{SR}\left(k,k\right)\right|^2 + N_0/2\right)^3}x_1^2 + \frac{2D_{k,R}}{\left(E_{k,R}D_{k,R} + N_0/2\right)^3}x_2^2 > 0 \tag{A.12}$$

G_{SR}, $D_{k,R}$, N_0 and $|D_{SR}(k,k)|$ are positive values, thus $\mathbf{H}_2$ is a positive definite matrix which proves the convexity term of the denominator term in (A.10). Accordingly $g_2(E_{k,S}, E_{k,R})$ is a concave function. As a result scaling with $E_{k,S}$ or E does not affect the concavity nature of $g_2(E_{k,S}, E_{k,R})$. Since $g_1(E_{k,S}, E_{k,R})$ and $g_2(E_{k,S}, E_{k,R})$ are concave function, ε_k is also concave function. As result, $f_1 = Q\left(\sqrt{a\varepsilon_k}\right)$ is convex. Since the sum of convex functions is convex, (A.1) turns out to be convex.

A.2 OBL

For this problem, the objective function will follow the general form in (2.8). By using the values of a_k and c_k in for M-PSK (2.10) and (2.11), we have

$$P \approx \sum_{k=1}^{N} \frac{(M_k - 1)}{mN} Q\left(\sqrt{\frac{2}{N_0}\sin^2\left(\frac{\pi}{M_k}\right)\varepsilon_k}\right) = \sum_{k=1}^{N} \frac{\left(2^{b_k} - 1\right)}{mN} Q\left(\sqrt{\frac{2}{N_0}\sin^2\left(\frac{\pi}{2^{b_k}}\right)\varepsilon_k}\right) \tag{A.13}$$

By relaxing the integer variable b_k to be continuous [59] and defining

$$f_2 = \frac{\left(2^{b_k} - 1\right)}{mN} Q\left(\sqrt{\frac{2}{N_0}\sin^2\left(\frac{\pi}{2^{b_k}}\right)\varepsilon_k}\right) \tag{A.14}$$

then P is convex if f_2 is convex. To test the convexity of f_2, we find the second derivative with respect to b_k which yields

$$\frac{\partial^2 f_2}{\partial b_k^2} = \frac{(\ln 2)^2 2^{b_k}}{mN} Q\left(\sqrt{\frac{2}{N_0}\sin^2\left(\frac{\pi}{2^{b_k}}\right)\varepsilon_k}\right)$$
$$+\frac{(\ln 2)2^{b_k}}{mN}\left(\frac{1}{\sqrt{2\pi}}\right)\exp\left(-\frac{2}{N_0}\sin^2\left(\frac{\pi}{2^{b_k}}\right)\varepsilon_k\right)\cos\left(\frac{\pi}{2^{b_k}}\right)\frac{(\ln 2)\pi}{2^{b_k}}$$
$$+\frac{(\ln 2)2^{b_k}}{mN}\left(\frac{1}{\sqrt{2\pi}}\right)\exp\left(-\frac{2}{N_0}\sin^2\left(\frac{\pi}{2^{b_k}}\right)\varepsilon_k\right)\cos\left(\frac{\pi}{2^{b_k}}\right)\frac{(\ln 2)\pi}{2^{b_k}}$$
$$+\frac{\left(2^{b_k}-1\right)}{mN}\left(\frac{1}{\sqrt{2\pi}}\right)\exp\left(-\frac{2}{N_0}\sin^2\left(\frac{\pi}{2^{b_k}}\right)\varepsilon_k\right)\sin\left(\frac{\pi}{2^{b_k}}\right)\left(\frac{(\ln 2)\pi}{2^{b_k}}\right)^2$$
$$+\frac{\left(2^{b_k}-1\right)}{mN}\left(\frac{1}{\sqrt{2\pi}}\right)\exp\left(-\frac{2}{N_0}\sin^2\left(\frac{\pi}{2^{b_k}}\right)\varepsilon_k\right)\cos\left(\frac{\pi}{2^{b_k}}\right)\frac{(\ln 2)}{2^{b_k}}\left(\frac{4}{N_0}\sin\left(\frac{\pi}{2^{b_k}}\right)\varepsilon_k\right)\left(\cos\left(\frac{\pi}{2^{b_k}}\right)\right)\frac{(\ln 2)\pi}{2^{b_k}} \tag{A.15}$$

Since $b_k \geq 1$, therefore the values of all cos(.) and sin(.) function are positive. And since exp(.) is a positive function, thus (A.15) is always positive. Then as a result f_2 is convex and accordingly P is convex.

A.3 OBPL

Replacing a_k and c_k in for M-PSK in the general form of the objective function in, we have

$$P = \sum_{k=1}^{N} \frac{\left(2^{b_k}-1\right)}{mN} Q\left(\sqrt{\frac{2}{N_0}\sin^2\left(\frac{\pi}{2^{b_k}}\right)\varepsilon_k\left(E_{k,S}, E_{k,R}\right)}\right) \tag{A.16}$$

Define f_3 to be

$$f_3 = \frac{\left(2^{b_k}-1\right)}{mN} Q\left(\sqrt{\frac{2}{N_0}\sin^2\left(\frac{\pi}{2^{b_k}}\right)\varepsilon_k\left(E_{k,S}, E_{k,R}\right)}\right), \tag{A.17}$$

To prove the convexity of P, we need to prove that f_3 is convex. First note that $\sin\left(\pi/2^{b_k}\right)$ can be bounded as $0 \leq \sin\left(\pi/2^{b_k}\right) \leq 1$. Noting Q functions monotonically decreasing

property, it is straightforward to show that

$$\frac{\left(2^{b_k}-1\right)}{mN}Q\left(\sqrt{\frac{2}{N_0}\varepsilon_k\left(E_{k,S},E_{k,R}\right)}\right)\leq\frac{\left(2^{b_k}-1\right)}{mN}Q\left(\sqrt{\frac{2}{N_0}\sin^2\left(\frac{\pi}{2^{b_k}}\right)\varepsilon_k\left(E_{k,S},E_{k,R}\right)}\right)\leq\frac{\left(2^{b_k}-1\right)}{2mN} \tag{A.18}$$

Further define $f_4=\left(2^{b_k}-1\right)/(2mN)$ and $f_5=\left(\left(2^{b_k}-1\right)/mN\right)Q\left(\sqrt{(2/N_0)\,\varepsilon_k\left(E_{k,S},E_{k,R}\right)}\right)$. f_5 is convex function if f_3 and f_4 are convex functions. We know that f_4 is convex function, thus we need to show that f_5 is convex. f_5 can be bounded as $f_6<f_5<f_7$ where f_6 and f_7 are defined as

$$f_6=Q\left(\sqrt{(2/N_0)\,\varepsilon_k\left(E_{k,S},E_{k,R}\right)}\right)$$

and

$$f_7=(1/2mN)\exp\left(b_k-(1/N_0)\,\varepsilon_k\left(E_{k,S},E_{k,R}\right)\right).$$

Noting $\exp(.)$ is a convex non-decreasing function and $(b_k-(1/N_0)\,\varepsilon_k\left(E_{k,S},E_{k,R}\right))$ is convex, f_7 is convex in $(b_k,E_{k,S},E_{k,R})$[64]. Since f_6 and f_7 are convex, f_5 is convex and accordingly f_3 is convex given that P of the OBPL is convex in $(b_k,E_{k,S},E_{k,R})$.

Appendix B

Convexity Proof of DF Problem

In this appendix, we provide the proof of convexity for (3.10). Define f_1 as

$$f_1 = cQ\left(\sqrt{a\varepsilon_k}\right) \tag{B.1}$$

where ε_k is given by

$$\varepsilon_k = \left|\mathbf{D}_{SD}\left(k,k\right)\right|^2 E_{k,S} + \left|\mathbf{D}_{R_iD}\left(k,k\right)\right|^2 G_{R_iD} E_{k,R_i} \tag{B.2}$$

The second derivative of f_1 is obtained as

$$\frac{d^2 f_1}{d\varepsilon_k^2} = c\left(\frac{a\sqrt{a}}{4\sqrt{2\pi\varepsilon_k}} + \frac{\sqrt{a}}{4\varepsilon_k\sqrt{2\pi\varepsilon_k}}\right)\exp\left(-\frac{a\varepsilon_k}{2}\right) \tag{B.3}$$

Since a, c and ε_k are positive quantities, $d^2 f_1/d\varepsilon_k^2$ is always positive. This indicates that f_1 is convex in ε_k. Noting that $Q(.)$ function is a convex non-increasing function in ε_k and ε_k is concave in $E_{k,S}$ and $E_{k,R}$ (note that the hessian matrix of ε_k is negative semi-definite),

we can conclude that ε_k is convex. Now define f_2 as

$$f_2 = \alpha Q\left(\sqrt{a\left|\mathbf{D}_{SD}\left(k,k\right)\right|^2 E_{k,S}}\right) Q\left(\sqrt{a\left|\mathbf{D}_{SR_i}\left(k,k\right)\right|^2 G_{SR_i} E_{k,S}}\right) \tag{B.4}$$

The second derivative of f_2 is given by

$$\begin{aligned}
\frac{\partial^2 f_2}{\partial E_{k,S}^2} &= \frac{\alpha}{4}\sqrt{\frac{a|\mathbf{D}_{SD}(k,k)|^2}{2\pi E_{k,S}^3}}\left(1+aE_{k,S}\right)\exp\left(-\frac{a|\mathbf{D}_{SD}(k,k)|^2 E_{k,S}}{2}\right) Q\left(\sqrt{a\left|\mathbf{D}_{SR_i}\left(k,k\right)\right|^2 G_{SR_i} E_{k,S}}\right) \\
&+\frac{\alpha a\sqrt{G_{SR_i}}}{4\pi E_{k,S}}\left|\mathbf{D}_{SD}\left(k,k\right)\right|\left|\mathbf{D}_{SR_i}\left(k,k\right)\right|\exp\left(-\frac{a|\mathbf{D}_{SD}(k,k)|^2 E_{k,S}}{2}\right)\exp\left(-\frac{a\left|\mathbf{D}_{SR_i}(k,k)\right|^2 G_{SR_i} E_{k,S}}{2}\right) \\
&+\frac{\alpha}{4}\sqrt{\frac{aG_{SR_i}}{2\pi E_{k,S}^3}}\left(1+aG_{SR_i}E_{k,S}\right)\left|\mathbf{D}_{SR_i}\left(k,k\right)\right| Q\left(\sqrt{a\left|\mathbf{D}_{SD}\left(k,k\right)\right|^2 E_{k,S}}\right) \\
&\qquad\qquad \times\exp\left(-\frac{a\left|\mathbf{D}_{SR_i}(k,k)\right|^2 G_{SR_i} E_{k,S}}{2}\right)
\end{aligned} \tag{B.5}$$

Since $\alpha,\ a,\ c,\ \left|\mathbf{D}_{SR_i}\left(k,k\right)\right|,\ \left|\mathbf{D}_{SD}\left(k,k\right)\right|,\ G_{SR_i}$ and $E_{k,S}$ are positive, we can conclude from (B.5) that $d^2 f_1/dE_{k,S}^2$ is positive, therefore is a convex function. Since f_1 and f_2 are convex functions and the sum of convex function is also convex [64], we can conclude that (3.10) is a convex function.

Bibliography

[1] I.-K. Fu, Y.-S. Chen, P. Cheng, Y. Yuk, R. Y. Kim, and J. S. K., "Multicarrier technology for 4g wimax system [wimax/lte update]," *IEEE Commun. Mag.*, vol. 48, no. 8, pp. 50–58, Aug. 2010. 1, 2

[2] A. Nosratinia, T. E. Hunter, and A. Hedayat, "Cooperative communication in wireless networks," *IEEE Commun. Mag.*, vol. 42, no. 10, pp. 74–80, Oct. 2004. 2

[3] R. Pabst, B. H. Walke, D. C. Schultz, P. Herhold, H. Yanikomeroglu, S. Mukherjee, H. Viswanathan, M. Lott, W. Zirwas, and M. Dohler, "Relay-based deployment concepts for wireless and mobile broadband radio," *IEEE Commun. Mag.*, vol. 42, no. 9, pp. 80–89, Sept. 2004. 2

[4] J. N. Laneman and G. W. Wornell, "Distributed space-time-coded protocols for exploiting cooperative diversity in wireless networks," *IEEE Trans. Inf. Theory*, vol. 49, no. 10, pp. 2415–2425, Oct. 2003. 2, 4, 47

[5] J. N. Laneman, D. N. C. Tse, and G. W. Wornell, "Cooperative diversity in wireless networks: Efficient protocols and outage behavior," *IEEE Trans. Inf. Theory*, vol. 50, no. 12, pp. 3062–3080, Dec. 2004. 2, 3, 4

[6] R. U. Nabar, H. Bolcskei, and F. W. Kneubuhler, "Fading relay channels: Performance limits and space-time signal design," *IEEE J. Sel. Areas Commun.*, vol. 22, no. 6, pp. 1099–1109, Aug. 2004. 3

[7] H. Ochiai, P. Mitran, and V. Tarokh, "Design and analysis of collaborative diversity protocols for wireless sensor networks," in *IEEE 60th Vehicular Technology Conference*, Fall-2004. 3, 15, 42

[8] A. Sendonaris, E. Erkip, B. Aazhang, Q. Inc, and C. A. Campbell, "User cooperation diversity. part i. system description," *IEEE Trans. Commun.*, vol. 51, no. 11, pp. 1927–1938, Nov. 2003. 4

[9] ——, "User cooperation diversity. part ii. implementation aspects and performance analysis," *IEEE Trans. Commun.*, vol. 51, no. 11, pp. 1939–1948, Nov. 2003. 4

[10] F. H. P. Frank and M. D. Katz, *Cooperation in Wireless Networks: Principles and Applications: Real Egoistic Behavior Is to Cooperate!* Springer-Verlag New York, Inc. Secaucus, NJ, USA, 2006. 4

[11] M. Uysal, Ed., *Cooperative Communications for Improved Wireless Network Transmission: Frameworks for Virtual Antenna Array Applications*, 1st ed. IGI Global, 2009. 4

[12] J. W. Mark and W. Zhuang, *Wireless Communications and Networking.* Prentice Hall, 2003. 4

[13] Y. Wu and W. Y. Zou, "Orthogonal frequency division multiplexing: A multi-carrier modulation scheme," *IEEE Trans. Consum. Electron.*, vol. 41, no. 3, pp. 392–399, Aug. 1995. 5

[14] W. Y. Zou and Y. Wu, "Cofdm: An overview," *IEEE Trans. Broadcast.*, vol. 41, no. 1, pp. 1–8, May 1995. 5

[15] G. Caire, G. Taricco, and E. Biglieri, "Bit-interleaved coded modulation," *IEEE Trans. Inf. Theory*, vol. 44, no. 3, pp. 927–946, May 1998. 5

[16] Z. Liu, Y. Xin, and G. Giannakis, "Linear constellation precoding for OFDM with maximum multipath diversity and coding gains," *IEEE Trans. Commun.*, vol. 51, no. 3, pp. 416–427, Mar. 2003. 6, 35, 36

[17] A. Goldsmith, *Wireless Communications.* Cambridge University Press, 2005. 6

[18] S. T. Chung and A. J. Goldsmith, "Degrees of freedom in adaptive modulation: A unified view," *IEEE Trans. Commun.*, vol. 49, no. 9, pp. 1561–1571, Sep. 2001. 6

[19] Y. Gabbai and S. I. Bross, "Achievable rates for the discrete memoryless relay channel with partial feedback configurations," *IEEE Trans. Inf. Theory*, vol. 52, no. 11, pp. 4989–5007, Nov. 2006. 6, 7

[20] A. J. Goldsmith and S. G. Chua, "Variable-rate variable-power mqam for fading channels," *IEEE Trans. Commun.*, vol. 45, no. 10, pp. 1218–1230, Oct. 1997. 6

[21] L. Lin, R. D. Yates, and P. Spasojevic, "Adaptive transmission with discrete code rates and power levels," *IEEE Trans. Commun.*, vol. 51, no. 12, pp. 2115–2125, Dec. 2003. 6

[22] L. Lin, R. D. Yates, P. Spasojevic, S. T. Inc, and M. D. Rockville, "Adaptive transmission with finite code rates," *IEEE Trans. Inf. Theory*, vol. 52, no. 5, pp. 1847–1860, May 2006. 6

[23] S. Catreux, V. Erceg, D. Gesbert, and R. W. H. Jr., "Adaptive modulation and mimo coding for broadband wireless data networks," *IEEE Commun. Mag.*, vol. 40, no. 6, pp. 108–115, Jun. 2002. 6

[24] Y. Ko and C. Tepedelenlioglu, "Orthogonal space-time block coded rate-adaptive modulation with outdated feedback," *IEEE Trans. Wireless Commun.*, vol. 5, no. 2, pp. 290–295, Feb. 2006. 6

[25] F. Kharrat-Kammoun, S. Fontenelle, and J. J. Boutros, "Accurate approximation of qam error probability on quasi-static mimo channels and its application to adaptive modulation," *IEEE Trans. Inf. Theory*, vol. 53, no. 3, pp. 1151–1160, Mar. 2007. 6

[26] J. Ham, M.-S. Kim, C. Lee, and T. Hwang, "An adaptive modulation algorithm for performance improvement of mimo ml systems," *IEEE Commun. Lett.*, vol. 12, no. 11, pp. 819–821, Nov. 2008. 6

[27] J. C. Roh and B. D. Rao, "Efficient feedback methods for mimo channels based on parameterization," *IEEE Trans. Wireless Commun.*, vol. 6, no. 1, pp. 282–292, Jan. 2007. 6

[28] Z. Zhou, B. Vucetic, M. Dohler, and Y. Li, "Mimo systems with adaptive modulation," *IEEE Trans. Veh. Technol.*, vol. 54, no. 5, pp. 1828–1842, Sept. 2005. 6

[29] C. Assimakopoulos and F. Pavlidou, "Transmission Systems Unified models for adaptive OFDM systems when QAM or PSK modulation is applied," *European Trans. on Telecommun.*, vol. 18, no. 7, pp. 777–790, Nov. 2007. 7

[30] T. Hunziker and D. Dahlhaus, "Optimal power adaptation for ofdm systems with ideal bit-interleaving and hard-decision decoding," in *IEEE International Conference on Communications*, vol. 5, 2003, pp. 3392–3397. 7

[31] Y. Rong, S. A. Vorobyov, and A. B. Gershman, "Adaptive ofdm techniques with one-bit-per-subcarrier channel-state feedback," *IEEE Trans. Commun.*, vol. 54, no. 11, p. 1993, Nov. 2006. 7

[32] C. K. Sung, S.-Y. Chung, J. H., and I. Lee, "Adaptive bit-interleaved coded ofdm with reduced feedback information," *IEEE Trans. Commun.*, vol. 55, no. 9, pp. 1649–1655, Sept. 2007. 7

[33] S. Ye, R. S. Blum, and L. J. Cimini, "Adaptive ofdm systems with imperfect channel state information," *IEEE Trans. Wireless Commun.*, vol. 5, no. 11, pp. 3255–3265, Nov. 2006. 7

[34] Y. Li, J. C. Chuang, and N. R. Sollenberger, "Transmitter diversity for ofdm systems and its impact on high-rate data wireless networks," *IEEE J. Sel. Areas Commun.*, vol. 17, no. 7, pp. 1233–1243, Jul. 1999. 7

[35] C. Mutti, D. Dahlhaus, and T. Hunziker, "Optimal power loading for multiple-input single-output ofdm systems with bit-level interleaving," *IEEE Trans. Wireless Commun.*, 2006. 7

[36] Q. Yong-Hong and P. Ya-Han, "Adaptive bit and power allocation with adaptive transmit diversity for broadband miso/ofdm wireless transmission," vol. 2, 2003, pp. 1472–1476. 7

[37] H. Bolcskei and E. Zurich, "Mimo-ofdm wireless systems: Basics, perspectives, and challenges," *IEEE Trans. Wireless Commun.*, vol. 13, no. 4, p. 31, Aug. 2006. 7

[38] P. Tan, Y. Wu, and S. Sun, "Link adaptation based on adaptive modulation and coding for multiple-antenna ofdm system," *IEEE J. Sel. Areas Commun.*, vol. 26, no. 8, pp. 1599–1606, Oct. 2008. 7

[39] P. Xia, S. Zhou, and G. B. Giannakis, "Multiantenna adaptive modulation with beamforming based on bandwidth-constrained feedback," *IEEE Trans. Commun.*, vol. 53, no. 3, pp. 526–536, Mar. 2005. 7

[40] ——, "Adaptive mimo-ofdm based on partial channel state information," *IEEE Trans. Signal Process.*, vol. 52, no. 1, pp. 202–213, Jan. 2004. 7

[41] Y.-H. Pan and S. Aissa, "Dynamic resource allocation with beamforming for mimo ofdm systems: performance and effects of imperfect csi," *IEEE Trans. Wireless Commun.*, 2007. 7

[42] N. Ahmed, M. A. Khojastepour, A. Sabharwal, and B. Aazhang, "Outage minimization with limited feedback for the fading relay channel," *IEEE Trans. Commun.*, vol. 54, no. 4, pp. 659–669, Mar. 2006. 7

[43] N. Ahmed and B. Aazhang, "Throughput gains using rate and power control in cooperative relay networks," *IEEE Trans. Commun.*, vol. 55, no. 4, pp. 656–660, Apr. 2007. 7

[44] A. P. T. Lau and S. Cui, "Joint power minimization in wireless relay channels," *IEEE Trans. Wireless Commun.*, vol. 6, no. 8, pp. 2820–2824, Aug. 2007. 7

[45] A. S. Ibrahim, A. K. Sadek, W. Su, and K. J. R. Liu, "Cooperative communications with relay-selection: When to cooperate and whom to cooperate with?" *IEEE Trans. Wireless Commun.*, vol. 7, no. 7, Jul. 2008. 7

[46] J. Adeane, M. R. D. Rodrigues, and I. J. Wassell, "Centralised and distributed power allocation for co-operative networks," *Electron. Lett.*, vol. 43, no. 1, pp. 39–40, Jan. 2007. 8

[47] I. Hammerstrom and A. Wittneben, "On the optimal power allocation for nonregenerative ofdm relay links," in *Proc. IEEE International Conference on Communications*, vol. 10, 2006, pp. 4463–4468. 8

[48] ——, "Power allocation schemes for amplify-and-forward mimo-ofdm relay links," *IEEE Trans. Wireless Commun.*, vol. 6, no. 8, pp. 2798–2802, Aug. 2007. 8

[49] Y. Ma, N. Yi, and R. Tafazolli, "Bit and power loading for ofdm-based three-node relaying communications," *IEEE Trans. Signal Process.*, vol. 56, pp. 3236–3247, Jul. 2008. 8, 9, 48, 71, 72

[50] W. Ying, Q. Xin-chun, W. Tong, and L. Bao-ling, "Power allocation and subcarrier pairing algorithm for regenerative ofdm relay system," in *Proc. IEEE 65th Vehicular Technology Conference*, Spring-2007, pp. 2727–2731. 8

[51] N. Yi, Y. Ma, and R. Tafazolli, "Rate-adaptive bit and power loading for ofdm based df relaying," in *Proc. IEEE 68th Vehicular Technology Conference*, Spring-2008, pp. 1340–1344. 8, 9, 71, 72

[52] B. Can, H. Yomo, and E. D. Carvalho, "Link adaptation and selection method for ofdm based wireless relay networks," *Journal of Commun. and Netw.*, vol. 9, no. 2, pp. 118–127, Jun. 2007. 8

[53] B. Gui and L. J. C. Jr, "Bit loading algorithms for cooperative ofdm systems," *EURASIP Journal Wireless Commun. and Netw.*, vol. 2008, no. 2, 2008. 9, 71, 72

[54] N. Yi, Y. Ma, and R. Tafazolli, "Bit and power loading for OFDM with an amplify-and-forward cooperative relay," in *IEEE 19th International Symposium on Personal, Indoor and Mobile Radio Communications*, 2008, pp. 1–5. 9, 71, 72

[55] M. Hajiaghayi, M. Dong, and B. Liang, "Using limited feedback in power allocation design for a two-hop relay ofdm system," in *Proc. IEEE International Conference on Communications*, Jun. 2009. 9, 36

[56] S. P. Boyd and L. Vandenberghe, *Convex optimization*. Cambridge Univ. Press, 2004. 9, 10, 49, 91

[57] D. Li and X. Sun, *Nonlinear Integer Programming.* Springer Science, 2006. 9, 10, 11, 29

[58] J. A. Snyman, *Practical Mathematical Optimization: An Introduction to Basic Optimization Theory and Classical and New Gradient-based Algorithms.* Springer, 2005. 9, 10, 11, 22

[59] T. Ibaraki and N. Katoh, *Resource Allocation Problems: Algorithmic Approaches.* Mit Press Series In The Foundations Of Computing, 1988. 9, 10, 11, 27, 71, 93

[60] O. Amin and M. Uysal, "Adaptive power loading for ofdm cooperative networks," in *Proc. 11th Canadian Workshop on Information Theory*, 2009, pp. 187–191. 11

[61] ——, "Optimal bit and power loading for amplify-and-forward cooperative ofdm system," *accepted in IEEE Trans. Wireless Commun.*, 2010. 11

[62] ——, "Adaptive power loading for multi-relay ofdm regenerative networks with relay selection," *under review in IEEE Trans. Commun.*, 2010. 11

[63] O. Amin, S. S. Ikki, and M. Uysal, "On the performance analysis of multi-relay cooperative diversity systems with channel estimation errors," *under review in IEEE Trans. Veh. Technol.*, 2010. 12

[64] ——, "Adaptive bit loading for multi-relay cooperative ofdm with imperfect channel estimation," *under review in IEEE Trans. Veh. Technol.*, 2010. 12

[65] H. Mheidat and M. Uysal, "Impact of receive diversity on the performance of amplify-and-forward relaying under aps and ips power constraints," *IEEE Commun. Lett.*, vol. 10, no. 6, pp. 468–470, Jun. 2006. 17, 63

[66] J. N. Laneman, "Cooperative diversity in wireless networks: algorithms and architectures," Ph.D. dissertation, 2002. 17

[67] J. G. Proakis, *Digital Communication.* McGraw-Hill, 2001. 19, 48

[68] R. M. Corless, G. H. Gonnet, D. E. G. Hare, D. J. Jeffrey, and D. E. Knuth, "On the Lambert W function," *Adv. Comp. Math*, vol. 5, no. 1, pp. 329–359, 1996. 24, 51

[69] O. Amin, B. Gedik, and M. Uysal, "Channel estimation for amplify-and-forward relaying: Cascaded against disintegrated estimators," *IET Commun.*, vol. 4, no. 10, pp. 1207–1216, Oct. 2010. 36, 37, 38, 58

[70] S. M. Kay, *Fundamentals of Statistical Signal Processing: Estimation Theory.* PTR Prentice Hall, 1993. 38, 64

[71] M. M. Fareed and M. Uysal, "On relay selection for decode-and-forward relaying," *IEEE Trans. Wireless Commun.*, vol. 8, no. 7, pp. 3341–3346, 2009. 43

[72] A. Bletsas, A. Khisti, D. P. Reed, and A. Lippman, "A simple cooperative diversity method based on network path selection," *IEEE J. Sel. Areas Commun.*, vol. 24, no. 3, pp. 659–672, 2006. 63, 68

[73] P. A. Anghel and M. Kaveh, "Exact symbol error probability of a cooperative network in a rayleigh-fading environment," *IEEE Trans. Wireless Commun.*, vol. 3, no. 5, pp. 1416–1421, 2004. 64

[74] S. S. Ikki and M. H. Ahmed, "Performance of multiple-relay cooperative diversity systems with best relay selection over rayleigh fading channels," *EURASIP Journal Advances in Signal Process.*, vol. 1, p. 5, 2008. 69

[75] J. M. Torrance and L. Hanzo, "Upper bound performance of adaptive modulation in a slow rayleigh fading channel," *Electron. Lett.*, vol. 32, pp. 718–719, 1996. 70

[76] B. J. Choi and L. Hanzo, "Optimum mode-switching-assisted constant-power single- and multicarrier adaptive modulation," *IEEE Trans. Veh. Technol.*, vol. 52, no. 3, pp. 536–560, 2003. 72, 74

[77] B. Rankov and A. Wittneben, "Spectral efficient protocols for half-duplex fading relay channels," *IEEE J. Sel. Areas Commun.*, vol. 25, no. 2, pp. 379–389, 2007. 87

[78] W. Wang and R. Wu, "Capacity maximization for OFDM two-hop relay system with separate power constraints," *IEEE Trans. Veh. Technol.*, vol. 58, no. 9, pp. 4943–4954, 2009. 87

[79] S. Shahbazpanahi and M. Dong, "Achievable rate region and sum-rate maximization for network beamforming for bi-directional relay networks," in *IEEE International Conference on Acoustics Speech and Signal Processing*, 2010, pp. 2510–2513. 87

[80] Z. Li, X. G. Xia, and B. Li, "Achieving full diversity and fast ml decoding via simple analog network coding for asynchronous two-way relay networks," *IEEE Trans. Commun.*, vol. 57, no. 12, pp. 3672–3681, 2009. 87

[81] F. Li, G. Zhu, G. Su, and X. Ke, "An optimal transmission scheme for two-way relaying networks with power constraint," in *Proc. 19th Annual Conference Wireless and Optical Communications*, 2010, pp. 1–4. 87

[82] Y. Jia and A. Vosoughi, "Two-way relaying for energy constrained systems: Joint transmit power optimization," in *Proc. IEEE International Conference Acoustics Speech and Signal Processing*, 2010, pp. 3026–3029. 87

[83] C. Hausl, O. Iscan, and F. Rossetto, "Optimal time and rate allocation for a network-coded bidirectional two-hop communication," in *2010 European Wireless Conference*, 2010, pp. 1015–1022. 87

[84] M. Dong and S. Shahbazpanahi, "Optimal spectrum sharing and power allocation for ofdm-based two-way relaying," in *Proc. IEEE International Conference on Acoustics Speech and Signal Processing*, 2010, pp. 3310–3313. 87

[85] F. Pancaldi, G. Vitetta, R. Kalbasi, N. Al-Dhahir, M. Uysal, and H. Mheidat, "Single-carrier frequency domain equalization," *IEEE Commun. Mag.*, vol. 25, no. 5, pp. 37–56, Sept. 2008. 88

[86] D. Falconer, S. L. Ariyavisitakul, A. Benyamin-Seeyar, and B. Eidson, "Frequency domain equalization for single-carrier broadband wireless systems," *IEEE Commun. Mag.*, vol. 40, no. 4, pp. 58–66, Apr. 2002. 88

[87] J. Yuan, Y. Du, L. Going, and J. Li, "A bit-loading algorithm in sc-fde system," in *Proc. IEEE Radio and Wireless Symposium*, 2006, pp. 27–30. 88